UNIVERSIDADE DE LISBOA
FACULDADE DE CIÊNCIAS
DEPARTAMENTO DE QUÍMICA E BIOQUÍMICA

Development of Liposomal Formulations for Treatment of Hepatic Ischemia and Reperfusion Injury

Luís Filipe Pereira dos Santos

Mestrado em Bioquímica
Especialização em Bioquímica Médica

Dissertação orientada por:
Doutora Maria Luísa Teixeira Azevedo Rodrigues Corvo
Professor Doutor Federico Herrera Garcia

2022

AGRADECIMENTOS

Esta Dissertação que hoje podem ver é o fruto de um ano de trabalho árduo e complicado, misturado de altos e baixos, que é o culminar de um percurso de crescimento pessoal, espiritual e académico longo e trabalhoso. Todo este percurso só foi possível graças ao apoio e à força de várias pessoas que estiveram, estão e estarão ao longo da minha vida pessoal e profissional, as quais agradeço imenso.

Queria agradecer ao *Drug Delivery and Immunotherapy Laboratory* do iMED.ULisboa/FFUL no Pólo do Lumiar, representado neste percurso pela Doutora Maria Luísa Corvo, pela oportunidade dada. Queria agradecer a ajuda e o apoio dado pela Ana Casaca, a Jacinta, a Doutora Manuela Colla e a Doutora Manuela Gaspar. Em particular, queria agradecer à Margarida Silva por me guiar dentro do laboratório, de me ensinar como fazer as formulações lipossomais e pela ajuda. Também queria agradecer em particular à Clarinda Costa pelo apoio no laboratório quando necessitava de estar mais tempo e pela ajuda indispensável na utilização dos aparelhos do laboratório, em conjunto com a Catarina. Por fim, queria agradecer ao Denys Holovanchuk pelo empurrão que me ajudou a dar para poder levar estes estudos para outro patamar, mesmo que tenha sido só por pouco tempo.

Queria agradecer também ao *Cell Structure and Dynamics Laboratory* do BioISI, FCUL, representado neste percurso pelo Professor Doutor Federico Herrera Garcia, por me acolher no seu laboratório numa altura complicada e por me dar a oportunidade de poder levar os meus estudos para outro patamar. Queria agradecer à Mafalda Migueis, à Daniela Alves e ao Pedro Peralta por me ajudarem a integrar no laboratório, por me ensinarem e ajudarem em novas técnicas e pelos momentos de diversão e humor que ajudavam a animar o ambiente, também com a ajuda da Patrícia Nascimento (mesmo que tenha sido um período breve). *In particular, I would like to thank Mickael Diallo, a person who, even though he was totally out of my Dissertation's study field and with a lot of personal and academic work, taught me all the basis for handling cellular cultures. I also thank Mika for the various good and bad moments that allowed me to get on with this project and for the fun and joy he brought to the laboratory.* Também queria agradecer em particular à Fernanda Murtinheira, uma pessoa muito especial nesta Dissertação que, no meio de todo o seu trabalho e sem conhecimento de como a quercetina e os lipossomas funcionavam, deu-me o impulso necessário para continuar com este projeto, quando tudo me parecia estar a correr mal. Graças ao seu apoio pessoal e com os ensinamentos dela de novas técnicas e de novas perspetivas, este projeto conseguiu dar frutos.

Queria também agradecer aos vários professores que tive ao longo deste percurso académico que me incentivaram e cultivaram o meu gosto por querer saber mais do Mundo e da Humanidade, em especial na área das ciências, sem esquecer também as pessoas detrás. Também queria agradecer aos meus colegas e amigos que fui conhecendo e fazendo durante este percurso por toda a força e alegria que me deram para conseguir seguir em frente com os meus objetivos.

Queria agradecer também a toda a minha família, em especial aos meus pais, ao meu irmão, à minha madrinha e aos meus avós, por me darem a força e o apoio necessário para me guiarem neste caminho, por acreditarem sempre em mim e por me encorajarem a seguir este caminho. Sem estas pessoas, eu não teria a força de continuar e de estar onde estou hoje.

Por fim, dedico esta Dissertação às várias pessoas que estiveram na minha vida mas que já não se encontram hoje entre nós, que deram o ânimo e a força necessária para poder estar onde estou hoje. Espero que ao verem isto, estejam orgulhosos do caminho que alcancei, onde quer que estejam.

ABSTRACT

Hepatic Ischemia and Reperfusion Injury, a medical condition derived from Hepatic Ischemia and Reperfusion, a clinical phenomenon commonly associated with medical interventions, such as a hepatic resection, is a very complex biological process that is associated with poor hepatic functional recovery, mortality and morbidity in humans. This complex process has numerous variables that can influence the outcome of existing treatments, which can only mitigate partially the damage. A possible treatment option is the administration of natural compounds extracted from plants that display antioxidant and/or anti-inflammatory properties, both of which are hallmarks of Hepatic Ischemia and Reperfusion Injury, such as resveratrol, curcumin, or quercetin. Quercetin not only displays these properties but also has protective effects against Hepatic Ischemia and Reperfusion Injury in rats. However, there are some drawbacks to quercetin's administration in humans, such as low bioavailability, lack of systematic data about quercetin as a nutraceutical in humans and the existence of side effects and drug interactions as a supplement, all of which can possibly limit quercetin's use. For that reason, the main goal of this research project is to discover a viable solution to overcome some of quercetin's administration issues by incorporating quercetin into a liposomal formulation. To develop this quercetin liposomal formulation, it was first determined the optimal quercetin-to-lipid molar ratio to use for the formulation preparation, using a saturation curve of the incorporation of quercetin in the lipid bilayer of the liposomes. Preliminary data from this saturation curve indicated that the optimal quercetin-to-lipid molar ratio to be used was 1:10 (mol/mol). Next, the effect of free quercetin and the optimal quercetin liposomal formulation were compared for their effect against oxidative stress and toxicity caused by rotenone, a Complex I mitochondrial respiratory chain inhibitor, in C6 rat glioma cells. Cell viability was analyzed after 24 and 48 hours of rotenone incubation and oxidative stress after 4 and 16 hours of incubation, using MTT Assays and Flow Cytometry, respectively. Preliminary results indicated that, although neither quercetin form had any protective effect against rotenone-induced toxicity, both quercetin forms reduced similarly rotenone-induced oxidative stress. These preliminary results suggest that, *in vitro,* quercetin can be a good treatment option for conditions that involve oxidative stress and that this liposomal formulation can be a viable solution for quercetin cell delivery. Ultimately, these results suggest that the developed quercetin liposomal formulation is a possible pharmacological treatment for Hepatic Ischemia and Reperfusion Injury. However, this *in vitro* cell model does not reflect the entirety of the Hepatic Ischemia and Reperfusion Injury process and the biological clearance mechanisms for liposomal formulation. For that reason, it is required to conduct further studies to evaluate if this quercetin liposomal formulation can be a viable pharmacological treatment for Hepatic Ischemia and Reperfusion Injury.

Keywords: Quercetin; Rotenone; Oxidative Stress; Liposomes; Hepatic Ischemia and Reperfusion Injury.

RESUMO ALARGADO

A Isquemia e Reperfusão é um fenómeno clínico que pode afetar diversos órgãos no organismo humano como o coração ou os rins, e que é derivado de várias situações como procedimentos cirúrgicos como um transplante de órgão ou por situações imprevisíveis como um enfarte do miocárdio. Por exemplo, este fenómeno pode afetar o fígado, sendo aqui conhecido como Isquemia e Reperfusão Hepática, uma condição médica tipicamente associada a intervenções cirúrgicas como um transplante de fígado. Devido a esta estreita interligação com intervenções médicas, a ocorrência da Isquemia e Reperfusão Hepática é possível de ser prevista. Além do mais, os danos causados por esta condição médica, referidos como a Lesão por Isquemia e Reperfusão Hepática, levam a que seja considerada como uma das principais causas da mortalidade, morbilidade e pobre recuperação da função hepática em humanos. A Lesão por Isquemia e Reperfusão Hepática pode ser sumariada como um processo biológico complexo com numerosas variáveis, estando também relacionado com a indução do *stress* oxidativo e do processo inflamatório, o que resulta em danos no fígado. Pela existência de diversas variáveis associadas como a duração e a severidade da isquemia, acrescentando que existem muitas mais variáveis não conhecidas, atualmente, não existem estratégias de tratamento direcionadas a prevenir ou tratar os efeitos da Lesão por Isquemia e Reperfusão Hepática, para além de mitigar os danos causados por essa condição médica. Existem diversas opções de tratamento a serem estudadas como a administração de compostos naturais extraídos de plantas que apresentam propriedades antioxidantes e/ou anti-inflamatórias, ambas marcas da Lesão por Isquemia e Reperfusão Hepática, tais como o resveratrol, a curcumina ou a quercetina. A quercetina é um flavonoide que exibe ambas as propriedades, tendo sido já estudada como forma de tratamento para outras condições médicas como doenças respiratórias. Para além do mais que a quercetina tem também efeitos protetores contra a Lesão por Isquemia e Reperfusão Hepática em ratos. Embora seja uma opção promissora, a administração de quercetina a humanos tem alguns contratempos como um baixo nível de biodisponibilidade, falta de informação sistematizada sobre o uso da quercetina como um nutracêutico em humanos, com sinais de alerta em outros modelos de estudo, e a existência de efeitos secundários e de interações com outros fármacos como um suplemento, o que limita o uso da quercetina. Para tentar solucionar alguns destes contratempos da administração de quercetina a humanos, uma possível solução é a incorporação da quercetina numa formulação lipossomal. Para tentar melhorar ainda esta administração, a formulação lipossomal usada pode ser desenhada de forma a melhorar o tempo de circulação da quercetina no organismo, permitindo assim que possa chegar às células-alvo para ter um efeito terapêutico mais apropriado. Por essa razão, o principal objetivo deste projeto de investigação é descobrir esta solução viável para a administração da quercetina a humanos, ao incorporar a quercetina numa formulação lipossomal.

Em relação à formulação lipossomal a usar, como é direcionada para o tratamento da Lesão por Isquemia e Reperfusão Hepática que é um processo inflamatório, a estratégia para o design desta formulação será com base na estratégia de direcionamento passivo. Com base nesta estratégia, foi utilizado polietilenoglicol na composição lipídica da formulação lipossomal de forma a mascarar os lipossomas do sistema imunitário do organismo, aumentando assim o tempo de circulação desta formulação lipossomal. Para além disto, existe também a restrição do tamanho dos lipossomas para valores de tamanho inferiores a 200 nm, de forma a passar as junções que foram abertas entre as células endoteliais dos vasos sanguíneos derivadas da indução do processo inflamatório e também para ultrapassar as barreiras de remoção de compostos do fígado e dos rins, aumentando mais o tempo de circulação da formulação lipossomal. Um dos aspetos-chave para o desenvolvimento desta formulação lipossomal com quercetina é saber a proporção ideal de quercetina para lípido a ser usada para a preparação da referida formulação. Isto visa permitir à formulação ter a quantidade adequada de quercetina incorporada, de forma a ter o melhor efeito terapêutico possível, sem haver desperdício de

fármaco. Para tal, foi realizada uma curva de saturação da incorporação de quercetina na matriz lipídica dos lipossomas. Os resultados obtidos desta curva de saturação indicaram que a proporção molar ideal de quercetina e lípido a ser usada era de 1:10 (mol/mol). Em seguida, os efeitos da quercetina livre e da formulação lipossomal de quercetina foram comparados de forma a estudar os efeitos de cada forma de quercetina contra a toxicidade e o *stress* oxidativo causado pela rotenona, em células C6 de glioma de rato, usando ensaios de MTT e Citometria de Fluxo, respetivamente. Como descrito anteriormente, o *stress* oxidativo é considerado uma das marcas-chave da Lesão por Isquemia e Reperfusão Hepática e este processo pode ser induzido *in vitro* com recurso à rotenona. A rotenona é um inibidor do Complexo I da cadeia respiratória mitocondrial que tem uma ação celular semelhante a alguns aspetos da Lesão por Isquemia e Reperfusão Hepática. Em relação aos ensaios de análise da viabilidade celular (ensaios de MTT), de acordo com um resultado preliminar, foi determinado que a viabilidade celular era analisada após 24 e 48 horas de incubação com rotenona, intervalos de tempo em que a rotenona causou um efeito na viabilidade celular. Com base neste resultado, para testar o efeito protetor de ambas as formas de quercetina, as células C6 foram pré-incubadas por 6 e 24 horas com as formas livre e lipossomal da quercetina, tendo sido analisada também a co-incubação da quercetina livre por 24 e 48 horas. Os resultados preliminares destas várias abordagens indicaram que nenhuma das formas da quercetina teve qualquer efeito protetor na viabilidade celular contra a toxicidade induzida pela rotenona. Para realizar os ensaios de análise do *stress* oxidativo (citometria de fluxo), foram usados dois tipos de marcadores para a análise, o DCF que reflete os níveis celulares de espécies reativas de oxigénio, de forma a avaliar o nível de *stress* oxidativo, e o DAPI, um marcador para avaliar a viabilidade celular. De acordo com um resultado preliminar, foi determinado que o *stress* oxidativo era analisado após 4 e 16 horas de incubação com rotenona, intervalos de tempo em que a rotenona não teve efeito na viabilidade celular. Isto foi depois confirmado durante os ensaios de citometria de fluxo para as 4 horas de incubação. De acordo com os resultados preliminares, ambas as formas da quercetina reduziram igualmente o *stress* oxidativo induzido pela rotenona.

Estes resultados preliminares sugerem que, *in vitro*, a quercetina pode ser uma boa opção de tratamento para condições médicas que envolvam o *stress* oxidativo, como a Lesão por Isquemia e Reperfusão Hepática, e que a formulação lipossomal usada pode ser uma solução viável para a entrega da quercetina nas células. Para finalizar, estes resultados sugerem que a formulação lipossomal desenvolvida com quercetina pode ser considerado como um possível tratamento farmacológico para a Lesão por Isquemia e Reperfusão Hepática. No entanto, existem algumas questões a ponderar sobre o modelo celular *in vitro* usado, pois não reflete a totalidade do processo da Lesão por Isquemia e Reperfusão Hepática, refletindo mais a parte da Isquemia. Para além do mais que neste modelo celular, não são refletidos os mecanismos biológicos de remoção de compostos do organismo para a formulação lipossomal. Por essa razão, é necessário realizar estudos adicionais para avaliar se esta formulação lipossomal desenvolvida com quercetina pode ser um tratamento farmacológico viável para a Lesão por Isquemia e Reperfusão Hepática.

Palavras-Chave: Quercetina; Rotenona; *Stress* Oxidativo; Lipossomas; Lesão por Isquemia e Reperfusão Hepática.

INDEX

LIST OF TABLES

LIST OF FIGURES

LIST OF ABBREVIATURES

A

Acetyl-CoA – Acetyl Coenzyme A;
ADP – Adenosine Diphosphate;
ALP – Alkaline Phosphatase;
ALT – Alanine Amino-Transferase;
AMP – Adenosine Monophosphate;
AP-1 – Activator Protein 1;
$AscH^{\bullet}$ – Ascorbyl Radical;
$AscH_2$ – Ascorbic Acid;
AST – Aspartate Amino-Transferase;
ATP – Adenosine Triphosphate;

B

Bcl-2 – B-Cell Lymphoma-2;

C

Ca^{2+}-ATPase – P-Type Ca^{2+} Transporter;
cAMP – Cyclic Adenosine Monophosphate;
CBP – CREB-Binding Protein;
C/EBP – CCAAT/Enhancer-Binding Protein;
Cerebral IR – Cerebral Ischemia and Reperfusion;
Chol – Cholesterol;
Complex I – NADH:Ubiquinone Oxidoreductase;
Complex II – Succinate Dehydrogenase;
Complex III – Cytochrome bc_1 Complex;
Complex IV – Cytochrome c Oxidase;
Complex V – F_1F_0ATP Synthase;
COX-1 – Cyclooxygenase-1;
COX-2 – Cyclooxygenase-2;
CREB – CRE-Binding Protein;
Cyt C – Cytochrome C;
Cryo-TEM – Cryo-Transmission Electron Microscopy;

D

DAPI – 4',6-Diamidino-2-Phenylindole, Dihydrochloride;
DCF – 2',7'-Dichlorofluorescein;
$DCFH_2$-DA – 2′,7′-Dichlorodihydrofluorescin Diacetate;
d_H – Particle Hydrodynamic Diameter;
DLS – Dynamic Light Scattering;
DMEM – Dulbecco's Modified Eagle Medium;
DMSO – Dimethyl Sulfoxide;
DNA – Deoxyribonucleic Acid;
DSPE – 1,2-Distearoyl-Sn-Glycero-3-Phosphoethanolamine;
DSPE-PEG2000 – N-(Carbonyl-Methoxypolyethylene Glycol-2000)-1,2-Distearoyl-sn-Glycero-3-Phosphoethanolamine;

E
EGCG – Epigallocatechin Gallate;
eNOS – Endothelial Nitric Oxide Synthase;

F
Fe-S Clusters – Iron-Sulfur Clusters;
*f(*k*a)* – Henry's Function;
FMN – Flavin Mononucleotide;

G
G1 – Correlation Function of the Dynamic Light Scattering Technique;
GSH – Reduced Form of Glutathione;
GSSG – Oxidized Form of Glutathione;

H
H_2O_2 – Hydrogen Peroxide;
Hepatic IR – Hepatic Ischemia and Reperfusion;
Hepatic IRI – Hepatic Ischemia and Reperfusion Injury;
$HO^{\bullet}$ – Hydroxyl Radical;
HOCl – Hypochlorous Acid;
HPLC – High-Pressure Liquid Chromatography;
Hypothermic MP – Hypothermic Mechanical Perfusion;
Hypothermic Oxygenated MP – Hypothermic Oxygenated Mechanical Perfusion;

I
ICAM-1 – Intercellular Adhesion Molecule-1;
IE/EE – Incorporation/Encapsulation Efficiency;
IκB – NF-κB Inhibitory Protein;
IKK – IκB Kinase;
IL-1 – Interleukin 1;
IL-1β – Interleukin 1 Beta;
IL-6 – Interleukin 6;
IL-8 – Interleukin 8;
IL-12 – Interleukin 12;
iNOS – Inducible Nitric Oxide Synthase;
IPost – Ischemic Postconditioning;
IPre – Ischemic Preconditioning;
IR – Ischemia and Reperfusion;
IV – Intravenous;

K
k*a* – Ratio between Particle Radius and Electric Double Layer Thickness;

L
L_d – Fluid, Liquid-Disordered Phase of the Lipid Bilayer;
L_o – Fluid, Liquid-Ordered Phase of the Lipid Bilayer;
LTB_4 – Leukotriene B4;
LTC_4 – Leukotriene C4;

M

M3 – Mixed Mode Measurement;
M3-PALS – Mixed Mode Measurement – Phase Analysis Light Scattering;
MAPK – Mitogen-Activated Protein Kinase;
MCP-1 – Monocyte Chemoattractant Protein-1;
MP – Mechanical Perfusion;
MPTP – Mitochondrial Permeability Transition Pore;
mRNA – Messenger Ribonucleic Acid;
MTT – 3-(4,5-Dimethylthiazol-2-yl)-2,5-Diphenyl Tetrazolium Bromide;

N

Na^+/K^+-ATPase – Na^+/K^+-Exchanging ATPase;
NAD^+ – Oxidized Form of Nicotinamide Adenine Dinucleotide;
NADH – Reduced Form of Nicotinamide Adenine Dinucleotide;
NADPH – Dihydronicotinamide-Adenine Dinucleotide Phosphate;
NF-κB – Nuclear Factor Kappa B;
$NO^{\bullet}$ – Nitric Oxide;
Normothermic MP – Normothermic Mechanical Perfusion;
NP – Nanoparticle;
NPs – Nanoparticles;

O

$O_2^{\bullet -}$ – Superoxide Radical;
$^1O_2$ – Singlet Oxygen;
o-dihydroxyl – Ortho-Dihydroxyl;
$ONOO^-$ – Peroxynitrite;

P

P_β – Ripple Phase of the Lipid Bilayer;
PALS – Phase Analysis Light Scattering;
PBS – Phosphate Buffer Solution;
PdI – Polydispersity Index;
PEG – Polyethylene Glycol;
PEG2000 – Polyethylene Glycol with a Molecular Weight of 2000 Da;
PGE_2 – Prostaglandin E2;

Q

Q – Ubiquinone;
QH_2 – Ubiquinol;
Q:L – Quercetin-to-Lipid;

R

RNA – Ribonucleic Acid;
RNS – Radical Nitrogen Species;
$ROO^{\bullet}$ – Peroxyl Radical;
ROS – Radical Oxygen Species;

S

S_o – Gel, Solid-Ordered Phase of the Lipid Bilayer;
SPC – Soybean Phosphatidylcholine;
STAT3 – Signal Transducer and Activator of Transcription 3;

T

T_m – Lipid Bilayer's Main Phase Transition Temperature;
TNF-α – Tumor Necrosis Factor Alpha;

U

U_E – Electrophoretic Mobility;
UV – Ultraviolet;

Z

Z-average – Mean Hydrodynamic Diameter;

#

5-HETE – 5-Hydroxyeicosatetraenoic Acid;
5-HPETE – 5-Hydroperoxyeicosatetraenoic Acid;
5-LOX – 5-Lipoxygenase;

Others

$[Compound]_I$ – Initial Compound Concentration (Before Liposomal Preparation);
$[Compound]_F$ – Final Compound Concentration (After Liposomal Preparation);
$[Lipid]_I$ – Initial Lipid Concentration (Before Liposomal Preparation);
$[Lipid]_F$ – Final Lipid Concentration (After Liposomal Preparation);

1. INTRODUCTION

1.1. Ischemia and Reperfusion and Hepatic Ischemia and Reperfusion:

1.1.1. General Concepts and Mechanisms:

Ischemia and Reperfusion (IR) is a common clinical phenomenon that can affect a variety of organs such as the brain (e.g., stroke), the heart (e.g., myocardial infarction) and the liver (e.g., liver resection), among others, and is one of the main sources of morbidity and mortality for humans [1, 2]. The medical condition that can be developed as a consequence of IR can lead to other clinical disorders [2]. Such conditions can be triggered by organ transplant, hypotensive shock, cerebrovascular diseases (e.g., aneurism), or peripheral vascular disease [1, 3, 4].

Hepatic IR is the above-mentioned medical condition specific to the liver and is a common and sometimes unavoidable event during hepatic surgery (e.g., liver transplantation) [1, 5-10]. Unlike IR in other possible organs (e.g., Cerebral IR), the occurrence of Hepatic IR is very commonly predicted because it is mainly caused by programmed medical interventions. Most surgical interventions in the liver involve an ischemic period after which the blood flow must be restored and, consequently, the injuries associated with this medical condition (Hepatic Ischemia and Reperfusion Injury – Hepatic IRI) are the main cause of liver dysfunction or post-operation functional failure and a cause of mortality, morbidity and low recovery of liver function [1, 5-7, 10-15].

Ischemia is defined as the interruption of blood flow into the organ, causing a reduction in the oxygen and nutrient supplies and ultimately resulting in cell damage. Reperfusion is defined as the reestablishment of the blood flow after ischemia [3, 7, 16]. Counterintuitively, reperfusion causes an increase in cell damage and death, as a result of the harm caused by the ischemic situation and microcirculation failure [2-5, 7, 8, 11, 14, 16]. This additional damage further complicates the patient's clinical situation, which was already unstable due to the original medical condition [2, 14, 16].

From a molecular point of view, Hepatic IRI can be divided into two phases. Initially, the interruption of oxygen supply to the liver provokes the halt of the mitochondrial respiratory chain, stopping the production of adenosine triphosphate (ATP) from this pathway [5, 17, 18]. The lack of nutrient supply derived from ischemia causes the cell metabolism to switch from aerobic to anaerobic, resulting in an abrupt reduction in ATP production and an increase in lactic acid formation (Figure 1.1) [5, 10, 17, 18]. These modifications result in cellular acidosis as well as a gradual halt of the ATP-dependent cellular metabolic activities (Figure 1.1) [5, 18]. Meanwhile, to maintain normal cell function, the existing ATP continues to be used, being converted to adenosine diphosphate (ADP), then to adenosine monophosphate (AMP) and lastly converted in successive steps to hypoxanthine (Figure 1.2), which accumulates in the liver [3, 19]. This results in an intracellular ATP depletion which causes an imbalance in ionic transport by interrupting the activity of Na^+/K^+ and Ca^{2+}-ATPases and an increase in cyclic adenosine monophosphate (cAMP) levels, a second messenger that signals nutrient deficiency [3, 5, 10, 17, 18]. The halt of the Na^+/K^+-ATPase activity increases the intracellular Na^+ levels, causing an increase in water entrance to maintain cell homeostasis [3, 18]. This water influx results in cellular swelling, triggering serious damage to hepatocytes (Figure 1.1) [11, 18]. The deregulation of intracellular Na^+ levels is exacerbated by cellular acidosis that causes an increase in intracellular H^+ concentration, which has to leave the cell via Na^+/H^+ exchanger, causing Na^+ to be further imported by the cell (Figure 1.1) [18]. Also, the levels of intracellular Ca^{2+} concentration increase due to the increase in the Na^+/Ca^{2+} exchanger function caused by the increase in the intracellular Na^+ levels and to the halt of the Ca^{2+}-ATPase activity (Figure 1.1) [3, 18].

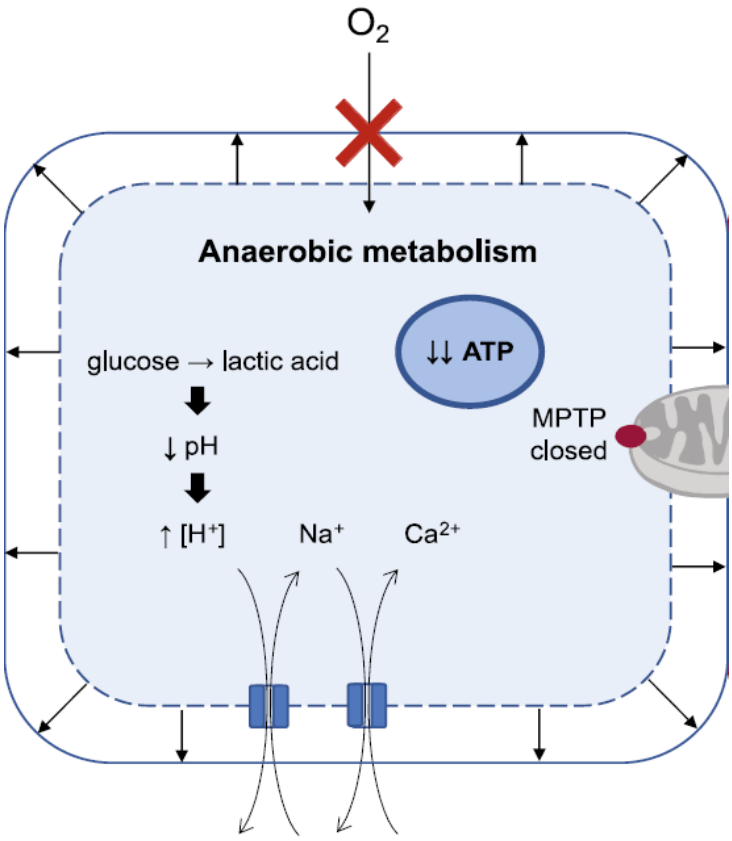

Figure 1.1 – **Ischemic Phase Outline of Hepatic Ischemia and Reperfusion Injury.** The interruption of the oxygen supply by ischemia causes the decrease in intracellular ATP levels and the alteration of the cell metabolism from aerobic to anaerobic, which causes an increase in lactic acid production. These modifications decrease the cellular pH and alter the intracellular ion homeostasis (H^+, Na^+ and Ca^{2+}), resulting in cellular acidosis and cellular swelling. Adapted from [11].

Ca^{2+} overload activates Ca^{2+}-dependent proteases (e.g., calpains) which degrade various types of cellular proteins such as cytoskeleton-associated proteins, leading to cell damage [3, 5, 18, 20]. The activation of calpains induces the conversion of xanthine dehydrogenase, one of the interconvertible forms of xanthine oxidoreductase, to xanthine oxidase, another form of the enzyme (Figure 1.2) [3, 19]. This change of activity is then involved in future steps of this cascade of events (Figure 1.2) [3, 19]. An increase in cAMP levels causes an alteration of the regulation of the phosphorylation of enzymes involved in carbohydrate metabolism. This alteration leads to an increase in the levels of acidic metabolites (e.g., ketone bodies), increasing the levels of metabolic acidosis, which can block the signaling interactions of the cell, homeostasis and mitochondrial damage [5, 17]. These ionic alterations and ATP depletion can cause microcirculation failure and cell death, as circulation issues are especially relevant since reperfusion cannot reach the liver tissue homogeneously, resulting in some areas having a complete lack of blood flow [5, 8, 10]. Also, it can induce dysfunctional responses in the cell (e.g., mitochondrial dysfunction), activating stress responses (e.g., endoplasmic reticulum stress response) and pathways, blocking the synthesis of new proteins [10, 18].

After the restoration of blood flow during the reperfusion process, the sudden excess of oxygen and nutrients triggers a cascade of events that includes the recruitment of immune cells, the generation of radical oxygen species (ROS) and radical nitrogen species (RNS), and the release of pro-inflammatory cytokines, chemokines and adhesion molecules [3, 15, 18]. These phenomena lead to the activation of the innate immune response and subsequently, to inflammation and oxidative stress, the hallmarks of Hepatic IRI [3, 10, 15]. This cascade of events can be divided into two different phases, the initial and the late phase of reperfusion [3, 6-8, 10, 21, 22]. The initial phase (1 to 2 hours after reperfusion) is marked mainly by the activation of Kupffer cells (resident liver macrophages) [18] and the production

of ROS and RNS [6-8, 10, 21, 22]. With the restoration of oxygen supply, the hypoxanthine accumulated during ischemia reacts with O_2 via xanthine oxidase to produce superoxide radicals ($O_2^{\bullet-}$) (Figure 1.2) [3, 10, 19].

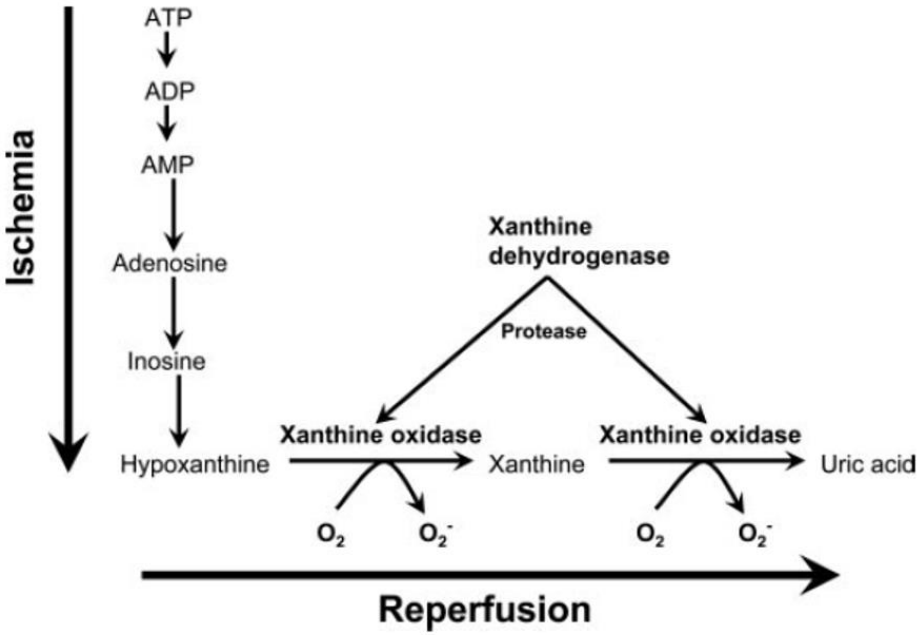

Figure 1.2 – **ATP Degradation Mechanism during Ischemia and Beginning of ROS Production during Reperfusion.** For cells to maintain normal cell function during ischemia, ATP is still used and converted in successive steps to hypoxanthine, which accumulates in the liver. At the same time, the conversion of xanthine dehydrogenase to xanthine oxidase via calpains (Ca^{2+}-dependent protease) occurs. Reperfusion of the liver causes the accumulated hypoxanthine to react via xanthine oxidase with O_2 to produce $O_2^{\bullet-}$, triggering the ROS production start. Adapted from [19].

$O_2^{\bullet-}$ can be converted enzymatically via superoxide dismutase to O_2 and hydrogen peroxide (H_2O_2) and, if it is not removed, H_2O_2 can be reduced via transition metal ions (e.g., Fe^{2+}; Fenton reaction) to form hydroxyl radicals ($HO^{\bullet}$) (Figure 1.3) [8, 19, 23, 24]. The production of these ROS induces cell damage via oxidative stress such as protein oxidation, DNA damage, or lipid peroxidation, in which lipid peroxidation promotes the formation of peroxyl radicals ($ROO^{\bullet}$) (Figure 1.3) [5, 15, 18, 21].

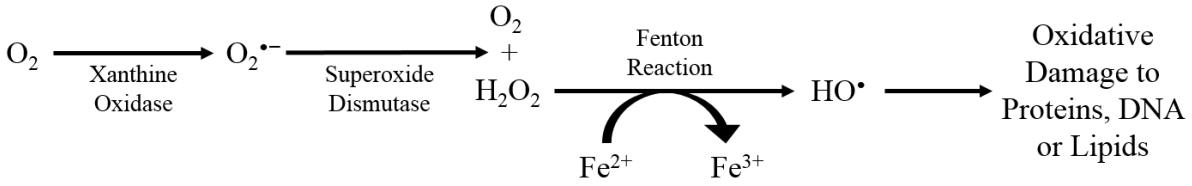

Figure 1.3 – **ROS Production Cascade and Cellular Effects.** After liver reperfusion, the enzymatic reaction between the accumulated hypoxanthine and O_2 via xanthine oxidase produces $O_2^{\bullet-}$, which subsequently can be converted to O_2 and H_2O_2. In the presence of transition metal ions such as Fe^{3+}, H_2O_2 can be reduced to $HO^{\bullet}$, triggering oxidative cell damage to proteins, DNA, or lipids [5, 8, 15, 18, 19, 21, 23, 24].

Alongside a concomitant Ca^{2+} overload caused by ischemia and the reversion of the cellular acidosis, ROS production can lead to mitochondrial dysfunction, causing the formation of a mitochondrial permeability transition pore (MPTP), leading to an increase in ATP depletion and cell death (Figure 1.4) [10, 11, 18, 25]. ROS production can also activate Kupffer cells (Figure 1.4) [10, 22]. These activated cells can also induce an increase in ROS levels via NADPH oxidase formation of $O_2^{\bullet-}$, which increases oxidative stress levels, resulting in an increase in cell damage [3, 5, 10, 17, 18, 26]. Concomitantly, activated Kupffer cells also produce pro-inflammatory cytokines, such as tumor necrosis factor alpha (TNF-α), interleukin 1 beta (IL-1β) and

interleukin 6 (IL-6), all of which activate the inflammatory response (Figure 1.4) [3, 7, 8, 15, 17, 18, 21, 25]. In normal situations, a countermeasure for this is the constitutive production of small quantities of nitric oxide ($NO^{\bullet}$) by the endothelial nitric oxide synthase (eNOS) in the liver [5, 15, 18, 27]. However, $NO^{\bullet}$ can be produced in larger quantities in stress situations via inducible nitric oxide synthase (iNOS) and react with $O_2^{\bullet-}$, forming the very reactive peroxynitrite ($ONOO^-$) [4, 18, 23, 27]. RNS production can also induce cell damage, worsening the effects of Hepatic IRI [18, 27]. Activation of Kupffer cells also leads to the production of chemokines [e.g., monocyte chemoattractant protein-1 (MCP-1)] and the activation of the expression of adhesion molecules [e.g., intercellular adhesion molecule-1 (ICAM-1)] [3, 5, 7, 8, 10, 17, 18, 22, 25]. Chemokines and adhesion molecules promote the recruitment, adhesion and extravasation of neutrophils to the liver, the hallmark of the late phase of reperfusion (6 and 48 hours after reperfusion) [3, 7, 8, 21]. The recruitment of neutrophils causes the release of proteases via neutrophil degranulation, which is the exocytosis of granules from neutrophils, causing also cell damage and the release of oxidants via NADPH oxidase activation by contact between neutrophils and hepatocytes (Figure 1.4). This release of oxidants consists of the additional formation of a cascade of ROS molecules, resulting in mitochondrial dysfunction, leading to higher levels of cell damage to the liver (Figure 1.4) [3, 5, 7 10, 21]. The increase in cell damage alongside ROS production increase – which increases the activation of Kupffer cells – induces the exacerbation of the inflammatory response (Figure 1.4), increasing over time the cell injury [22].

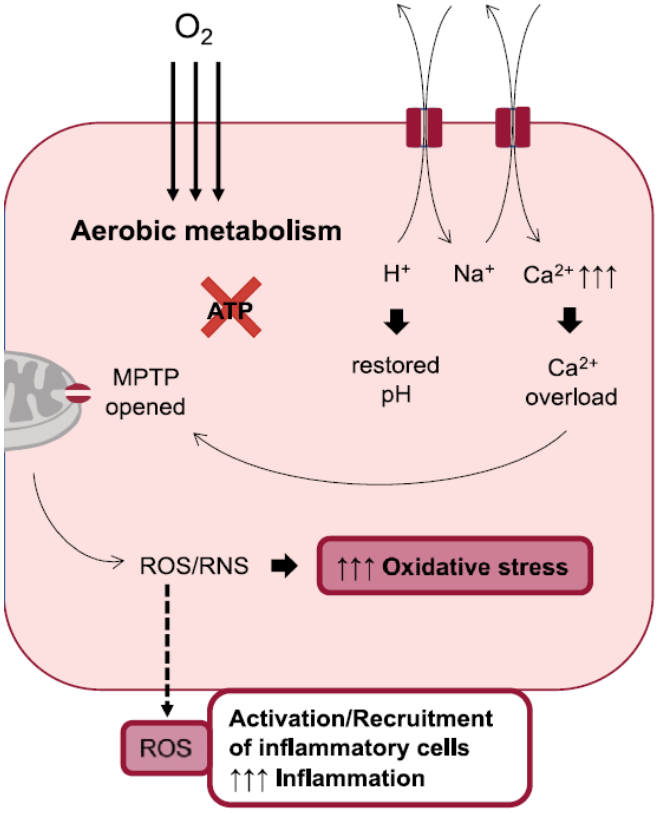

Figure 1.4 – **Reperfusion Phase Outline of Hepatic Ischemia and Reperfusion Injury.** The reestablishment of oxygen supply causes the cell metabolism to revert to aerobic, which reverts the cellular acidosis. However, this promotes the Ca^{2+} import, overloading the Ca^{2+} levels, resulting in mitochondrial permeability transition pore opening. Reperfusion promotes also ROS and RNS production, increasing oxidative stress and cell damage. ROS can lead to the activation of Kupffer cells and the subsequent neutrophil recruitment, inducing and promoting the inflammatory response. Adapted from [11].

1.1.2. Rotenone-Induced Oxidative Stress has Parallelisms with Hepatic Ischemia and Reperfusion Injury:

Oxidative stress is one of the hallmarks of Hepatic IRI [3, 15] and it can be induced *in vitro* by inhibiting the mitochondrial respiratory chain (Figure 1.5). The mitochondrial respiratory chain is a part of the oxidative phosphorylation system which produces ATP [28, 29]. Each mitochondrion is formed by two membranes, an outer membrane that encloses the organelle and an inner membrane that surrounds the matrix, which folds into itself, resulting in the formation of cristae. These cristae contain the oxidative phosphorylation system [28-31]. This system is comprised of five protein complexes, NADH:Ubiquinone Oxidoreductase (Complex I), Succinate Dehydrogenase (Complex II), Cytochrome bc_1 Complex (Complex III), Cytochrome c Oxidase (Complex IV) and F_1F_0ATP Synthase (Complex V), with Complex V not being part of the mitochondrial respiratory chain (Figure 1.5) [28, 30, 31]. First, glucose is converted into pyruvate in the glycolytic pathway and pyruvate is then converted to acetyl coenzyme A (acetyl-CoA) via pyruvate dehydrogenase. Acetyl-CoA enters the citric acid cycle in the mitochondrial matrix, where it promotes the conversion of NAD^+ to NADH [29, 32]. NADH is then oxidized by Complex I to NAD^+, which can return to the citric acid cycle to continue its function, transferring its electrons to ubiquinone and thus reducing it to ubiquinol (Figure 1.5). Alongside, Complex II catalyzes the oxidation of succinate to fumarate and these electrons are transferred to ubiquinone, complementing ubiquinol production (Figure 1.5). The generated ubiquinol is transferred to Complex III, where it is oxidized back to ubiquinone, transferring its electrons to cytochrome c (Figure 1.5). Cytochrome c is then transferred to Complex IV and here, cytochrome c transfers its electrons to O_2, the final electron acceptor, generating H_2O (Figure 1.5) [28, 29, 31]. At the same time, each electron transfer process in Complexes I, III and IV result in proton transport to the mitochondrial inner membrane space (Figure 1.5). This transport generates a proton electrochemical gradient that causes the protons to pass through Complex V to the mitochondrial matrix, transferring the electrochemical gradient to Complex V. This transfer allows for a conformation alteration of part of Complex V, allowing the phosphorylation of ADP to ATP, which is released to supply energy to the cells (Figure 1.5) [28, 31, 33, 34].

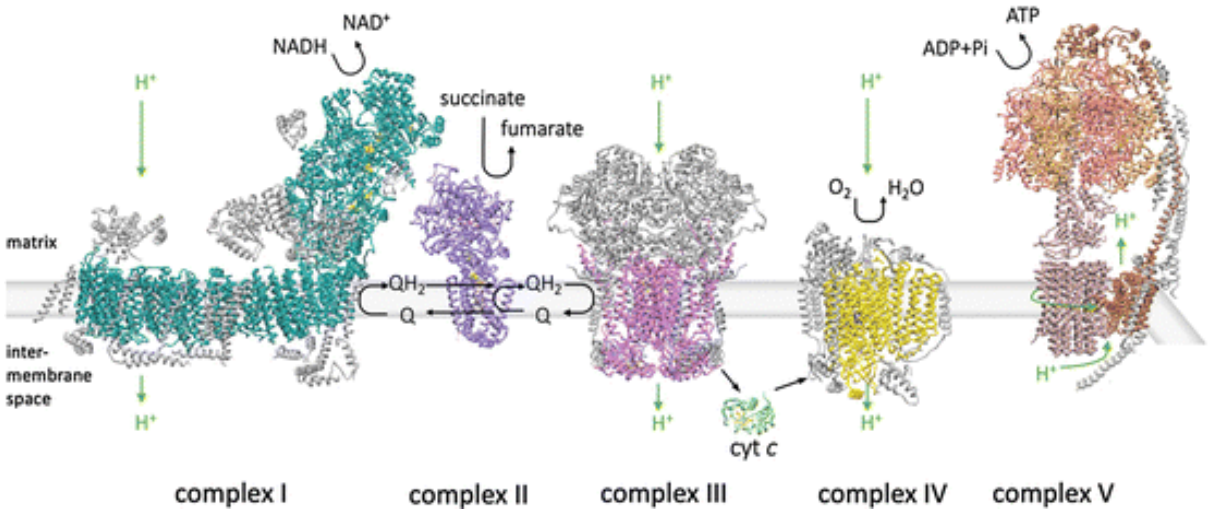

Figure 1.5 – **Oxidative Phosphorylation System Schematic.** Representation of the Oxidative Phosphorylation System composed of the Mitochondrial Respiratory Chain (Complexes I-IV) associated with ATP Synthase (Complex V). Adapted from [28].

Rotenone ($C_{23}H_{22}O_6$) is a natural lipophilic molecule that derives from the roots, stems, bark, leaves and seeds of certain plant species (*Lonchocarpus* and *Derris* species), which inhibits Complex I of the mitochondrial respiratory chain (Figure 1.6) [35-40].

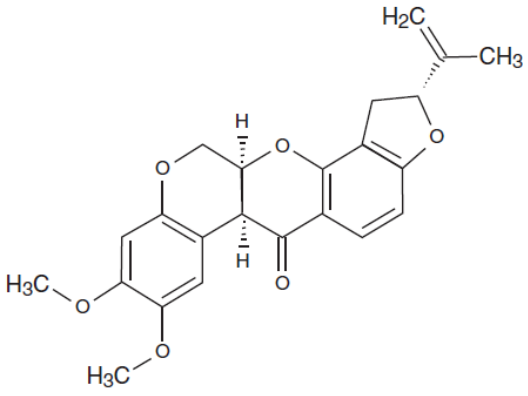

Figure 1.6 – **Rotenone's Chemical Structure.** Retrieved from [35].

After the citric acid cycle, in Complex I, NADH interacts with a flavin mononucleotide (FMN) at the top of this Complex, transferring its electrons to FMN. FMN electrons are then transferred along Complex I through a series of seven iron-sulfur clusters (Fe-S clusters) to the ubiquinone, reducing it to ubiquinol [28, 29, 31]. Rotenone blocks the ubiquinone binding site and the subsequent transfer of electrons from the Fe-S clusters to ubiquinone [35-37, 41]. This interrupts the electron flow needed for the oxidative phosphorylation process, causing a decrease in ATP production [36].

Comparing the mechanism behind Rotenone-Induced Oxidative Stress and Hepatic IRI, it is possible to draw some parallelisms. In both situations, the mitochondrial respiratory chain is blocked, reducing ATP production. In Hepatic IRI, the lack of oxygen supply caused by ischemia causes the halt of Complex IV [42], while rotenone blocks Complex I [36, 39, 43, 44]. With the mitochondrial respiratory chain blocked by rotenone, the free electrons are released and can react with O_2, triggering ROS formation and causing cell damage [39, 43, 45, 46]. ROS production is also observed during the initial phase of reperfusion in Hepatic IRI when accumulated hypoxanthine formed during ischemia reacts with O_2 via xanthine oxidase to produce $O_2^{\bullet-}$ [3, 10, 19, 23]. As mentioned before, Ca^{2+} overload and calpain activation are commonly found in Hepatic IRI [3, 5, 10, 18, 19]. These alterations are also seen during rotenone treatment. For example, differentiated SH-SY5Y human neuroblastoma cells treated with rotenone display a significant increase in free Ca^{2+} levels and μ-calpain activation [47]. The activation of calpains by rotenone is also observed in rat retinal cell cultures [43]. The production of pro-inflammatory cytokines such as TNF-α, IL-1β and IL-6 is one of the central features of Hepatic IRI [3, 7, 17, 18, 21, 25]. For example, mitochondria from rat brain cells exposed to rotenone display a significant increase in the levels of TNF-α, IL-1β and IL-6 [44]. In a stress situation such as Hepatic IRI, the production of $NO^{\bullet}$ via iNOS is increased largely, causing the production of RNS, worsening the effects of Hepatic IRI [4, 18, 23, 27]. This effect on $NO^{\bullet}$ and iNOS levels is also seen during rotenone treatment, such as in mitochondria from rat brain cells supplemented with rotenone, which displays a significant increase in these levels [44]. A protective shield against oxidative stress is glutathione, an antioxidant, which in a stress situation such as Hepatic IRI, the reduced form of glutathione (GSH) levels are drained [48, 49]. This significant GSH decrease is also seen during rotenone treatment, such as in mitochondria from rat brain cells supplemented with rotenone [44].

1.2. Current Treatments for Hepatic Ischemia and Reperfusion Injury:

There are many known and unknown variables that can influence the medical outcome of existing treatments/interventions for Hepatic IRI, such as the ambiguity of the time window to administer the treatment and the duration and severity of ischemia, among others [11-13, 25, 50, 51]. For this reason, presently, there is no standard treatment strategy for preventing or treating the effects of Hepatic IRI. The current treatments can improve the damage provoked by the pathology but new treatment approaches in a real attempt to address this medical condition are being developed [11, 50, 51]. The available treatments can be divided into physical or pharmacological approaches [11].

The physical approach includes treatments related to ischemic preconditioning (IPre), ischemic postconditioning (IPost) and mechanical perfusion (MP). In the IPre option, the liver is subjected to a shorter period of ischemia (5 to 15 minutes) and then to a longer period of reperfusion (10 to 20 minutes), or cycles of alternate periods of ischemia and reperfusion, before exposing the organ to a large ischemic period [12, 18, 25, 50, 52]. This approach produces lower oxidative stress in hepatocytes, allowing cells to adapt to the ischemic situation and promoting cell survival [18, 25]. IPost consists of subjecting the liver to short periods of regulated reperfusion right after the ischemic situation and before the reperfusion step [15, 18, 53, 54]. IPost allows for treatments after injury, in contrast with the preventive IPre approach [18]. IPre and IPost share the same mechanistic basis but IPost avoids the removal of endogenous protective compounds during total reperfusion [15, 18]. Although IPre and IPost are promising in humans, their beneficial effects on long-term patient morbidity and mortality are unclear, especially because it is difficult to identify *a priori* which are the optimal patients that can receive these treatments. This is because there are many variables that can influence the treatment outcome such as the liver condition severity, the patient's age and the ischemic duration [18, 50, 52, 54]. While IPre and IPost are associated with the interruption of blood flow to the liver, MP maintains the blood flow *ex vivo*. MP allows the liver to endure a longer period outside the organism, avoiding ischemia and the associated tissue damage [14, 55]. This is possible to achieve via two MP techniques, Hypothermic and Normothermic. Hypothermic MP uses cold temperatures (between 8 °C and 12 °C) to store the organ and reduce damage, needing a specific circulation fluid to maintain normal liver function. This circulation fluid can be more or less oxygenated, as seen in Hypothermic Oxygenated MP, which can combat hypoxia, improving Hepatic IRI damages [18]. On the other hand, Normothermic MP tries to imitate the liver's natural conditions, using only a diluted, hyperbaric oxygenated blood-based perfusate with the appropriate nutrients as circulation fluid. This method reduces the possible damage caused by hypothermia and possible hypoxia typical of Hypothermic MP [14, 18, 55].

The pharmacological approach includes a variety of compounds that can act on various targets of Hepatic IRI such as ROS or inflammation, for example [3, 5, 11, 17]. Various antioxidants have been identified as possible treatments for Hepatic IRI, such as melatonin and ascorbic acid [5]. Melatonin, an endogenous hormone produced in the brain, is reported to act as a ROS scavenger and by inducing the expression of antioxidant enzymes in the organism (e.g., superoxide dismutase), also being linked to ATP production maintenance and stabilization of mitochondrial function [5, 18, 27, 56, 57]. Melatonin shows promising preclinical results but still needs to be tested in patients [27]. Ascorbic Acid (Vitamin C) acts as a ROS scavenger, generally decreasing oxidative stress, but it can have the opposite effect at higher doses [5, 17]. A low dose of ascorbic acid can cause a decrease or a normalization of Hepatic IRI biomarkers (e.g., hepatocellular necrosis) *in vivo*. However, a 10-30 times higher dose worsens Hepatic IRI [21, 58]. This is because ascorbic acid can reduce metal ions (e.g., Fe^{3+} to Fe^{2+}), causing the production of $HO^{\bullet}$ radical by the Fenton reaction (Figure 1.7) [8, 19, 21, 23, 24, 59].

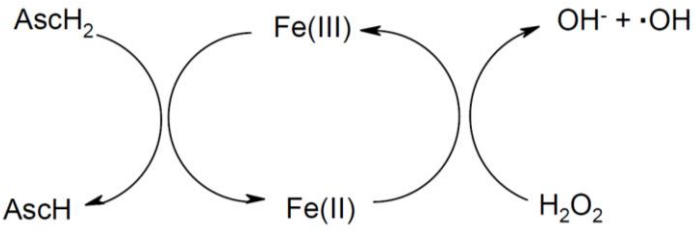

Figure 1.7 – **Countereffect of using Ascorbic Acid as a Hepatic IRI Pharmacological Treatment.** In higher doses, the therapeutic effect of ascorbic acid disappears because ascorbic acid can reduce Fe^{3+} to Fe^{2+}, forming a radical molecule. Fe^{2+} can then, according to the Fenton reaction, convert H_2O_2 to $HO^{\bullet}$, causing cell damage. Adapted from [59].

Immunosuppressors are commonly given as a treatment to ameliorate the consequences of Hepatic IRI [11]. For example, methylprednisolone is a synthetic corticosteroid that can reduce the production of pro-inflammatory cytokines TNF-α and IL-1β, among other molecules. This corticosteroid also decreases intracellular Ca^{2+} concentration, inhibiting calpain activation [20, 60, 61]. However, corticosteroids are rapidly cleared from the system, forcing their administration at higher doses to compensate for clearance, but producing harmful side effects (e.g., hypertension) [11, 62, 63]. Several compounds extracted from plants have also been tested to treat Hepatic IRI. For example, resveratrol has antioxidant properties, which act as a ROS scavenger, reducing oxidative stress but there are still some issues with its bioavailability and a possible prooxidative effect [5, 21, 26].

1.3. Quercetin as a Possible Treatment for Hepatic Ischemia and Reperfusion Injury:

1.3.1. Description of Quercetin:

A good example of the above-mentioned compounds extracted from plants is quercetin (3,3',4',5,7-pentahydroxyflavone), a flavonol (one of the six subclasses of flavonoids), that is usually found in the human diet (e.g., onions, berries, apples, grapes and tea) (Figure 1.8) [64-70].

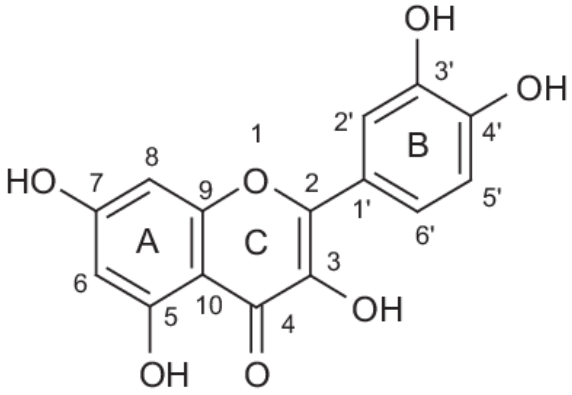

Figure 1.8 – **Quercetin's Chemical Structure.** Retrieved from [71].

Quercetin presents a yellow bright coloration and is poorly soluble in aqueous solutions but is soluble in organic solutions (e.g., alcohols) [68]. This molecule is an aglycone, a type of molecule without any linked sugar molecules. However, quercetin can also be found as a sugar-conjugated compound – quercetin glycosides – linked to a sugar molecule (e.g., glucose and galactose) via one of the hydroxyl groups, generally in position 3. This conjugation modifies quercetin's solubility, increasing its water solubility, and absorption in the intestinal tract, as different conjugations cause different absorption rates. For example, quercetin glucosides are better absorbed than quercetin rutinosides [64, 67-69]. Examples of quercetin glycosides are isoquercetin, which is quercetin conjugated with a glucose molecule in position 3, and rutin, which is quercetin conjugated with a

rutinose molecule in position 3 [67, 69]. Quercetin glycosides are the predominant form of quercetin in nature. For example, in a shallot, 99,2% is associated with the glycosylated forms and 0,8% with the aglycone form. In contrast, the aglycone form is the predominant one in nutritional supplements [64, 67]. Quercetin is considered to be one of the most universal compounds in plants and one of the most abundant flavonoids in the human diet [64, 67-69]. The estimated intake of flavonoids in a normal diet variates from country to country, ranging from 50 to 800 mg/day, being 60% to 75% associated with quercetin and its glycosylated forms [67-69]. Quercetin usually exists at low concentrations in plants (15 to 330 mg/kg), existing in other vegetables such as onions in higher concentrations (284 to 486 mg/kg) [69]. For supplement purposes, quercetin intake can go up to 1000 mg (usually 500 mg) [64] but oral doses of 150 mg/day are enough to increase quercetin's blood levels and have effects on humans [67].

1.3.2. Quercetin's Properties:

Quercetin has antioxidant, anti-inflammatory, antiaggregatory, anti-fibrotic, anti-allergic, immune-protective and anticarcinogenic properties and it is currently under study for the treatment of several diseases such as respiratory allergic diseases, cardiovascular diseases and cancer prevention, among others [64-66, 69, 70, 72-74].

When quercetin reacts with damaging molecules, it reduces their harmful effects, but this reaction converts quercetin into a radical [23]. The chemical structure of quercetin has three main features: the existence of the *o*-dihydroxyl group in positions 3' and 4' in the B ring; the conjugated system between the B ring and the oxo group in position 4 of the C ring via 2,3 double bond; and the existence of two hydroxyl groups between the oxo group in the B ring (Figure 1.9) [23]. These characteristics combined allow for an electron delocalization around quercetin's structure, creating a more stable radical molecule [23, 69]. This is the reason why quercetin is indicated as an efficient scavenger, with good antioxidant activity, being proposed to confer protection when the organism is under oxidative stress [23, 67, 69, 70].

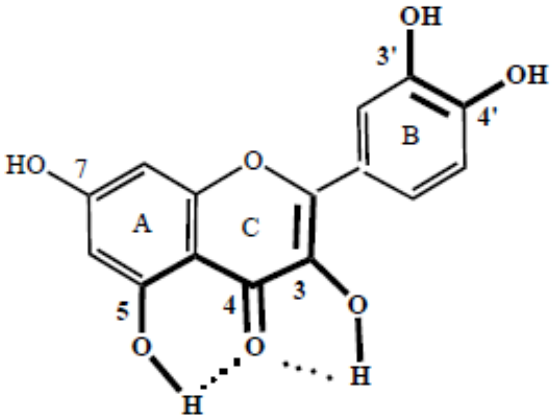

Figure 1.9 – **Quercetin's Main Features to be considered as an efficient Scavenger.** The reason behind quercetin being considered an efficient scavenger is derived from three main characteristics of quercetin's chemical structure: the existence of the o-dihydroxyl group in positions 3' and 4' in the B ring; the conjugated system between the B ring and the oxo group in position 4 of the C ring via 2,3 double bond; and the existence of two hydroxyl groups between the oxo group in the B ring. Retrieved from [23].

Quercetin is demonstrated to have antioxidant activity against hypochlorous acid (HOCl), singlet oxygen ($^1O_2$), $ONOO^-$ and $HO^\bullet$ production by transition metal ions (Fenton reaction, Figure 1.3), preventing the propagation of oxidative chain reactions [23, 67]. HOCl is formed by Cl^- oxidation of H_2O_2, catalyzed by myeloperoxidase, a hydrogen peroxide oxidoreductase found in granulocytes

(e.g., neutrophils and monocytes) [16, 75]. HOCl can react with quercetin, chlorinating it in positions 6 and 8 of the A ring, forming stable molecules [23, 75]. $^1O_2$ can be produced by peroxidases (e.g., myeloperoxidase), lipoxygenases, or as a subproduct of lipid peroxidation. $^1O_2$ can react with quercetin via hydroxyl group in position 3 and with the double bond between positions 2 and 3 of the C ring [23]. Quercetin inhibits $HO^{\bullet}$ production by chelating transition metals, such as Fe^{3+} and Cu^{2+}, by means of the hydroxyl and oxo groups in positions 3', 4' (B ring), 3, 4 and 5 (A and C ring). However, quercetin can also have indirect pro-oxidant activity by reducing iron (Fe^{3+} to Fe^{2+}) and copper (Cu^{2+} to Cu^{+}), producing more $HO^{\bullet}$ via Fenton reaction, similar to ascorbic acid (Figure 1.7), increasing oxidative stress [23, 75]. In rats, a long-term quercetin diet increased the levels of α-tocopherol, one of the Vitamin E forms and inhibitor of oxidative chain reactions [76], in the liver and serum [75]. This increase was observed concomitantly with a decrease in the concentration of malondialdehyde, a lipid peroxidation product [4].

Associated with the antioxidant activity, quercetin is also described as an anti-inflammatory compound. Anti-inflammatory effects of quercetin include the modulation of cytokine production (e.g., TNF-α) via the arachidonic acid metabolic cascade [e.g., cyclooxygenase-2 (COX-2)] and the regulation of gene expression (e.g., TNF-α mRNA), among others (Figure 1.10) [23, 68].

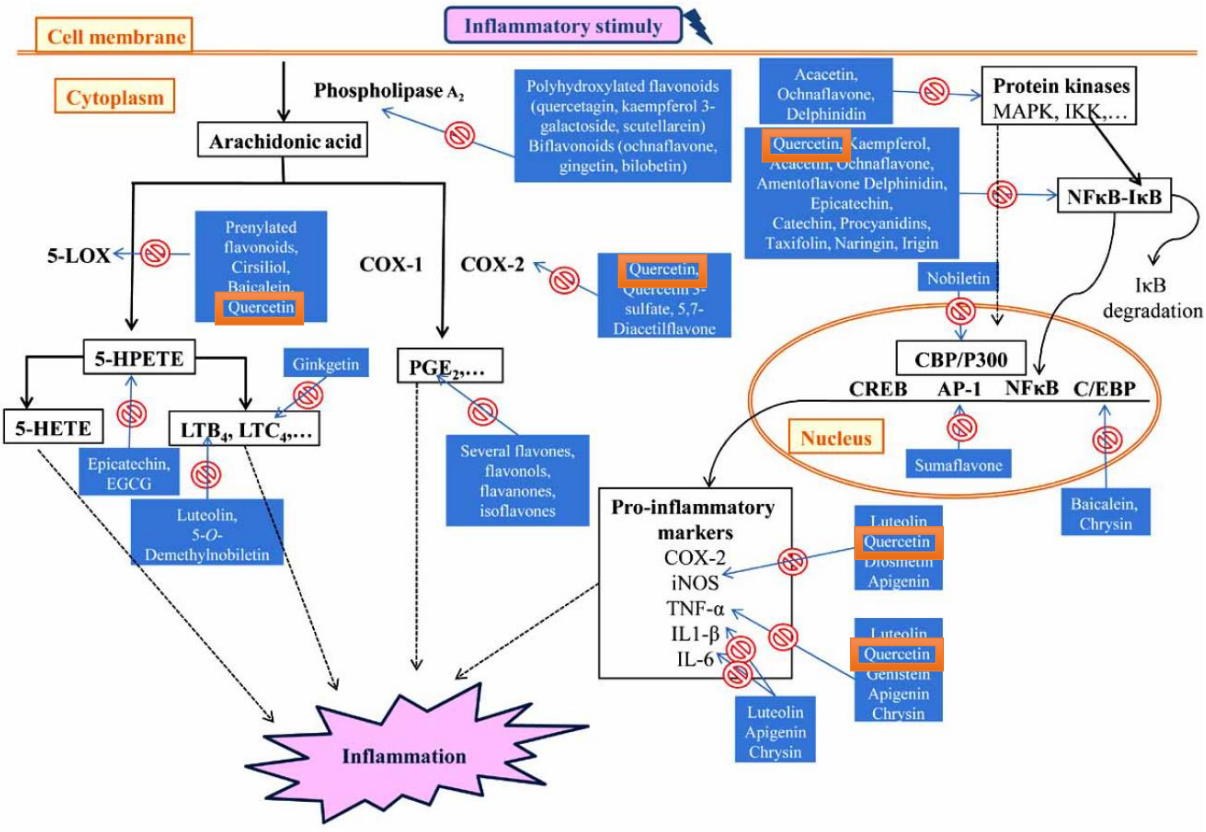

Figure 1.10 – **Flavonoid Modulation Targets of the Inflammatory Response Cascade.** After an inflammatory stimulus, the inflammatory response cascade is activated, dividing into two sections, the arachidonic acid metabolic cascade and the regulation of transcription factors, both leading to inflammation. Each part of this cascade is possible to modulate via a flavonoid, in order to reduce inflammation. In the orange squares, it is possible to observe where quercetin can modulate the inflammatory response cascade. Adapted from [23].

Quercetin suppresses lipopolysaccharide-induced TNF-α production in mouse macrophages and interleukin 8 (IL-8) in lung cells [23]. Quercetin also decreases the expression levels of iNOS and $NO^{\bullet}$ production, both involved in the inflammatory cascade [67, 68, 77]. Quercetin inhibits COX-2 expression and activity, and 5-lipoxygenase (5-LOX) activity, blocking the arachidonic acid inflammatory cascade [23]. Also, quercetin inhibits interleukin 1 (IL-1)-stimulated IL-6 production

and secretion in mast cells, and blocks the interleukin 12 (IL-12)-induced tyrosine phosphorylation of signal transducer and activator of transcription 3 (STAT3) in activated T cells, decreasing their proliferation [68]. Quercetin also inhibits TNF-α and IL-1 mRNA production in microglia, reducing neuronal cell death induced by microglial activation [68]. Quercetin inhibits the transcription factor NF-κB, an effect that can be connected with the inhibition of COX-2 and iNOS expression and activity, as both genes are regulated by NF-κB [23]. These anti-inflammatory effects are also observed *in vivo*. When quercetin is administered to obese rats, there is a reduction in TNF-α and $NO^{\bullet}$ production and in the expression of iNOS [23, 67, 69]. In a rat model of spinal cord injury, an intraperitoneal quercetin administration led to the recovery of more than half of the rats. However, higher quercetin concentrations blocked every animal from recovery [67, 69]. In humans, the anti-inflammatory actions of quercetin have some ambivalent results with the same oral quercetin administration [67, 69].

The administration of quercetin *in vitro* can alter the sensitizing effect and it suppresses histamine release by mast cells and basophils, suggesting anti-allergic properties [67, 69]. In guinea pigs and rat models for asthma, oral administration of quercetin reduced the levels of neutrophils and extravasation to lung cells, decreasing inflammation [67]. Also, quercetin could have anti-anaphylactic effects, as demonstrated in animal models. This is not confirmed in humans, but isoquercitin reduced ocular but not respiratory symptoms of anaphylaxis [67]. Quercetin can have anticarcinogenic properties by means of antioxidant, antiproliferative, pro-apoptotic and cell signaling mechanisms *in vitro* and *in vivo* [67]. Quercetin can reboot drug resistance and boost the efficiency of certain chemotherapeutic agents (e.g., daunomycin) and there is a correlation between administration of quercetin and reduction in cancer risk and cancer size in humans [67, 78].

In a rat model of Hepatic IRI *in vivo*, quercetin induced a decrease in liver enzymes [e.g., alanine amino-transferase (ALT), aspartate amino-transferase (AST) and alkaline phosphatase (ALP)], oxidative stress, inflammatory cytokines and on liver tissue damage, among others [5]. Quercetin reduced significantly the levels of GSH, superoxide dismutase and catalase, an enzyme that assists in the reduction of H_2O_2 to water and O_2 [79], but not significantly malondialdehyde [4]. Quercetin also reduced significantly the expression levels of TNF-α and NF-κB and increased significantly the levels of B-cell lymphoma-2 (Bcl-2), a protein involved in the inhibition of apoptosis [4, 80]. Additionally, quercetin was shown to reduce the levels of cell damage and the dilation of the liver blood sinusoids [4].

1.3.3. Quercetin's Bioavailability, Toxicity and Safety:

Quercetin has a low bioavailability in humans, which is approximately 2% of the oral intake. Even when injected into the blood circulation, quercetin has a low cell availability in humans as it is quickly metabolized in the body and secreted [67, 68, 72, 73, 81-84].

For humans, there is no systematic data on quercetin toxicity and safety as a nutraceutical and the existing studies were performed for short periods of administration and with low dosages. As a supplement, quercetin may aggravate adverse effects in pre-damaged kidneys and, with higher doses, some patients started to suffer headaches and a mild tingling of the extremities after each dose [64]. In rat and cell systems, the studies about quercetin toxicity and safety present points of concern that can be a warning for its use in humans [64]. However, these points are not completely reproducible, existing other studies that do not have these issues [66]. In *in vitro* studies in bacterial and eukaryotic cell systems, quercetin caused mutations, chromosomal aberrations, breaks in single-stranded DNA and the formation of micronuclei, among others, but these effects were not confirmed *in vivo* [64, 66].

In vitro studies in human cancer cells from a variety of tissues and organs (e.g., pancreas and colon) demonstrated that quercetin inhibits cell growth. However, this was not confirmed *in vivo*, where quercetin can enhance tumor growth in certain conditions [64]. When quercetin is administered orally in medium or high doses to rats, there is a variety of negative effects: reduction in body weight, increase in the relative organ weight such as the kidney and the liver, increase in polyp quantity, parathyroid hyperplasia (only in males) and appearance of calcium oxalate crystals in the urine. They also present a type of yellow-brown coloration in the glandular stomach and the small intestine, possibly caused by the coloration of quercetin or one of its metabolites [64, 66]. In male rats, quercetin can increase chronic progressive nephropathy, renal hyperplasia and renal tumors and also can cause sperm abnormalities. In female rats, quercetin can reduce offspring quantity [64, 66]. This outcome disparity comes also due to the different quercetin doses used in the studies and the analyzed time windows [64, 66].

Quercetin is also shown to interact with other compounds used for treatments, which can alter the bioavailability or the effect of those compounds [64, 67]. One example is digoxin, a drug used in cardiac treatments such as heart failure [67, 85]. In a pig model, quercetin administered jointly with digoxin resulted in the death of two of three pigs after 30 minutes of treatment. A lower dose of quercetin did not produce deadly effects but increased the maximum serum digoxin concentration by 413% [86].

1.3.4. How to Overcome Quercetin's Administration Problems?

In summary, the administration of quercetin raises numerous red flags, from its low solubility in physiological medium, low bioavailability, drug interactions and concerns in toxicity and safety for humans, all of which make the use of quercetin in humans a potential risk [64, 66-68, 72, 81-84]. To overcome some of these issues, quercetin can be incorporated into a lipid drug delivery system to improve quercetin's solubility and avoid the liver clearance barrier, improving quercetin's circulation time and therefore, reaching the intended target in a higher concentration. With the use of liposomal formulations, it is possible to improve quercetin's pharmacokinetic profile [81, 83, 87].

1.4. Liposomal Formulations:

1.4.1. Description:

Liposomes are spherical vesicles composed of one or more concentric lipid bilayers organized forming an aqueous core and they are one example of nanoparticles (NPs), alongside polymeric NPs, micelles, dendrimers and carbon-based NPs, among others [87-93]. These vesicles are formed via self-assembly of specific lipid molecules (e.g., phospholipids) in an aqueous medium [88, 90, 93]. Since the liposome is composed of an aqueous core surrounded by a lipid bilayer, hydrophilic compounds can be encapsulated in the aqueous core and hydrophobic compounds can be incorporated into the lipid bilayer (Figure 1.11) [87-89, 91-94]. Depending on their purpose, the surface of the liposomes can be bioconjugated with other molecules (e.g., antibodies or peptides) for active targeting, or some hydrophilic molecules [e.g., polyethylene glycol (PEG)] can be inserted into their surface to confer stealth properties (Figure 1.11). These strategies can increase liposome circulation time and improve the compound's pharmacokinetic profile, allowing compound delivery to the target site, which creates new possibilities for pharmacological treatments [87, 88]. Liposomes are considered to be biocompatible, biodegradable, non-toxic and non-immunogenic, lowering drug degradation and leading to a safer drug administration [87, 89, 91-93, 95]. Also, liposomes can improve drug

pharmacokinetic profiles, facilitating the achievement of optimal concentrations and effectiveness [91, 96].

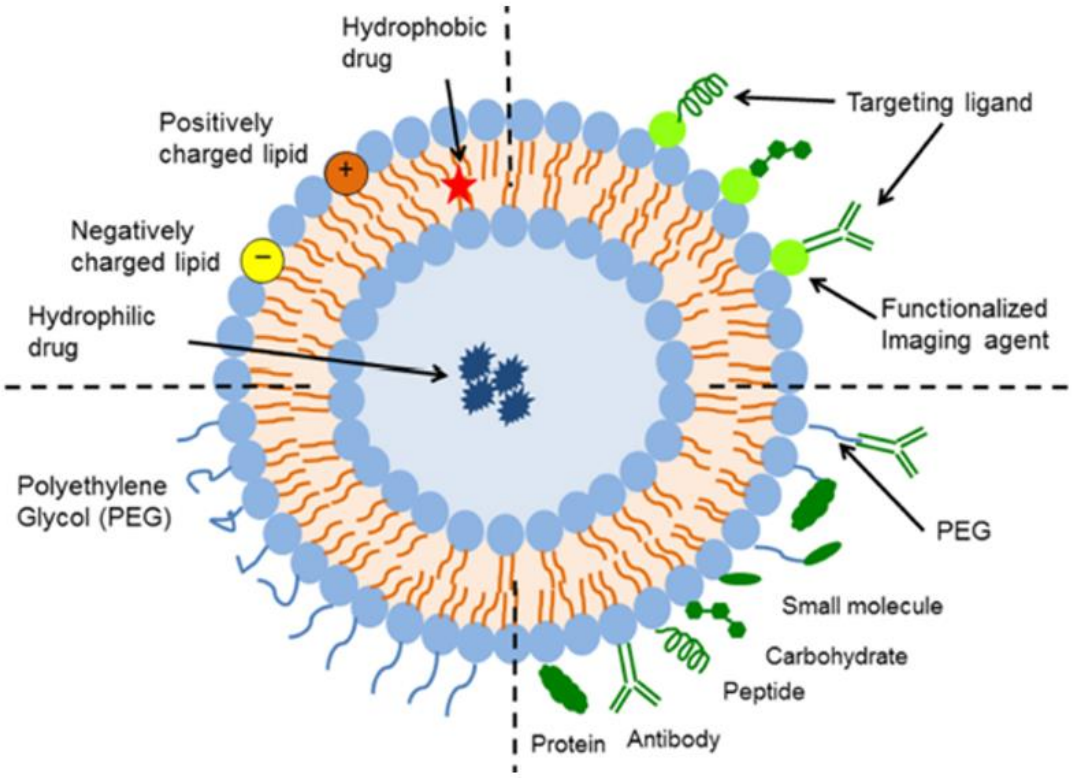

Figure 1.11 – **Liposomal Structure Schematization and Modification Possibilities.** Liposomes are vesicles made from a lipid bilayer that surrounds an aqueous core, which allows for the encapsulation of hydrophilic compounds in the aqueous core and the incorporation of hydrophobic compounds inside the lipid bilayer. Liposomes can be modified, from altering the phospholipid head group charge (cationic, anionic and neutral) to combining molecules to improve the liposomal function. For example, the use of modified lipids with PEG attached inhibits recognition from the organism's immune system. Lipids can be modified to attach also, with and without PEG or an imaging agent, other molecules such as proteins, antibodies, peptides, carbohydrates, or small molecules or imaging agents. Adapted from [92].

The discovery of liposomes is attributed to Doctor Alec Douglas Bangham [97-100]. During the beginning of the decade of 1960, Bangham observed that egg lectin, when in contact with water, rearranged itself in a vesicle structure [101]. This spontaneous assembly behavior of phospholipids into vesicles was referred to by Bangham as multilamellar smectic mesophases or, as named by Bangham, Banghasomes [97]. The first reference to liposomes comes from the work of Gerald Weissmann that describes them as microscopic vesicles made of one or more lipid bilayers [99, 100, 102]. Soon later, it was demonstrated that liposomes can entrap lysozymes inside their core [103, 104], which gave light to a new use for liposomes as enzyme or drug carriers for some therapies for storage diseases and ultimately for delivery into the organism [102, 103, 105]. Lastly, it was shown that when a drug is encapsulated into a liposome (e.g., actinomycin D), it can increase its efficiency compared to the free drug, extending the survival of animals, which opened up the gates for clinical use [102, 103, 106].

Currently, liposomes have many potential purposes that are in clinical trials or already approved to be commercialized, as they were the first NP system approved for clinical use [87, 89, 90]. Liposomes have a large array of possible uses: from models to study biomembranes [98, 107] to serve as a vehicle for delivery systems for cancer treatment, ocular disorder treatment, or vaccines, among others [87, 89, 90, 108-111]. For cancer treatment, one possibility is *Doxil*®, the first liposomal formulation approved to be released to the market, which is a doxorubicin-loaded liposomal formulation, a topoisomerase IIα inhibitor [87], with the therapeutic indication for cancer treatment (e.g., metastatic

ovarian cancer) [109]. For ocular disorders, a possible treatment that is commercialized is the use of *Visudyne*®, a verteporfin-loaded liposomal formulation, with the therapeutic indication for wet-age-related macular degeneration, a medical condition that is resulted from the growth of abnormal blood vessels that leak blood and fluids in the macula, causing loss of central vision [89, 108, 111]. Verteporfin is a photosensitizing agent that, when irradiated, releases ROS molecules into the abnormal blood vessels, causing them to close [89, 112]. One example of a liposomal-based vaccine is *Epaxal*®, based on virosomes, which are liposomes bioconjugated with viral particles, which in this case are the hepatitis A virus, neuraminidase and hemagglutinin, with the intent to prevent the organism against hepatitis A [89, 108, 110]. This liposomal formulation works by interacting with the immune system via neuraminidase and hemagglutinin, allowing for the hepatitis A virus to enter the macrophages in order to produce a protective response against this virus [110].

1.4.2. How to Characterize a Liposomal Formulation:

To characterize a liposomal formulation, it is fundamental to know several parameters that influence its therapeutic activity based on the physicochemical properties. These properties can influence the *in vivo* fate and targeting capabilities of this liposomal formulation [87, 93, 94]. These physicochemical properties include the (lipid) composition, the size, the polydispersity index, the zeta potential, the preparation method, the lamellarity and the incorporation/encapsulation efficiency.

1.4.2.1. Composition:

There are four main aspects to notice when analyzing the composition of a liposomal formulation: the lipid composition of the bilayer, the compound (drug) that uses the liposome as a vehicle and its localization in the liposome, the molecules (coating compounds, ligand-targeting moieties) that assist the liposome to perform its duty and the proportion (the molar ratio) between all these substances.

The base of the liposome structure is composed of one or more lipid bilayers and for this lipid bilayer to form, it is necessary to have a key element, phospholipids [87, 90]. Phospholipids are amphiphilic molecules composed of a glycerol molecule that is linked to a hydrophobic group composed of two acyl chains and also linked to a hydrophilic group composed of a phosphate group connected to a polar residue (e.g., choline). Phospholipids used to form the liposomal bilayers can be of natural or synthetic origin and, depending on the hydrophilic group charge, the liposomal surface charge can be neutral, cationic, or anionic [87, 93]. Phospholipids act as the key for the interaction between the drugs to be associated and the liposome for a better incorporation/encapsulation into the liposomes and determine how the way liposomes interact with cells [87, 90]. In this case, soybean phosphatidylcholine (SPC) is used in the lipid composition of the studied liposomal formulation, a phospholipid similar to phosphatidylcholine, one of the most abundant phospholipids in mammalian cell membranes [113]. The use of SPC allows for better interaction between liposomes and cells [114]. Associated with the phospholipids, cholesterol, a sterol molecule, can be used which can interact with the fatty acid chains of the phospholipids, fitting between the phospholipids [87, 115]. The sole use of phospholipids to form the lipid bilayer of the liposome permits the lipid bilayer to be in a ripple phase (Figure 1.12). This ripple phase is an intermediary phase between the gel, solid-ordered phase and the fluid, liquid-disordered phase, with the lipid bilayer alternating between these phases depending on the lipid bilayer's main phase transition temperature (Figure 1.12). In the gel, solid-ordered phase, the acyl chains of the phospholipids are completely extended, causing the phospholipids to be ordered tightly between them, resulting in the compactness and rigidity of the lipid bilayer. In the fluid, liquid-disordered phase, the acyl chains of the phospholipids are not as extended as before, resulting in a looser phospholipid organization in the membrane, resulting in a fluid membrane (Figure 1.12)

[115]. The addition of cholesterol to the lipid bilayer allows the bilayer to be in a fluid, liquid-ordered phase, a phase that conjugates both gel and fluid properties of the two previously described phases (Figure 1.12). Cholesterol acts in two forms: it can loosen the tight phospholipid organization in a rigid membrane, fluidifying this rigid lipid bilayer and it can organize tighter the loosen phospholipid organization of a fluid membrane, tightening this fluid lipid bilayer [115-117].

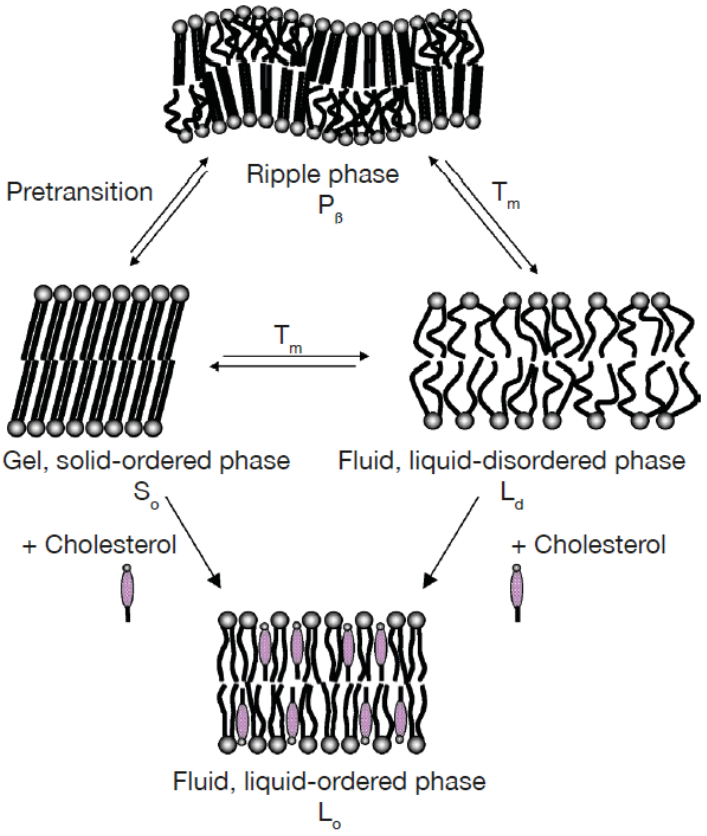

Figure 1.12 – **Relationship between the Different Bilayer Phases and the addition of Cholesterol.** A lipid bilayer composed only of phospholipids results in this bilayer being in a ripple phase, an intermediary phase between the gel, solid-ordered phase, marked by the rigidity of the membrane, and the fluid, liquid-disordered phase, marked by the fluidity of the membrane. These phases alternate between them depending on the lipid bilayer's main phase transition temperature. When cholesterol is added to this lipid bilayer, it switches to an extra phase, a fluid, liquid-ordered phase. This phase allows for the fluidity of rigid membranes and the rigidity of fluid membranes, conjugating here both gel and fluid properties of both gel and fluid phases. Removed from [115].

If the surface of the liposomal formulation is only composed of the head groups of the phospholipids, these liposomes are cleared rapidly from the bloodstream by the immune system, resulting in a low circulation residence time [87, 94, 118]. One of the solutions that can be used to overcome this problem is the use of certain molecules such as hydrophilic polymers, namely PEG [119] to coat the surface of the liposome (Figure 1.11) [87, 92-94, 118]. Due to the chemical structure and hydrophilia of PEG, it can interact with water, masking the liposome, which inhibits the liposome opsonization and destruction via the immune system, leading to an increase in the circulation time in the organism [87, 88, 92-95, 102, 120]. Usually, the coating with PEG is obtained by using the modified lipid [N-(carbonyl-methoxypolyethylene glycol-2000)-1,2-distearoyl-sn-glycero-3-phosphoethanolamine; DSPE-PEG2000], which is used in the lipid composition of the studied liposomal formulation. Furthermore, the use of PEG can also prevent aggregation between liposomes with a neutral surface charge, improving the stability of these liposomal formulations [95, 102, 120, 121]. Depending on the endpoint, PEG can be modified in terms of molecular weight [122]. In this case, it was used PEG with a molecular weight of 2000 Da (PEG2000) because it is considered the lowest molecular weight that

maintains the liposomal formulation distributed in the bloodstream without being removed from circulation by the organism's immune system [96]. However, it was described that, in some cases, the repeated administration of liposomes with PEG can induce the production of antibodies anti-PEG that, when injected again with a liposomal formulation with PEG, can activate the organism's immune response, clearing the liposomal formulation from the organism (Figure 1.13) [90, 92, 123].

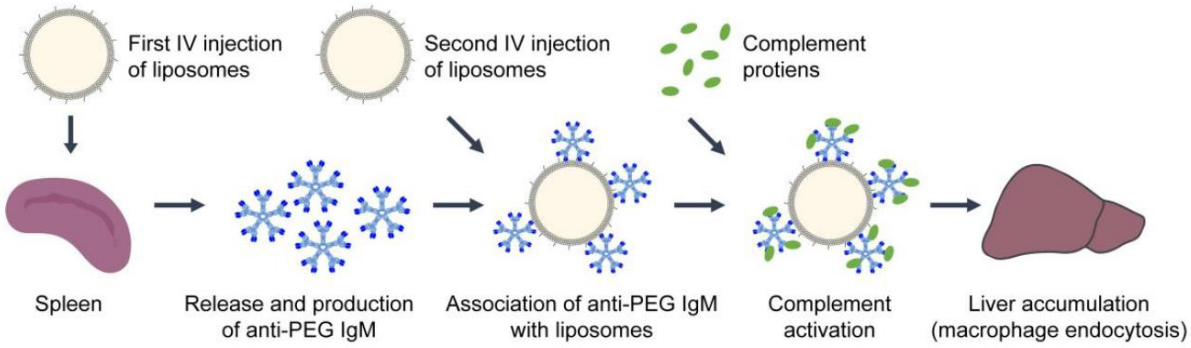

Figure 1.13 – **Triggering of the Immune Response with the repeated administration of a Liposomal Formulation with PEG.** One inconvenience of using PEG in a liposomal formulation is that, as these liposomes interact with the immune system, it can cause the production of anti-PEG antibodies (anti-PEG IgM) by B cells in the spleen and their release into the bloodstream. In the next administration of a liposomal formulation with PEG, PEG is recognized by the immune system, in which anti-PEG IgM are associated with the liposomes, triggering the immune response and the liposomal clearance from the organism. Retrieved from [90].

A solution designed to more specifically target the liposomes to sets of cells was its bioconjugation with other molecules such as antibodies, small molecules, or peptides (Figure 1.11). This allows for the direct targeting of specific cells, allowing for the liposomal formulation to release the drug in a specific cell, avoiding healthy tissues [93, 94, 120]. Ultimately, this strategy improves the drug's therapeutic effect and decreases the side effects [94].

1.4.2.2. Size and Polydispersity Index:

Two of the most relevant characteristics of a liposomal formulation are its size and its polydispersity index. Size can affect various biological factors such as drug pharmacokinetics, liposomal extravasation into tissues and liposomal clearance rate from the organism [87, 93]. Liposomes can present a diverse size assortment, from 60 nm to 100 μm, depending on the preparation method and their endpoint [87, 93, 122]. To determine the size of a liposomal formulation, it is used the measurement of the mean hydrodynamic diameter (Z-average), which corresponds to the mean value of the diameters of the correspondent spherical particles that have the same diffusion rate as the particles to be analyzed [124, 125]. The polydispersity index (PdI) corresponds to the degree of heterogeneity of the analyzed particle population, identifying the size distribution in a given particle population. This value is dimensionless, ranging between 0, which is the value for a homogeneous liposomal population, and 1, which is the value for a heterogeneous liposomal population [125, 126].

To measure these characteristics, it is commonly used the Dynamic Light Scattering (DLS) Technique [124]. In a given sample, there are particles of different sizes that are in suspension in an aqueous media. These particles are diffusing in this solvent, colliding randomly with the dispersant molecules and between each other, causing the particles to be in random movement, also described as Brownian motion. For each particle size, the diffusion rate is different because smaller particles have a higher diffusion rate and bigger particles have a lower diffusion rate and, by using the different diffusion rates, it is possible to calculate the particle size by using the Stokes-Einstein Equation (Equation 1.1: d_H – Particle Hydrodynamic Diameter; k – Boltzmann's Constant; T – Absolute Temperature; η – Viscosity of the Medium; D – Translational Diffusion Coefficient) [124, 125].

Equation 1.1 – $d_H = \frac{kT}{3\pi\eta D}$

When a laser crosses the sample, this laser interacts with the particles, modifying how the light from the laser arrives at a detector placed at an angle different than 90º from the laser source, causing a pattern of brighter and darker areas in the detector. As a result of these particles being in Brownian motion, this formed pattern of brighter and darker areas changes over time, causing light fluctuations that variate along time as a result of the random particle movement. This variation can be translated graphically along the time of analysis using a digital correlator. This digital correlation compares the difference in the light intensity of the formed pattern after a delay time, a small time interval, in order to produce a correlation relation along this delay time. This correlation is then quantified after each multiple of this delay time to a value between 0, which is no correlation, and 1, which is a perfect correlation, decreasing the correlation value over time. When this correlation value reaches 0, this correlation function can be used to calculate the particle size. The correlation variates depending on the particle size, as the correlation value decreases faster when analyzing smaller particles than bigger particles (Figure 1.14) [124, 125].

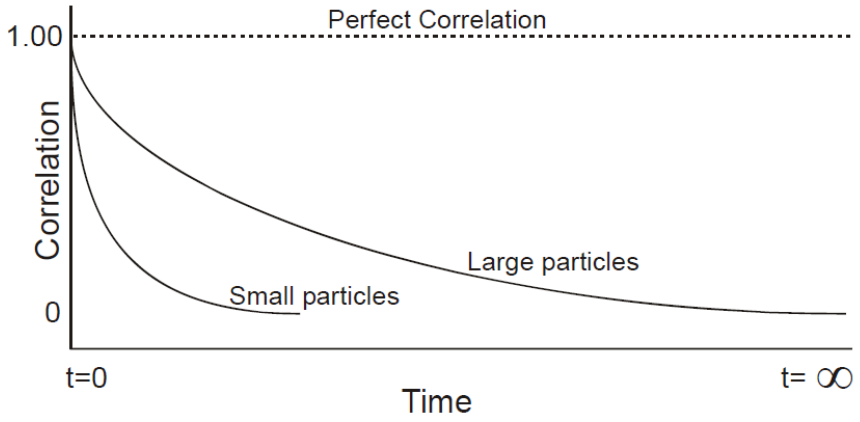

Figure 1.14 – **Correlation Function Graph of Different Size Particles.** When comparing the correlation relation of smaller and larger particles, it is possible to see that the correlation decay rate is higher for smaller particles than for larger particles. This is because, as the diffusion rate of particles depends on the particle size, smaller particles move quicker than larger particles. As particles move in different velocities, their correlation value is different, being reduced quicker in smaller particles than in larger particles, resulting in different correlation relation graphs. Retrieved from [124].

When analyzing a particle population, the function that is used is comprised of the sum of all the correlation functions of the various particles. In this case, the software behind the used device for this study (Zetasizer Nano S from Malvern Instruments) resorts to a cumulants analysis that fits the logarithm of the obtained correlation function (G1) to a single polynomial function (Equation 1.2: *t* – Delay Time) [124, 125].

Equation 1.2 – $ln(G1) = a + bt + ct^2 + dt^3 + \cdots$

This method only uses the values for the coefficients a, b and c, in which b corresponds to the value of D, which can be used in Equation 1.1 to determine the Z-average value, and the value of $2c/b^2$, which corresponds to the PdI value [124, 125].

1.4.2.3. Zeta Potential:

Consider a medium, at a specific pH, that contains various particles, each of which has an associated electric charge. For each particle, the existing ions in this suspension (e.g., from the solvent) have to rearrange themselves around these particles, resulting in the formation of an ion layer named the electric double layer. This electric double layer is made up of two layers: the Stern layer, constituted

of opposing charged ions that are firmly attached to the particle's surface, and a more diffused layer, made of various ions of diverse charges that are less attached to the particle [124, 126, 127]. When one particle moves, the ions in this second layer start to divide into two groups alongside a boundary called the slipping plane, in which the ions inside the boundary move with the particle and the ions outside this boundary do not follow said particle [127-129]. The electrostatic potential in this slipping plane corresponds to the Zeta Potential, which is represented in millivolts (Figure 1.15) [127, 129].

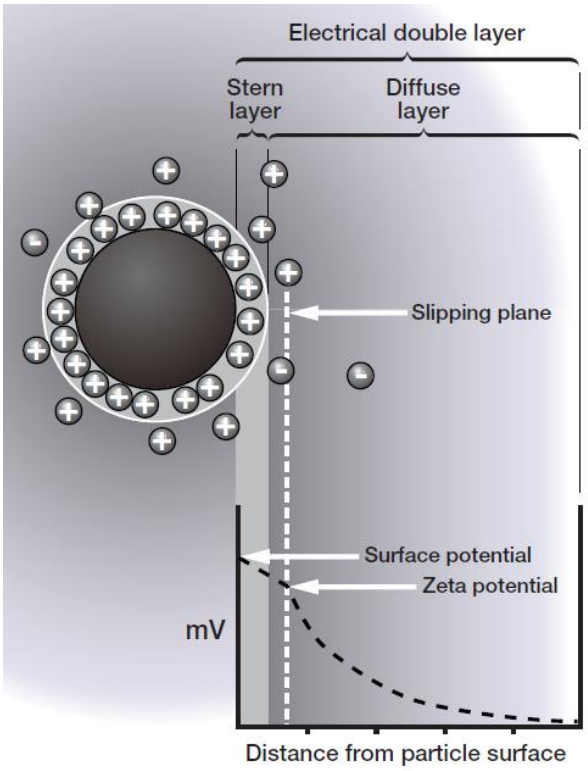

<u>Figure 1.15</u> – Electric Double Layer Representation around a Negatively Charged Particle and the Variation of the Electrostatic Potential *vs* the Distance from the Particle's Surface. Around this charged particle, the existing ions in the medium form an ion layer named the electric double layer which is composed of two different layers, the Stern layer and the Diffuse layer. When this particle moves, it creates an ion separation between two different layers within the Diffuse layer. The resulting border from this separation, known as the Slipping plane, is the point where the electrostatic potential is known as the zeta potential. Retrieved from [124].

Depending on their zeta potential value, particles can be classified into anionic (lower than – 30 mV), cationic (higher than 30 mV) and neutral (between – 10 mV and 10 mV) [93, 127, 129]. The zeta potential is a crucial characteristic because it predicts the stability of the liposomal formulation, as well as the interaction between liposomes and cells [128, 130, 131].

To measure the zeta potential value, it is normally used the Mixed Mode Measurement – Phase Analysis Light Scattering (M3-PALS) Technique [124]. As the zeta potential measurement is based on the electric charge from particles, this measurement needs to be made with a capillary cell that has, at each end, an electrode. When an electric current is applied to the system, it is created an electrical field inside the cell, which causes the particles to move to the opposite charge electrode. By analyzing the diffusion velocity of these particles and by knowing the electric field strength, it is possible to obtain the electrophoretic mobility value (U_E) [124, 125]. With this value, it is possible to obtain the mean zeta potential value by applying Henry's Equation (Equation 1.3: ζ – Zeta Potential Value; ε – Dielectric Constant; η – Viscosity of the Medium; $f(ka)$ – Henry's Function; ka – Ratio between particle radius and the thickness of the electric double layer) [124, 127, 129].

<u>Equation 1.3</u> – $U_E = \frac{2\varepsilon\zeta f(ka)}{3\eta}$

During the application of an electric field to the system, the sample is irradiated with a laser which, due to the Brownian motion of these particles, the light from the laser is shifted and it arrives at a detector placed at a specific angle from the laser source. The applied electric field is switched rapidly various times, creating fluctuations in the intensity of the scattering light during the time of analysis. By combining this information with the information from a reference laser, it is possible to obtain a representation of the phase shift along the time of analysis (Figure 1.16). With this representation, it is possible to obtain the mean of the slopes of the phase difference along the time of analysis, resulting in the mean U_E value [124, 125].

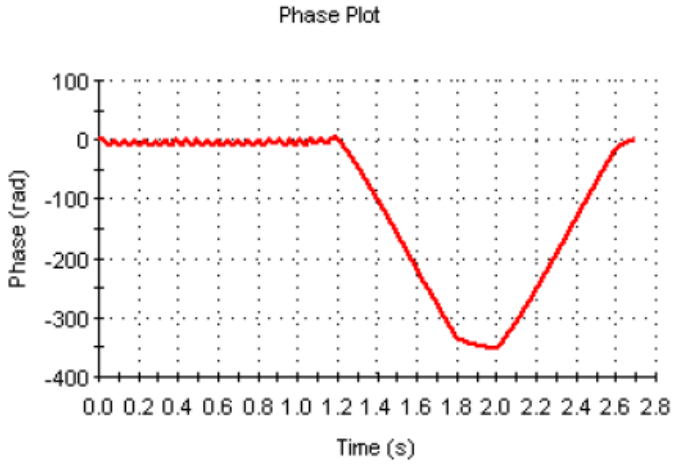

Figure 1.16 – **Phase Plot Example.** By comparing the information from the phase shift of the sample with the one from a reference beam, it is possible to obtain a phase plot. This phase plot is then the base to calculate the U_E value, by using the mean value of the various slopes in the plot, that is needed to calculate the zeta potential. Retrieved from [125].

This method has some issues because it is needed to be done in a specific place in the cell where the electroosmotic flow of the sample and the one induced externally are canceled. By using the M3 Technique, it is also performed a measurement where the electric field is switched slowly to obtain a better resolution, allowing for the measurement to be made at any point in the cell [124]. With this approach, it is possible to achieve the zeta potential distribution which, due to various factors (e.g., particle sedimentation), can be broader than supposed [124] and that is why the zeta potential values have a standard deviation of around 10% which in neutral particles can be around 5 mV.

1.4.2.4. Preparation Method:

The workflow to prepare a liposomal formulation is divided into four sections: choice and measurement of the raw materials, liposomal formation, purification/removal of the non-associated drug and analysis of the final liposomal formulation.

A variety of methods can be used to prepare a liposomal formulation, with the strategy being selected depending on the base conditions, such as the hydrophobicity/hydrophilicity of the base compound. An example of a preparation method is the Thin Film Hydration Method [97]. This method involves dissolving a lipid mixture with an organic solvent (e.g., chloroform, ethanol) and then, by organic solvent evaporation, the lipid mixture forms a lipidic film. Then, this lipid film is resuspended with an aqueous solution and, as explained before, the lipid mixture constitutes self-assemble into liposomes. Using this technique, if the compound to analyze is hydrophobic, it is added alongside the organic solvent and if the compound is hydrophilic, it is added alongside the aqueous solution. This method results in a suspension containing liposomes with a wide size range and some compound molecules that were not encapsulated/incorporated within the liposome [132, 133]. With the aim to reduce and homogenize the obtained sizes, the liposomal formulation can be extruded through a specific

membrane, usually a polycarbonate filter, with a predetermined pore size [132, 134]. If the liposomes are larger than these pores, they deform until the liposomal membrane breaks and reseals into smaller liposomes [135]. This liposomal formulation is passed then, through these membranes various times, reducing membrane pore size in each cycle, until the average size and polydispersity index are the desired ones [134, 135]. The final result is a suspension containing liposomes with homogeneous size [134]. In order to remove the compound molecules that were not encapsulated/incorporated into the liposome, a step of separation must be added. For example, a size-exclusion chromatography can be used if the free compound is smaller than the liposomes. Here, as the liposomes are out of the range of the gel beads, they are eluted in the void-volume, and on other hand, the free compound is retained in the column. This results in a liposomal formulation without the non-associated compound [136-138]. After the liposomal formulation purification, it is needed to analyze the liposomal formulation to know its physical and chemical parameters as well as the formulation stability [133].

1.4.2.5. Lamellarity:

The liposomal formulation preparation can, for example, result in the preparation of liposomes constituted with various concentric lipid bilayers or, in some cases, smaller liposomes within larger liposomes [139]. To analyze the liposomal internal organization, one characteristic used is Lamellarity, which corresponds to the number of concentric lipid bilayers inside a liposome [93, 140, 141]. This is one important characteristic because it can influence, for example, the compound percentage incorporated/encapsulated into the liposome, or the liposomal stability [91, 140, 141]. To measure this characteristic, one of the possible techniques to use is the Cryo-Transmission Electron Microscopy (Cryo-TEM) which allows to analyze the structure of the liposomal population and see the number of bilayers in a liposome [142].

1.4.2.6. Incorporation/Encapsulation Efficiency:

Depending on the liposomal properties (e.g., size), the used preparation method for the liposomal formulation, or the compound's properties (e.g., hydrophilicity), compounds are incorporated or encapsulated into a liposome in different amounts [91, 121, 143]. The dose of a drug is a critical parameter for an efficient treatment. If it is used a lower dose than the therapeutic one, the liposomal drug has a minimal or a non-therapeutic effect. However, if the used dose is higher, toxic effects can be observed. It is crucial to determine the exact drug amount that is associated with the liposomal formulation. To obtain the pretended dose in the final liposomal preparation, the initial conditions should be optimized. In order to adequate the preparation conditions to achieve the best liposomal formulation, the parameters of Incorporation/Encapsulation Efficiency (IE/EE) are used [91, 121]. IE/EE corresponds to the molar ratio between the concentration of the incorporated/encapsulated compound and the concentration of the compound added during the liposomal formulation preparation, normalized to liposomal lipid concentration [91, 144]. To calculate this characteristic, it is used the following equation (Equation 1.4: $[Compound]_I$ – Initial Compound Concentration (before liposomal preparation); $[Lipid]_I$ – Initial Lipid Concentration (before liposomal preparation); $[Compound]_F$ – Final Compound Concentration (after liposomal preparation); $[Lipid]_F$ – Final Lipid Concentration (after liposomal preparation)).

$$\textbf{Equation 1.4} - IE/EE = \frac{\frac{[Compound]_F}{[Lipid]_F}}{\frac{[Compound]_I}{[Lipid]_I}} \times 100\ (\%)$$

To measure IE/EE, it is needed to resort to two types of quantifications, lipid quantification and compound quantification, which are performed at the beginning and the end of the liposomal

formulation preparation. A possible technique to use for the lipid quantification is the Rouser's Method [145], which is based on the spectrophotometry determination of inorganic phosphorus in the sample. In this method, the liposomal sample suffers acid digestion with perchloric acid, which converts phosphate into inorganic phosphate. Then, inorganic phosphate reacts with ammonium molybdate, forming a complex between phosphate and molybdate. In the presence of ascorbic acid, this complex turns blue, which can be analyzed via spectrophotometry to determine the concentration of inorganic phosphorus in a sample. One possibility for compound quantification is to use the High-Pressure Liquid Chromatography (HPLC) Technique. For this technique, the liposomes have to be destroyed and the lipids solubilized, for example, in methanol. After this, the samples are injected into the HPLC device, and it is possible to see the elution profile of the solution. Knowing in advance at what time the compound is going to be eluted, it is possible to know at what peak corresponds to the compound and, by using a calibration curve, quantifying the concentration of the compound in the liposome [91].

1.4.3. Liposomal Targeting Properties:

When the liposomal formulation is administered to the organism, the formulation has to travel from the administration site to the target cells to deliver the incorporated/encapsulated drugs to have a therapeutic effect. For this, certain molecules (e.g, PEG, antibodies) can be associated with the liposomes in order to assist liposomes in targeting the intended target cells. To choose the adequate molecules to use for each situation, it is required to choose the adequate targeting strategy, which can be between the passive targeting strategy and the active targeting strategy (Figure 1.17 and 1.18) [120, 121].

The passive targeting strategy conjugates the target cells' characteristics (e.g., blood vessel's permeability) with the liposomal circulation time, which is related to the lipidic composition, and size in order to direct the liposomal formulation to the desired target cells. This targeting strategy is mainly directed at tumors (Figure 1.17) and/or at inflammation situations [120-122, 146, 147] and it is used in the studied liposomal formulation. In the tumor's example, as the tumor grows rapidly, the cells need the necessary oxygen and nutrients supply, which causes the rapid formation of new blood vessels to maintain the tumor's growth. By analyzing the tumor's microvasculature, it is possible to observe the formation of fenestrations, which are small openings in the blood vessels, turning them more permeable for the entrance of small compounds through them (Figure 1.17) [120, 121, 146, 147]. These fenestrations can be a way to deliver the liposomal formulation derived from the enhanced permeability and retention effect, which causes the liposomes to pass the blood vessels and, as the lymphatic system does not remove compounds, the formulation accumulates in tumors, resulting in the anticancer drug delivery in the tumor to treat it (Figure 1.17) [92, 120-122, 146-148]. As for inflammation conditions, such as Hepatic IRI, one of the characteristics of this biological cascade is the production of pro-inflammatory cytokines by immune cells [149]. These pro-inflammatory cytokines can cause the activation of the endothelial cells of the blood vessels, which are the cells that compose the blood vessel's structure that are connected tightly between them. This cell activation can cause the reorganization of the cell structure, which results in the opening of cell junctions, causing the blood vessel's structure to become more permeable to small compounds. The blood vessel's increased permeability is then used by the organism to pass immune cells to the extravascular medium to try and fight the inflammation cascade [149-151]. From a liposomal standpoint, by using the enhanced permeability and retention effect, the liposomal formulation can pass the blood vessels and accumulate in the inflamed cells, delivering the necessary drugs to combat the inflammation situation [92, 146]. As for the liposomal formulation design, in both cases, it is required a liposomal formulation with a

long circulation time, which can be possible with the use of PEG in its lipidic composition, and with a size smaller than 200 nm. These characteristics allow for the liposomes to pass the blood vessels and also the liver and the kidney clearance barriers, increasing circulation time [9, 87, 120, 121, 147, 148, 152, 153]. By administering intravenously this liposomal formulation, it can travel through the bloodstream, bypassing the clearance barriers and the immune system, reaching and delivering the necessary drugs to the target cells [120].

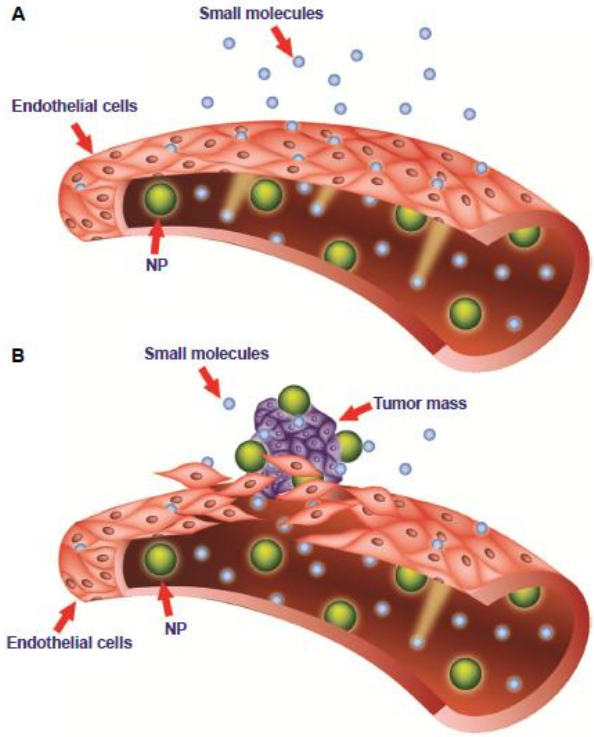

Figure 1.17 – **Passive Targeting Strategy Basis for Tumors. (A) –** In a normal, healthy situation, the structure of the newly formed blood vessels is intact, with the endothelial cells jointed tightly, only allowing the diffusion of very small molecules. Upon the reach of a liposomal formulation, as the blood vessel endothelium is not permeable to larger compounds, the liposomal formulation cannot pass these vessels, continuing its course through the bloodstream. **(B)** – For example, if a tumor grows in this place, as the tumor cells divide rapidly, the blood vessels have to be built quickly, which can cause the formation of fenestrations. If a liposomal formulation with adequate size and long circulation time is administered, it can pass through these fenestrations and accumulate around the tumor, allowing for a treatment option. Retrieved from [121].

However, in addition to the previously described PEG issues, the passive targeting strategy does not direct clearly the liposomal formulation to a specific set of cells, which can decrease the drug's pharmacological effect, which can be overcome by using the active targeting strategy (Figure 1.18) [120, 121]. The active targeting strategy functionalizes liposomes with certain molecules such as antibodies, growth factors, glycoproteins, or peptides that can target specific cell receptors. By targeting specific cell receptors, these liposomes can be directed specifically to a target cell, avoiding healthy tissues, in order to direct the drug's pharmacological effect [120-122]. This improves the drug's therapeutic effect and decreases the side effects [94, 122]. Also, these molecules can be conjugated or not with PEG in order to increase the liposomal circulation time [88, 94]. However, the simplicity of the passive targeting by itself can be more advantageous than the active strategy complexity of combining liposomes with specific molecules (Figure 1.18) [120]. In Figure 1.18, it is shown the comparison between passive targeting and active targeting strategy.

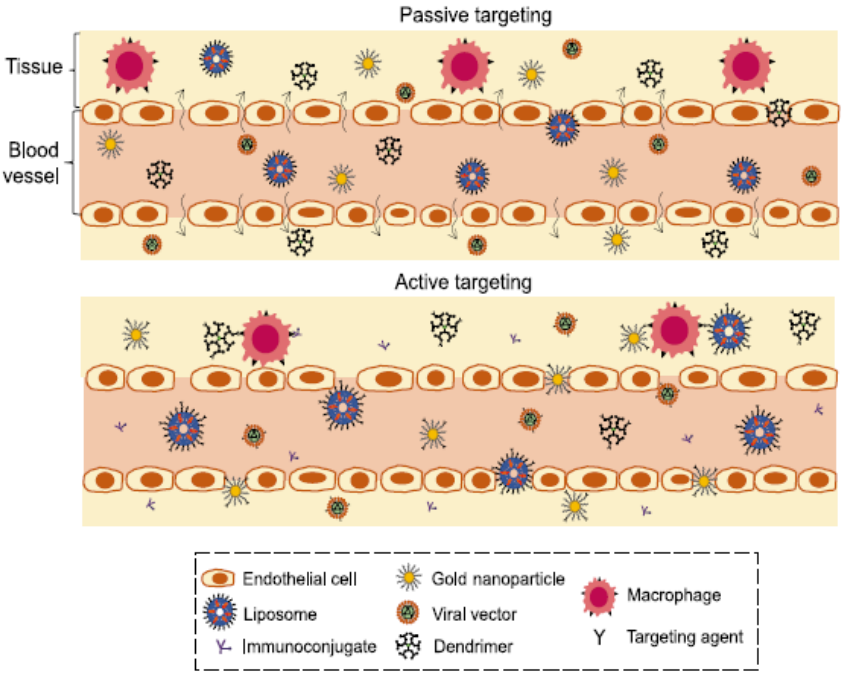

Figure 1.18 – **Comparison between the Passive and the Active Targeting Strategy for different NPs.** Each targeting strategy uses a different approach: in the passive targeting strategy, NPs are designed in a way to utilize the microenvironment, by taking advantage of the fenestrations, to be directed to the target cells; in the active targeting strategy, NPs are functionalized with a targeting agent that directs to a specific target cell, for example, a specific targeting agent directed to macrophages. Retrieved from [11].

1.4.4. Mechanisms of Liposomal Interaction with Cells:

Upon arriving at the target cells, the liposomal formulation accumulates around the cells and in order to deliver the incorporated/encapsulated drugs into the cells, this formulation has to interact with the cell surface. Depending on some liposomal characteristics such as the liposomal surface charge and size, liposomes can interact with cells in four different ways: adsorption, fusion, lipid exchange and endocytosis (Figure 1.19) [117, 121, 122, 136, 154, 155].

Adsorption is the association between the liposomes and the cell membrane. This can be done in two different types: specific, if there is any specific receptor or ligand in the liposome surface that allows for the cell connection (Figure 1.19 a), or nonspecific by, for example, electrostatic interactions (Figure 1.19 b) [121, 122, 136, 154-157]. After adsorption, over time, the cell's microenvironment (e.g., enzymes) can cause the degradation of the liposomal structure, which destabilizes the liposome. This destabilization can cause the release of the liposomal drug content into the extracellular fluid, which can enter the cell via diffusion or also micropinocytosis in order to perform its therapeutic effect [121, 122, 154, 155, 157]. The fusion between the liposomal membrane and the cell membrane allows for the drug content to enter directly into the cytoplasm and exert its therapeutic effect (Figure 1.19 c) [121, 122, 136, 154-157]. The lipid exchange mechanism is based on the transfer of the liposomal lipid molecules with the lipid molecules from the cell membrane, which can be done directly or mediated by lipid transfer proteins localized in the cell membrane (Figure 1.19 e) [121, 122, 136, 154, 155, 157]. The endocytosis mechanism, the most common interaction mechanism between these four, is based on the internalization of the liposomal formulation by the target cells (Figure 1.19 f) [121, 122, 154-158]. After the liposomes contact with the cell, the cell membrane folds inwards, surrounding the liposome, resulting in the formation of a vesicle, known as the endosome, that allows for the liposomal internalization (Figure 1.19 f). Over time, this endosome can fuse with a

lysosome and, as the lysosomal pH is very acidic, the lysosomal pH can cause the degradation and destabilization of the liposomal structure (Figure 1.19 g). This can result in the release of the drug content into the lysosome, which can diffuse into the cytoplasm in order for this drug cargo to exert its therapeutic effect (Figure 1.19) [121, 155, 157]. In some cases, before the fusion between the late endosome and the lysosome, the liposomal structure can destabilize the endosome, resulting in the release of the drug content into the cytoplasm in order for this drug cargo to exert its therapeutic effect (Figure 1.19 h) [121, 155].

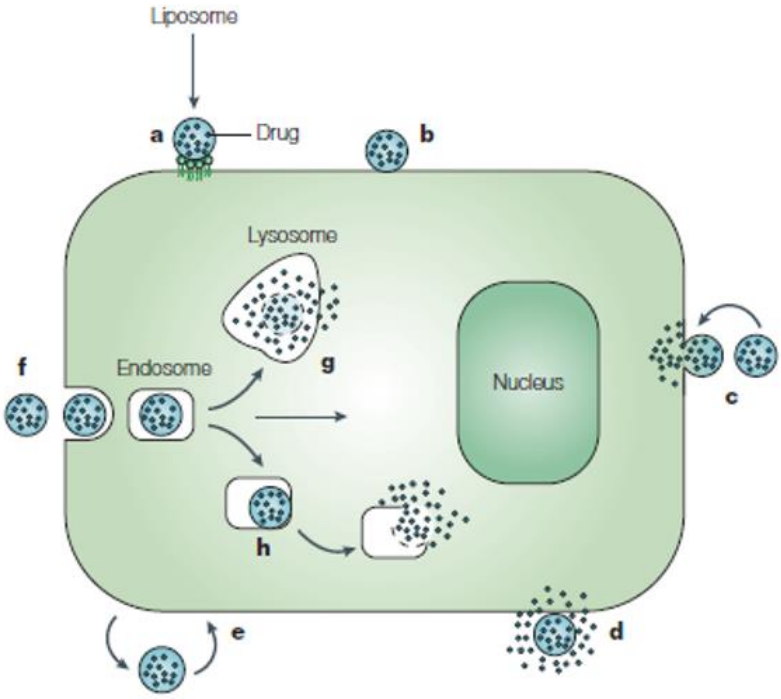

Figure 1.19 – **Possible Mechanisms for Liposomal Formulation-Cell Interaction.** When the liposomal formulation reaches the target cells, the liposomes have to interact with the cells in order to deliver the drug content in order to exert its therapeutic effect. This interaction can be done in four different mechanisms: adsorption, which can be specific **(a)** or nonspecific **(b)**, fusion **(c)**, lipid exchange **(e)**, which can be direct or mediated by cell transfer proteins, and endocytosis **(f)**. Due to the cell's microenvironment (e.g., enzymes) or by the interaction mechanism (lipid exchange), the liposomal structure can be destabilized, releasing the drug content into the extracellular fluid, which can enter the cell via diffusion or micropinocytosis **(d)**. In the endocytosis mechanism, the endosome containing the liposomes can fuse with a lysosome and, due to the lysosomal pH, the liposomal structure can be disrupted, releasing the drug cargo into the lysosome, diffusing then to the cell's cytoplasm **(g)**. Instead of fusing with the lysosome, the endosome containing the liposomes can be destabilized by the liposomal structure, resulting in the drug cargo being released into the cell's cytoplasm **(h)**. Adapted from [155].

2. OBJECTIVES

The main aim of this research project is to develop a liposomal formulation that incorporates quercetin in order to study the biological effects of quercetin against an insult, with the ultimate goal to develop a pharmacological treatment for Hepatic IRI. To achieve this goal, the chosen liposomal formulation must be optimized to incorporate the maximum possible concentration of quercetin. The optimized liposomal formulation is then tested for its protective effect against rotenone-induced toxicity and oxidative stress and compared with the effects from the free form of quercetin. It is expected to obtain data to understand if this quercetin liposomal formulation can be potentially useful in Hepatic IRI models.

3. METODOLOGY

3.1. Preparation of Liposomal Formulations with Quercetin to study the Saturation Curve of Quercetin Incorporation:

To study the highest possible quercetin concentration that can be incorporated into a liposomal formulation, without wasting any quercetin, it is needed to know what is the appropriate quercetin-to-lipid (Q:L) molar ratio to use in the liposomal formulation. For that, it was studied the effect of the incorporation of quercetin in liposomes for various Q:L molar ratios. Based on previous data, the chosen Q:L molar ratios were 0.50:10, 0.75:10, 1.00:10, 1.25:10, 1.50:10 and 2.00:10 (mol/mol).

For this procedure, a mixture of soybean phosphatidylcholine (SPC) (Lipoid GmbH), cholesterol (Chol) (C-3292; Sigma-Aldrich) and N-(Carbonyl-methoxypolyethylene glycol-2000)-1,2-distearoyl--sn-glycero-3-phosphoethanolamine (DSPE-PEG2000) (Lipoid GmbH) in the molar ratios of 8.00:1.50:0.50 were dissolved in chloroform in a round-bottom flask. At the same time, quercetin dihydrate (97%; A15807; Alfa-Aesar) in the corresponding Q:L molar ratio, with an increase in 10% on the theoretic mass, was dissolved in methanol and 90% of its volume was added to the round-bottom flask. After adding quercetin, the solution was mixed and then dried until all the solvent was evaporated with a BÜCHI Rotavapor RE-111 (BÜCHI) [associated with the BÜCHI 461 Water Bath and the Heto-Holten Sue300Q Recirculating Water Jet Pump Mixer (Helo-Holten A/S)], forming a yellow lipidic film. This lipidic film was then resuspended in 10 mM citrate buffer, pH 6.0 in 145 mM NaCl to a final lipid concentration of 32 mM, with the assistance of glass beads. This solution was then placed for 30 minutes in the dark and mixed every 10 minutes, forming a heterogeneous liposomal population in terms of size. To homogenize the size of the prepared liposomal suspension, this emulsion was then extruded using a Lipex Biomembranes Extruder (Lipex Biomembranes), passing one time and sequentially the suspension through Nucleopore® Polycarbonate Filters (Whatman®) with a pore size of 600 nm, 400 nm and 200 nm and lastly, the suspension was passed three times through the Nucleopore® Polycarbonate Filters (Whatman®) with a pore size of 100 nm. To validate that the liposomal population was at the desired size and if the PdI was below 0.1, the Z-average and PdI were measured. To separate the free quercetin from the liposomes, size-exclusion chromatography was then performed using an Econo-Pac® 10DG Desalting Column (#732-2010; Bio-Rad Laboratories, Inc.).

A sample was taken from the prepared suspension right before and at the end of the extrusion process and the end of the chromatography process. For every sample except the one taken before the extrusion process, it was measured the Z-average and the PdI and also the lipid and quercetin concentrations were quantified. For the chromatography sample, it was also measured the zeta potential. For the sample taken before the extrusion process, it was only quantified the lipid and quercetin concentrations.

3.2. Preparation of the Liposomal Formulations for Cell Studies:

Knowing the adequate Q:L molar ratio to use in the liposomal formulation, it was prepared the liposomal formulation to use for the cell studies. As the liposome's lipidic structure can interact with the cells, causing some sort of effect on their viability or proliferation, it is needed to prepare a liposomal formulation with quercetin incorporated and another without quercetin. It is considered the liposomal formulation without quercetin, also referred to as empty liposomal formulation, as SPC:Chol:DSPE-PEG2000 (molar ratios of 8.00:1.50:0.50) and the liposomal formulation with

quercetin as SPC:Chol:DSPE-PEG2000:Quercetin (molar ratios of 8.00:1.50:0.50:1.00). The procedure to prepare these two formulations followed the same line as described for the preparation of the formulations for the Saturation Curve (Point 3.1) with a few differences. The differences were: as the empty liposomal formulation did not have quercetin, all references to it did not enter in the preparation of this formulation; the samples taken from both formulations were different; the buffer for this procedure was previously filtered to be used. After the chromatography procedure, as these two formulations are to be used in cell studies, both were filtered in sterile conditions, using a FilterBio® CA sterile syringe filter with a pore size of 0.22 μm and a diameter of 25 mm (FBS25CA022S; FilterBio®). After that, the liposomal formulations were stored in the dark and in the cold.

A sample was taken from both suspensions right before and at the end of the extrusion process, the end of the chromatography process and the filtration process. For every sample, it was measured the Z-average and the PdI and also the lipid concentration was quantified. For the filtration sample, it was also measured the zeta potential. For the samples taken from the liposomal formulation with quercetin, it was also quantified the quercetin concentration.

3.3. Characterization of the Liposomal Formulations:

3.3.1. Mean Hydrodynamic Diameter and Polydispersity Index:

For the measurement of the Z-average and the PdI, the sample was diluted 1:100 in 10 mM citrate buffer, pH 6.0 in 145 mM NaCl in a cell and then, this dilution was analyzed via the DLS Technique using the Zetasizer Nano S (Malvern Instruments). To analyze the results, it was used the Zetasizer Software v8.00.4813 (Malvern Panalytical). For each sample, it was obtained a set of three different values for the Z-average and the PdI, each one obtained by a different measurement to the same sample. The final value of these two parameters to consider was the median of the three values obtained in the entire sample analysis. For the Z-average value to be considered acceptable, it has to be between 100 and 150 nm (0.1 and 0.15 μm), except in the sample taken before the extrusion process. For the PdI value to be considered acceptable, it has to be below 0.1, except in the sample taken before the extrusion process as the sample is heterogeneous in size due to the preparation method.

3.3.2. Zeta Potential:

The zeta potential value was determined by diluting the samples 1:100 in 10 mM citrate buffer, pH 6.0 in 145 mM NaCl in a capillary cell (DTS1070; Malvern Instruments) and this dilution was analyzed via the M3-PALS Technique using the Zetasizer Nano Z (Malvern Instruments). To analyze the results, it was used the Zetasizer Software v8.00.4813 (Malvern Panalytical). For each sample, it was obtained the direct value to this parameter. To be acceptable, the zeta potential value has to be between – 5 mV and 5 mV.

3.3.3. Lipid Quantification:

The lipid quantification was performed using Rouser's Method [145]. Each liposomal sample was diluted 1:20 for samples taken after the size exclusion chromatography or 1:30 before and after the extrusion process and filtration process in 10 mM citrate buffer, pH 6.0 in 145 mM NaCl. 0.05 mL of each sample was placed in a tube that was then placed in a dry bath at 180 ºC to dry completely. Tubes

were then cooled down to room temperature and then, 0.30 mL of 70% v/v perchloric acid was added to each tube and the tube was again placed in the dry bath for 45 minutes at 180 ºC to perform the acid digestion of the lipids. After this interval, to confirm that the acid digestion was finished, the tubes needed to be clear before taking them off the dry bath. After this procedure and the cooldown of the tubes, it was added to each tube, in this order, 1 mL of distilled water, 0.40 mL of 1.25% w/v ammonium molybdate and 0.40 mL of 5% w/v ascorbic acid, which was prepared right before using. Each tube was agitated vigorously and the tube set was then added to a bath at 100 ºC for 5 minutes. After cooling down, the absorbance of each sample tube was measured at a wavelength of 797 nm using the Shimadzu UV-Visible Spectrophotometer UVmini-1240 (Shimadzu Corporation). Simultaneously, a lipid calibration curve was made using fixed concentrations of 0, 10, 15, 20, 25, 30 and 40 μM from a 0.5 mM phosphate standard dilution, using the same procedure except for the initial reference about the needed dilution before the drying step.

To obtain the lipid concentration for each sample, the median value of each sample triplicate was converted to a lipid concentration by using the slope and the intersection value on the y-axis values obtained from the respective calibration curve.

3.3.4. Quercetin Quantification:

Quercetin quantification was performed by HPLC of the solubilized quercetin liposomal formulation in methanol. On the previous day, each liposomal sample is diluted with methanol and stored overnight in the dark and in the cold. As for the dilution factor, it is used a dilution of 1:25 for samples taken after the chromatography and a dilution of 1:50 for samples taken before and after the extrusion process and the filtration process. On the following day, the solubilized samples were filtered with FilterBio® PTFE syringe filter with a pore size of 0.22 μm and a diameter of 13 mm (FBS13PTFE022H; FilterBio®) to vials, right before the analysis. The samples were then placed in a Spark Holland Midas HPLC Autosampler (Spark Holland) and then analyzed via the HPLC system consisting of Beckman Coulter System Gold® 126 Solvent Module (Beckman Coulter), Beckman Coulter System Gold® 166 UV-Visible Detector (Beckman Coulter) with a Purospher® STAR RP-18 Endcapped (5 μm) HPLC column (1.50359.0001; Merck Millipore). The HPLC system was previously equilibrated with a ratio of 70% v/v of methanol and 30% v/v of distilled water acidified with 1% v/v trifluoracetic acid. The samples were analyzed at a wavelength of 360 nm. At the same time, a quercetin calibration curve using fixed concentrations of 0, 5, 10, 15, 20, 25, 30, 35, 40, 45 and 50 μg/mL was needed to prepare but it was used a fixed quercetin calibration curve, already developed using the same process.

In the HPLC analysis, it is obtained the values for the retention time and the area from each peak. The peaks corresponding to quercetin need to have a retention time similar to 4.6 seconds, based on previous assays from the laboratory. The peak area of each sample is then converted to a quercetin concentration by using the slope and the intersection value on the y-axis values obtained from the respective calibration which is then multiplied by the dilution factor.

3.4. Cell Culture:

The rat glioma C6 cell line (Catalogue Nº 92090409; Public Health England) was maintained in Dulbecco's Modified Eagle Medium (DMEM) with low glucose, stable glutamine and sodium pyruvate (L0066; Biowest) supplemented with 10% v/v heat-inactivated fetal bovine serum (F9556; Sigma-Aldrich, Co.) and 1% v/v penicillin-streptomycin solution (SV30010; GE Healthcare),

hereafter referred to as complete medium. Cells were maintained in a cell incubator at 37 ºC, with a relative humidity of 95% and 5% CO_2 v/v.

When cell confluency surpassed 70%, cells were passed according to the following description. After removing the medium, cells were trypsinized using warm TrypLE™ Express Enzyme (1X) with phenol red (12605-028; Gibco™) until they were completely detached (approximately 5 minutes). Trypsin was then neutralized with complete medium and the resulting cell suspension was transferred to a 15 mL Falcon tube to be centrifuged (300 g, 5 minutes, room temperature). After centrifugation, the supernatant was removed and cells were then resuspended in 10 mL of complete medium. Finally, cells were seeded at 1:20 dilution in a 100 mm culture dish. Medium was replaced with fresh warm complete medium every two days. For cell assays, cells were counted in a hematocytometer before seeding in the corresponding dishes.

3.5. MTT Assay for Determination of Cellular Viability for Free Quercetin and Quercetin Liposomal Formulation Analysis:

To determine what is the effect of the free form of quercetin on the cell viability of the used cell model, it was used the MTT Assay. The MTT Assay consists of a colorimetric assay designed to measure the relative amount of viable cells in a cell culture, using a specific compound, 3-(4,5-dimethylthiazol-2-yl)-2,5-diphenyl tetrazolium bromide (MTT). This assay is linked to mitochondrial function, allowing for the compound's toxicity analysis in cell proliferation and viability [159-161].

For the MTT assays, cells were counted and seeded in 96-well plates at a density of 10^4 cells per well and placed in the incubator overnight for them to attach to the dish surface. The next day, cells were incubated with free quercetin (1 – 100 μM), the liposomal formulation with quercetin (lipid concentration: 14 – 140 μM; quercetin concentration: 1 – 10 μM) or their vehicles [DMSO or empty liposomal formulation (lipid concentration: 14 – 140 μM)], as indicated in the corresponding experiments. The plate was then placed in the incubator for the corresponding incubation period (6, 8, 16, 24, or 48 hours) and then, rotenone (5 μM; R-8875; Sigma-Aldrich) or its vehicle (DMSO) were added and incubated for the indicated time (4, 16, 24 and 48 hours). At the end of the incubation period, the medium was aspirated and cells were washed three times with phosphate buffer solution (PBS) 1X. Finally, 100 μL of complete medium, in the same volume as previously, and MTT (475989; EMD Millipore Corporation; 0.5 mg/mL) were added and incubated for 2 hours. After the incubation period, the medium was gently aspirated (to not disturb the formazan crystals deposited in the bottom of the well), 100% v/v DMSO was added and the plate was incubated in agitation in the dark for 15 minutes at room temperature, in order to dissolve the formazan crystals. Absorbance was measured at 570 nm in a Tecan Sunrise Basic Microplate Reader (Sunrise™).

3.6. Flow Cytometry for Evaluation of ROS-Induced Oxidative Stress:

The effect of quercetin, both in the free form and in the incorporated form, on rotenone-induced oxidative stress, was analyzed by Flow Cytometry, using the specific cell-permeable probe, 2′,7′-dichlorodihydrofluorescin diacetate ($DCFH_2$-DA). In the presence of ROS, DFCH-DA is oxidized to 2',7'-dichlorofluorescein (DCF) and the fluorescence of DCF is proportional to the levels of ROS [162, 163]. Simultaneously, 4',6-diamidino-2-phenylindole (DAPI) was used as a viability staining, to differentiate healthy live cells from dead cells. This dye for nucleic acids is impermeable to the cell membrane and it only enters the cells when the cell membrane is disrupted [164, 165].

For this procedure, cells were seeded in 35 mm cell culture dishes at a density of 5 x 10^5 cells per dish and placed in the incubator overnight. The next day, free quercetin (10 μM), the liposomal formulation with quercetin (lipid concentration: 140 μM; quercetin concentration: 10 μM) or their vehicles [DMSO or empty liposomal formulation (lipid concentration: 140 μM)] were added and, 24 hours later, rotenone (5 μM) or its vehicle (DMSO) were added to the corresponding dishes. Four or sixteen hours later, the medium was aspirated and cells were washed three times with PBS 1X. In the end, fresh medium and $DCFH_2$-DA (10 μM; D6883; Sigma-Aldrich) were added and incubated at 37 ºC for 20 minutes in the dark. Cells were then washed three times with PBS 1X and trypsinized (1X) for 5 minutes. Trypsin was then neutralized with warm complete medium and the resulting cell suspension was transferred to a 1.5 mL Eppendorf tube to be centrifuged (300 g, 5 minutes, room temperature). The supernatant was then aspirated and the resulting pellet was resuspended with PBS 1X and with DAPI (1 μg/mL; 21875-034; Gibco™). Samples were then analyzed using the BD FACSCalibur™ Flow Cytometer (BD Biosciences), using a blue laser (488 nm). Regarding DCF and DAPI fluorescence analysis, the corresponding excitation wavelength is 350 nm and 494 nm, respectively, and the corresponding emission wavelength is 461 nm and 519 nm, respectively. For each experimental group, it was analyzed 10000 events/cells.

3.7. Statistical Analysis for Cell Studies:

For MTT Assays, each independent experiment was only performed once and each condition represents a set of 4, 8, or 16 technical replicates, in which for each condition, it was obtained the mean value and the standard error. Each experiment has a defined control group that was incubated only with DMSO in which the mean value for this group is considered to be 100%. All the mean values and standard errors from the other conditions are then converted to a percentage value in relation to the mean value of the control group. GraphPad Prism Version 9.1.0 (GraphPad Software, LLC) was used to construct the graphical representations and to perform a provisional statistical analysis. The sample data in these graphical representations are represented as mean value ± standard error, for each condition. The provisional statistical analysis was performed using the Student's *t*-test, with the modification of using the corresponding number of replicates of each condition, as informed in the legend of each Figure, instead of the number of independent experiments. This provisional analysis was performed by comparing each condition with the respective control for each experiment (vehicle for the white bars or vehicle with rotenone for the black bars). The results were considered statistically significant when $p < 0.05$.

For Flow Cytometry, each independent experiment was only performed once with each condition only being made once. For each condition, the sample was divided between two major groups, the dead cell group and the live cell group, based on the DAPI fluorescence levels. The live cell group was then further divided between the DCF-negative and the DCF-positive group, based on the DCF fluorescence levels. FlowJo vX.07 (FlowJo, LLC) software was used to analyze data and construct some graphical representations. The remaining graphical representations were made with the software GraphPad Prism Version 9.1.0 (GraphPad Software, LLC) and the sample data are represented as the obtained value (percentage of DCF-positive cells) or the geometric mean value of the data (DCF fluorescence intensity).

4. RESULTS

4.1. Free Quercetin does not protect cells against Rotenone-Induced Toxicity:

Mitochondrial dysfunction and oxidative stress are some of the key features of Hepatic IRI [3, 5, 15, 42, 49, 51]. Rotenone is an inhibitor of the Complex I of the mitochondrial respiratory chain that causes oxidative stress in various cellular models at low micromolar concentrations [43, 44, 166, 167]. C6 cells were treated with 5 μM rotenone or its vehicle (DMSO 0.15%) for 4, 16, 24 and 48 hours in order to determine the time course of rotenone toxicity in these cells through the MTT assay (Figure 4.1).

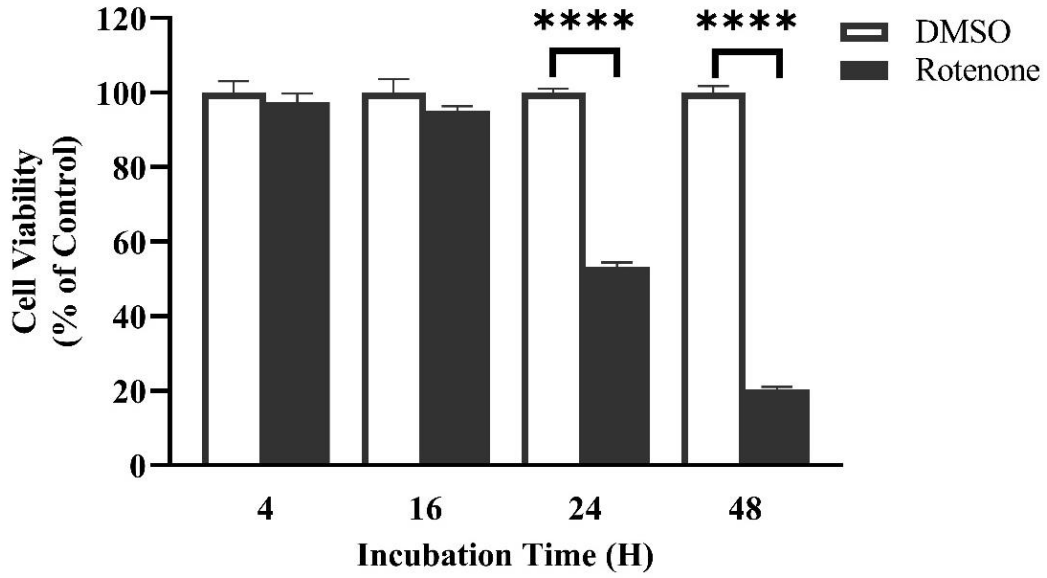

Figure 4.1 – **Rotenone reduced Cell Viability.** Cell Viability Analysis via MTT Assay of the C6 cell culture incubated with rotenone (5 μM; Black bars) for 4, 16, 24 and 48 hours, compared to the respective control (DMSO 0.15%; White bars). Data were represented as the mean value ± standard error of one independent experiment (N = 1). The standard error was calculated in each case with 4 replicates (4H), 8 replicates (16H) and 16 replicates (24/48H). Provisional statistical analysis was performed with a Student's *t*-test (N = 4 for 4H, N = 8 for 16H and N = 16 for 24/48H), by comparing each rotenone incubation condition (Black bars) with the respective control (White bars). **Analysis Legend:** ***** – $p < 0.0001$.

Cell viability only decreased after 24 hours of incubation with rotenone, reducing to almost 50% *vs* control, and to 20% *vs* control after 48 hours. This could be because the mechanism behind oxidative stress is a complex mechanistic cascade that triggers programmed cell death mechanisms, where DNA, RNA and proteins have to be synthesized *de novo* to dismantle the cell [168, 169]. For this reason, 24 hours was preferentially selected as the optimal rotenone incubation time to test quercetin's effects, unless otherwise indicated.

Quercetin is reported to be protective against insults between the concentrations of 10 μM and 30 μM, not having any toxicity itself within this range of concentrations. From 30 μM onward, quercetin inhibits cell growth and/or viability in a dose-dependent manner until 100 μM, which is the boundary for cell studies, as it is close to the solubility limit for quercetin in DMSO [170-172]. To test the effect of free quercetin on rotenone-induced toxicity, C6 cells were co-incubated with a range of quercetin concentrations (10 – 100 μM) with or without rotenone (5 μM) for 24 and 48 hours, and the viability was determined via MTT Assay (Figure 4.2 A/B). Quercetin alone decreased cell viability after 24 hours of incubation at concentrations as little as 10 μM (Figure 4.2 A). This effect was slightly diluted after 48 hours of incubation, as it was only observed from 25 μM (Figure 4.2 B). The only quercetin concentration that prevented rotenone-induced toxicity was 100 μM at 24 hours (42% *vs* control) but this was somewhat masked by the potent reduction of cell number induced by

quercetin alone (48% *vs* control) (Figure 4.2 A). Furthermore, this effect was temporary, as it disappeared after 48 hours of co-incubation (5% *vs* control) (Figure 4.2 B).

In order to give more time for quercetin to have a protective effect against rotenone, cells were preincubated with quercetin (1, 5, 10, 25 and 50 μM) for 6 hours before adding rotenone (5 μM) for 24 and 48 hours (Figure 4.2 C/D). In this case, 50 μM was the maximum quercetin concentration, since 100 μM concentration was too toxic and within the boundary of quercetin solubility. The effect of quercetin preincubation on rotenone-induced toxicity improved protection after 24 hours of rotenone incubation, as 25 and 50 μM concentrations displayed a slight increase tendency of recovery (Figure 4.2 C). Here, the viability increased from approximately 30% (25 μM) and 35% *vs* control (50 μM) to approximately 47% and 52% *vs* control, respectively (Figure 4.2 C/D). On the other hand, these additional 6 hours of quercetin preincubation did not increase quercetin toxicity *vs* the 24 hours of co-incubation (Figure 4.2 A/B). Increasing quercetin preincubation time to 24 hours with the same concentrations (1, 5, 10, 25 and 50 μM) did not prevent rotenone-induced toxicity, maintaining the viability around 4% *vs* control, but it did increase quercetin toxicity (Figure 4.2 E).

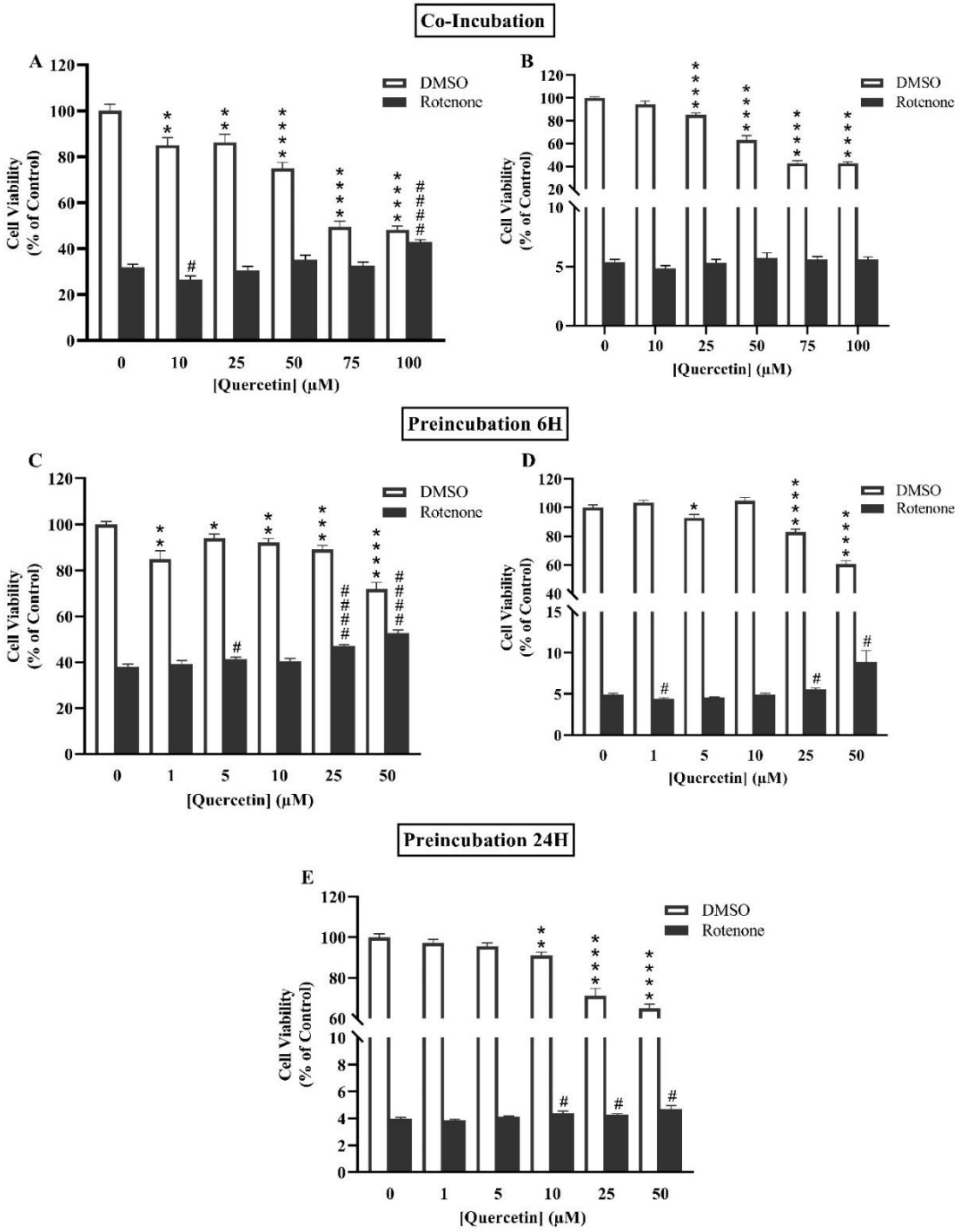

Figure 4.2 – **Free Quercetin did not protect Cell Viability against Rotenone-Induced Toxicity. (A, B)** – Cell Viability Analysis via MTT Assay of the C6 cell culture co-incubated with rotenone (5 μM; Black bars) and quercetin (10 – 100 μM) for 24 **(A)** and 48 **(B)** hours, compared to the respective control (DMSO 0.25%; White bars). **(C, D, E)** – Cell Viability Analysis via MTT Assay of the C6 cell culture preincubated with quercetin (1 – 50 μM) for 6 **(C, D)** and 24 **(E)** hours and incubated with rotenone (5 μM; Black bars) for 24 **(C, E)** and 48 **(D)** hours, compared to the respective control (DMSO 0.15%; White bars). Data were represented as the mean value ± standard error, calculated with 8 replicates in each case, from one independent experiment (N = 1). Provisional statistical analysis was performed with a Student's *t*-test (N = 8), with two comparations: comparing (*) each corresponding quercetin concentration ([Quercetin] (μM) = 1, 5, 10, 25, 50, 75 and 100; White bars) with the respective control ([Quercetin] (μM) = 0; White bar); comparing (#) each corresponding quercetin concentration incubated with rotenone ([Quercetin] (μM) = 1, 5, 10, 25, 50, 75 and 100; Black bars) with the respective control ([Quercetin] (μM) = 0; Black bar). **Analysis Legend:** *, # – $p < 0.05$; ** – $p < 0.01$; *** – $p < 0.001$; ****, #### – $p < 0.0001$.

In summary, based on these results, free quercetin did not have major effects on rotenone-induced toxicity and the concentrations at which it showed some effect against rotenone-induced toxicity were

toxic themselves. However, these results were preliminary and further studies should be carried out to confirm them. In light of these results, it was hypothesized that a liposomal formulation could improve the performance of free quercetin against a rotenone insult.

4.2. Saturation Curve of Quercetin Incorporation into Liposomes:

An important aspect of preparing a liposomal formulation for drug delivery is the molar ratio between the drug concentration and the total lipid concentration. This is because the used drug concentration has to be very well balanced with the lipid concentration to avoid a liposomal formulation without a therapeutic effect or an economic loss during the liposomal formulation preparation. Due to this, the molar ratio between the drug concentration and the total lipid concentration needs to be set to the maximum drug concentration that can be incorporated/encapsulated into the liposome in order to deliver the best possible therapeutic effect with the least possible amount of drug loss. For that reason, it was performed a saturation curve of the incorporation of quercetin into a liposomal formulation, using a range of theoretic quercetin-to-lipid (Q:L) molar ratios. Based on previous data, the chosen theoretic Q:L molar ratios to analyze were 0.50:10, 0.75:10, 1.00:10, 1.25:10, 1.50:10 and 2.00:10 (mol/mol). To ensure that there were no issues during the preparation of the liposomal formulations, it was measured the Z-average and the PdI after the extrusion and the chromatography process, as well as the zeta potential after the chromatography process (Table 4.1).

Table 4.1 – **Results of the Z-average (μm), PdI and Zeta Potential (mV) Values of the analyzed Liposomal Formulations with Quercetin after the Extrusion and the Chromatography Process.** The lipidic composition of the liposomal formulation was SPC:Chol:DSPE-PEG2000 (8.00:1.50:0.50) and the theoretic Q:L molar ratios were 0.50:10, 0.75:10, 1.00:10, 1.25:10, 1.50:10 and 2.00:10 (mol/mol). Data were from one independent experiment (N = 1).

Theoretic Q:L Molar Ratio of the Formulation (mol/mol)	Procedure	Z-average (μm)	PdI	Zeta Potential (mV)
0.50:10	After Extrusion	0.14	0.068	-
	After Chromatography	0.14	0.074	0
0.75:10	After Extrusion	0.14	0.071	-
	After Chromatography	0.14	0.076	- 2
1.00:10	After Extrusion	0.13	0.066	-
	After Chromatography	0.13	0.055	- 1
1.25:10	After Extrusion	0.14	0.078	-
	After Chromatography	0.14	0.079	- 2
1.50:10	After Extrusion	0.14	0.060	-
	After Chromatography	0.14	0.059	- 1
2.00:10	After Extrusion	0.14	0.068	-
	After Chromatography	0.14	0.069	- 3

The values for the three parameters were within the expected range (Table 4.1): the Z-average was between 0.10 and 0.15 μm (100 and 150 nm), the PdI was below 0.1 and the zeta potential was between – 5 mV and 5 mV (Table 4.1). By comparing the Z-average and PdI values between the extrusion and the chromatography procedures, these did not differ largely between the two procedures, indicating that there were no issues with the liposomal formulations during the purification process (Table 4.1).

In each phase of the preparation and purification of the liposomal formulation, there is a possible loss of lipid and/or quercetin concentration which could be due to the process itself or because the liposomal drug loading capacity has reached its maximum. For each liposomal formulation, the lipid

and quercetin concentrations were quantified before the extrusion process (1) and after the chromatography process (2) and the initial (1) and final (2) Q:L molar ratio values were calculated (Table 4.2).

Table 4.2 – Initial and Final Q:L Calculated Molar Ratio Values of the analyzed Liposomal Formulations with Quercetin before the Extrusion (Initial) and after the Chromatography (Final) Process. The lipidic composition of the liposomal formulation was SPC:Chol:DSPE-PEG2000 (8.00:1.50:0.50) and the theoretic Q:L molar ratios were 0.50:10, 0.75:10, 1.00:10, 1.25:10, 1.50:10 and 2.00:10 (mol/mol). Data were from one independent experiment (N = 1).

Theoretic Q:L Molar Ratio of the Formulation (mol/mol)	Initial Q:L Molar Ratio (μmol/μmol)	Final Q:L Molar Ratio (μmol/μmol)
0.50:10	0.045	0.041
0.75:10	0.066	0.061
1.00:10	0.064	0.056
1.25:10	0.091	0.066
1.50:10	0.076	0.088
2.00:10	0.155	0.145

When comparing the obtained Q:L molar ratio values, it was possible to observe, for practically all the theoretic Q:L molar ratios, a decreasing tendency from the initial to the final Q:L molar ratio due to the liposomal formulation process itself (Table 4.2). The exception was for the liposomal formulation with the theoretic Q:L molar ratio of 1.25:10 which showed an increasing tendency. This could be because the obtained Q:L molar ratios were derived from two different quantifications which means that if there is an error in the quantification process or if the samples were not taken appropriately, these values could be different than expected. Also, these values were from only one liposomal formulation, not a group of replicates.

The saturation curve of the incorporation of quercetin into the liposomal formulation was obtained from the graphical representation of the initial *vs* the final Q:L molar ratio values of Table 4.2 for the various liposomal formulations with quercetin (Figure 4.3).

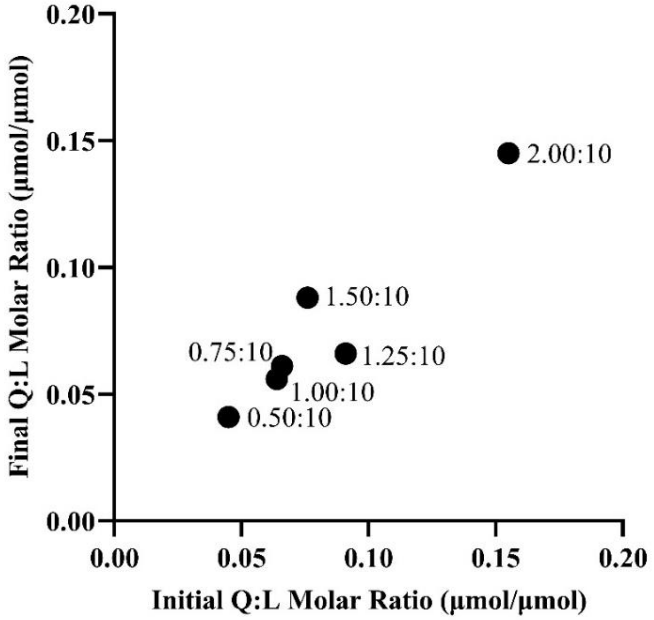

Figure 4.3 – Saturation Curve of the Incorporation of Quercetin into the Liposomal Formulation. The lipidic composition of the liposomal formulation is SPC:Chol:DSPE-PEG2000 (8.00:1.50:0.50) and the theoretic Q:L molar ratios are 0.50:10, 0.75:10, 1.00:10, 1.25:10, 1.50:10 and 2.00:10 (mol/mol). Data were from Table 4.2, representing one independent experiment (N = 1). The legend values correspond to the theoretic Q:L molar ratios of each liposomal formulation.

Theoretically, the saturation curve representation is expected to follow a hyperbolic tendency, reaching a plateau when the final Q:L molar ratio value stabilizes around the same value, with the increase in the initial Q:L molar ratio value, indicating that the liposomal saturation is achieved. This saturation curve did not reach the saturation plateau, indicating that the saturation point was not reached (Figure 4.3). However, this result was preliminary and further studies should be carried out to confirm them. Considering the studied Q:L molar ratios, the chosen Q:L molar ratio to be used in the liposomal formulation for the cell studies was 1.00:10 (mol/mol), as it represented a more comfortable value in line with other data from the laboratory [72].

4.3. Preparation of the Liposomal Formulations for Cell Studies:

Considering the Q:L molar ratio of 1.00:10 (mol/mol), it was needed to prepare the liposomal formulation to be used in the cell studies [SPC:Chol:DSPE-PEG2000:Quercetin (molar ratios of 8.00:1.50:0.50:1.00)]. As there is a possibility that the liposomal structure might affect the cell viability, it has to be prepared a liposomal formulation without quercetin [SPC:Chol:DSPE-PEG2000 (molar ratios of 8.00:1.50:0.50)], referred to as empty liposomal formulation. To ensure that there were no issues during the preparation of the liposomal formulations, it was measured the Z-average and the PdI before and after the extrusion process, after the chromatography and the filtration process, as well as the zeta potential after the filtration process, for both liposomal formulations (Table 4.3).

Table 4.3 – Results of the Z-average (μm), PdI and Zeta Potential (mV) Values of the analyzed Liposomal Formulations (Empty and With Quercetin) before and after the Extrusion Process, after the Chromatography and the Filtration Process. The composition of the empty liposomal formulation was SPC:Chol:DSPE-PEG2000 (8.00:1.50:0.50) and the composition of the liposomal formulation with quercetin was SPC:Chol:DSPE-PEG2000:Quercetin (8.00:1.50:0.50:1.00). Data were from one independent experiment (N = 1).

Liposomal Formulation	Procedure	Z-average (μm)	PdI	Zeta Potential (mV)
Empty Liposomal Formulation	Before Extrusion	1.50	0.886	-
	After Extrusion	0.12	0.051	-
	After Chromatography	0.12	0.062	-
	After Filtration	0.12	0.054	- 2
Liposomal Formulation with Quercetin	Before Extrusion	0.84	0.989	-
	After Extrusion	0.12	0.053	-
	After Chromatography	0.12	0.056	-
	After Filtration	0.12	0.058	- 3

The values for the three parameters taken after the extrusion process were within the expected range (Table 4.3): the Z-average was between 0.10 and 0.15 μm (100 and 150 nm), the PdI was below 0.1 and the zeta potential was between – 5 mV and 5 mV. By comparing the Z-average and PdI values before and after the extrusion process, it was possible to observe the supposed size reduction and homogenization, suggesting that the extrusion process worked properly (Table 4.3). Considering the liposomal formulations separately, the Z-average and PdI values did not differ greatly between them in the steps after the extrusion process, indicating that there were no issues with the liposomal formulations during the purification process (Table 4.3). By comparing both formulations between them, the values for the three parameters were very similar, not indicating any difference between both formulations.

Because the empty liposomal formulation did not present any concerns, the lipid concentration of this formulation was quantified before and after the extrusion process, after the chromatography and the filtration process (Table 4.4).

Table 4.4 – Lipid Concentration Values of the Empty Liposomal Formulation quantified before and after the Extrusion Process, after the Chromatography and the Filtration Process. The composition of the empty liposomal formulation was SPC:Chol:DSPE-PEG2000 (8.00:1.50:0.50). Data were from one independent experiment (N = 1).

Procedure	Lipid Concentration (mM)
Before Extrusion	33.37
After Extrusion	31.03
After Chromatography	21.22
After Filtration	21.55

In each step, the lipid concentration values were almost all within the expected (Table 4.4). Initially, the lipid concentration was similar to the theoretic lipid concentration (32 mM) and, almost after each successive step, this value decreased, as supposed. The lipid concentration value after the chromatography process was lower than the value after the filtration process, which could be explained by the sensitivity of the quantification method, causing this minor disparity. Based on this, for future cell studies, the considered lipid concentration of the empty liposomal formulation was 21.55 mM.

As the liposomal formulation with quercetin did not present any concerns, the lipid and quercetin concentrations of this formulation were quantified before and after the extrusion process, after the chromatography and the filtration process and for those steps, it was calculated the Q:L molar ratio and the yield (Table 4.5). The yield value derives from considering as 100% the Q:L molar ratio value taken before the extrusion process.

Table 4.5 – Lipid and Quercetin Concentration Values of the Liposomal Formulation with Quercetin quantified before and after the Extrusion Process, after the Chromatography and the Filtration Process. The composition of the liposomal formulation with quercetin was SPC:Chol:DSPE-PEG2000:Quercetin (8.00:1.50:0.50:1.00). Data were from one independent experiment (N = 1).

Procedure	Lipid Concentration (mM)	Quercetin Concentration (mM)	Final Q:L Molar Ratio (μmol/μmol)	Yield (%)
Before Extrusion	33.47	2.81	0.084	100
After Extrusion	30.51	2.68	0.088	105
After Chromatography	22.03	1.60	0.073	86
After Filtration	21.90	1.56	0.071	85

In each step, the lipid and quercetin concentration values were within the expected, displaying a concentration value decrease in each successive process (Table 4.5). Also, the initial lipid concentration was similar to the theoretic lipid concentration (32 mM). With the Q:L molar ratio and yield values, it was possible to observe that, for almost all the steps, these values decreased with each successive step as expected. As the ratio is the result of two different quantifications, a slight deviation on one of these quantifications can lead to a deviation from the normal behavior. In conclusion, for future cell studies, it was considered that the liposomal formulation with quercetin has a lipid concentration of 21.90 mM and a quercetin concentration of 1.56 mM.

4.4. A Liposomal Formulation with Quercetin does not protect cells against Rotenone-Induced Toxicity:

Since the free form of quercetin had weak protective effects against rotenone-induced toxicity, a liposomal formulation with quercetin was prepared and tested under the same conditions described earlier (Figure 4.2 C-E). C6 cells were preincubated with the empty liposomal formulation [SPC:Chol:DSPE-PEG2000 (8.00:1.50:0.50); lipid concentration: 14 – 140 μM], free quercetin (quercetin concentration: 1 – 10 μM) and the liposomal formulation with quercetin [SPC:Chol:DSPE-PEG2000:Quercetin (8.00:1.50:0.50:1.00); lipid concentration: 14 – 140 μM; quercetin concentration: 1 – 10 μM] for 6 hours before adding rotenone (5 μM) for 24 and 48 hours, and the viability was analyzed via MTT Assay (Figure 4.4 A/B).

The empty liposomal formulation did not affect cell viability on its own (between 91% and 97.5% *vs* control), nor prevented rotenone-induced toxicity, which in this experiment reduced cell viability to between 34% and 35% (24H) and between 3% and 4% (48H) *vs* the respective control (Figure 4.4 A/B). The quercetin liposomal formulation recovered rotenone-induced toxicity after 24 hours of incubation to 43.2% (5 μM) and 42.8% (10 μM) *vs* control (Figure 4.4 A). This effect faded after 48 hours of incubation to 4.3% (5 μM) and 3.9% (10 μM) *vs* control (Figure 4.4 B). In the absence of rotenone, the quercetin liposomal formulation decreased cell viability after 24 hours of incubation at the concentration of 5 μM (79.3% *vs* control) but the results were not dose-dependent, as the viability was higher at the concentration of 10 μM (88.7% *vs* control) (Figure 4.4 A). After 48 hours of incubation, the dose-dependent effect of the quercetin liposomal formulation was also not observed (Figure 4.4 B). Free quercetin had similar effects on rotenone-induced toxicity compared to the quercetin liposomal formulation (Figure 4.4 A/B). Increasing the preincubation time for free quercetin and both liposomal formulations to 24 hours (lipid concentration: 14 – 140 μM; quercetin concentration: 1 – 10 μM) did not improve free and liposomal quercetin cytoprotection (Figure 4.4 C).

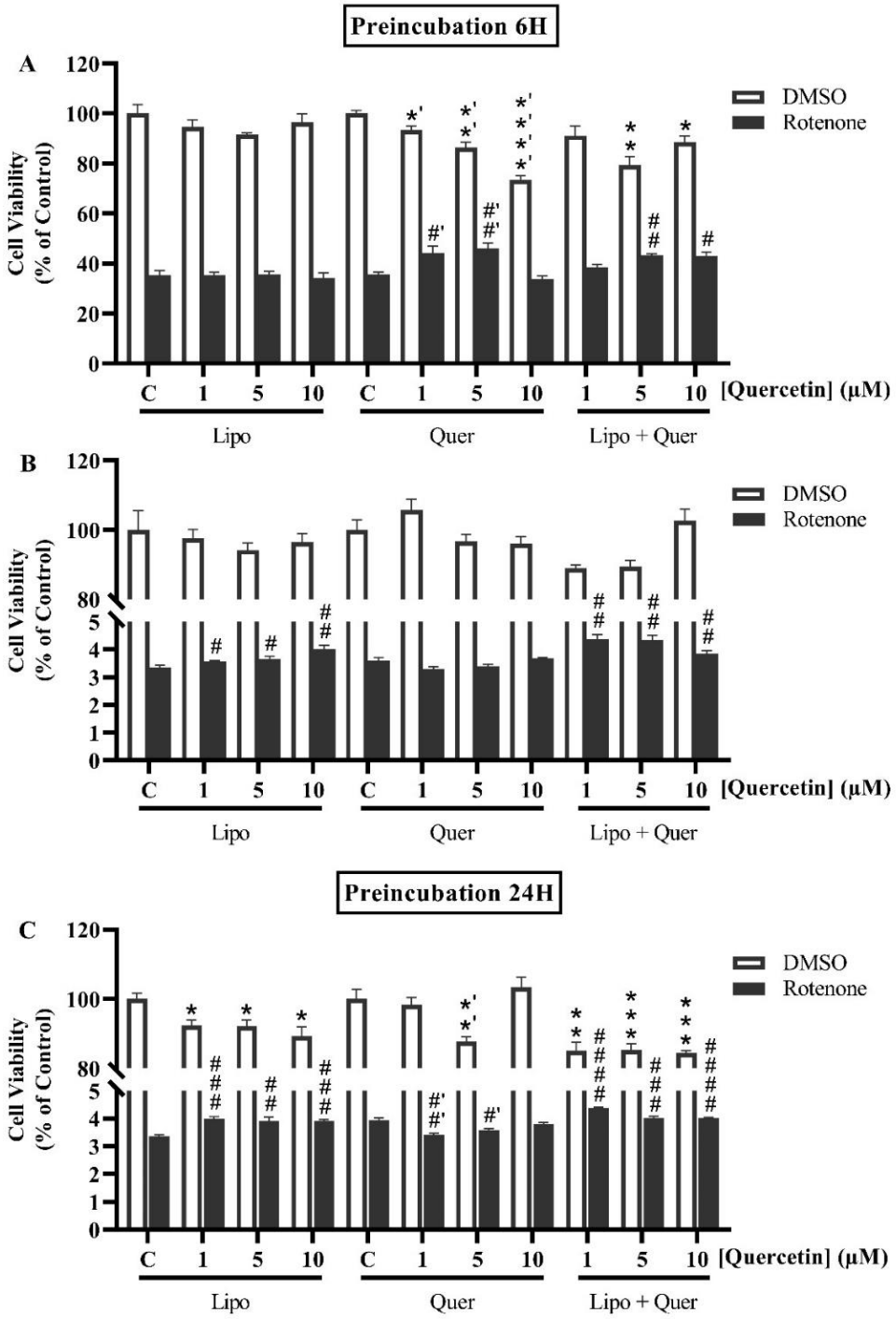

Figure 4.4 – **Quercetin Liposomal Formulation did not protect Cell Viability in Rotenone-Induced Toxicity.** Cell Viability Analysis via MTT Assay of the C6 cell culture preincubated with the empty liposomal formulation [Lipo; SPC:Chol:DSPE-PEG2000 (8.00:1.50:0.50); lipid concentration: 14 – 140 μM], free quercetin (Quer; quercetin concentration: 1 – 10 μM) and the quercetin liposomal formulation [Lipo + Quer; SPC:Chol:DSPE-PEG2000:Quercetin (8.00:1.50:0.50:1.00); lipid concentration: 14 – 140 μM; quercetin concentration: 1 – 10 μM] for 6 **(A, B)** and 24 **(C)** hours and incubated with rotenone (5 μM; Black bars) for 24 **(A, C)** and 48 **(B)** hours, compared to the respective control (C; DMSO 0.05% for the Lipo group or 0.15% for the Quer and the Lipo + Quer group; White bars). Data were represented as the mean value ± standard error, calculated with 4 replicates in each case, from one independent experiment (N = 1). Provisional statistical analysis was performed with a Student's *t*-test (N = 4). The analysis was performed by comparing each corresponding quercetin concentration ([Quercetin] (μM) = 1, 5 and 10; White bars) with the respective control (Lipo/Lipo + Quer group: C from Lipo group (*) and Quer group: C from Quer group (*'); White bars) ; comparing each free quercetin concentration c with rotenone ([Quercetin] (μM) = 1, 5 and 10; Black bars) with the respective control (Lipo/Lipo + Quer group: C from Lipo group (#) and Quer group: C from Quer group (#'); Black bars). **Analysis Legend:** *, *', #, #' – $p < 0.05$; **, *' *', ##, #'#' – $p < 0.01$; ***, ### – $p < 0.001$; *'*'*'*', #### – $p < 0.0001$.

Based on these results, the quercetin liposomal formulation did not have a serious influence on rotenone-induced toxicity, being those effects similar to the ones from free quercetin. Nevertheless, these results were still preliminary (N = 1, only one liposomal formulation analyzed) and these results had a great variability between similar experimental conditions (Figures 4.2 C/D/E and Figure 4.4 A/B/C, respectively), requiring further studies to corroborate them. In light of this, it was thought to shift the focus from analyzing rotenone's action from a cell viability standpoint to an oxidative stress standpoint (rotenone-induced oxidative stress).

4.5. The Free Form of Quercetin and the Quercetin Liposomal Formulation reduces equally Rotenone-Induced Oxidative Stress:

One of the shared hallmarks between rotenone's effects and Hepatic IRI is the production of ROS, which leads to the development of oxidative stress [3, 10, 19, 39, 43, 45, 46]. Oxidative stress can be evaluated by using a specific probe, $DCFH_2$-DA, which evaluates the ROS production in cells [162, 163]. For this approach, it was chosen an incubation time for rotenone long enough to produce oxidative stress but short enough to avoid cell toxicity. Based on previous data (Figure 4.1), the preferentially selected incubation time for rotenone for this analysis was 4 hours. C6 cells were preincubated with the empty liposomal formulation [SPC:Chol:DSPE-PEG2000 (8.00:1.50:0.50); lipid concentration: 140 µM], free quercetin (quercetin concentration: 10 µM) and the liposomal formulation with quercetin [SPC:Chol:DSPE-PEG2000:Quercetin (8.00:1.50:0.50:1.00); lipid concentration: 140 µM; quercetin concentration: 10 µM) for 24 hours before adding rotenone (5 µM) for 4 hours. The DAPI fluorescence intensity histograms of the dead cell group were analyzed to validate that the toxicity effects of rotenone were irrelevant in these conditions (Figure 4.5). As it is possible to observe, rotenone did not cause any major alterations in the cell viability after 4 hours of incubation in any of the conditions, which was in line with the previous results (Figure 4.1).

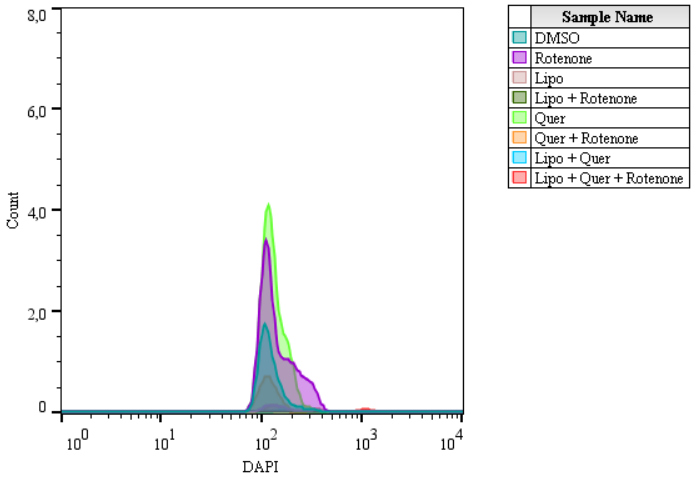

Figure 4.5 – Rotenone did not reduce Cell Viability. DAPI fluorescence intensity distribution of the dead cell group of each condition via Flow Cytometry of the C6 cell culture preincubated with the empty liposomal formulation [Lipo; SPC:Chol:DSPE-PEG2000 (8.00:1.50:0.50:1.00); lipid concentration: 140 µM], quercetin (Quer; quercetin concentration: 10 µM) and the quercetin liposomal formulation [Lipo + Quer; SPC:Chol:DSPE-PEG2000:Quercetin (8.00:1.50:0.50:1.00); lipid concentration: 140 µM; quercetin concentration: 10 µM] for 24 hours and incubated with rotenone (Rotenone/X + Rotenone; 5 µM) for 4 hours, compared to the respective control (DMSO; DMSO 0.15%). Data derived from one independent experiment (N = 1).

The DCF fluorescence intensity distribution and their mean values, alongside the percentage of DCF-positive cells of the live cell group, were analyzed to observe the effects of free quercetin and both liposomal formulations on rotenone-induced oxidative stress (Figure 4.6). Rotenone itself caused

an increase in the mean DCF fluorescence value compared to the control (145.0 *vs* control), indicating that rotenone induced ROS formation and subsequently, oxidative stress (Figure 4.6 B). This was reflected in the increase in the percentage of DCF-positive cells compared to the control (43.5% *vs* control) (Figure 4.6 D). The empty liposomal formulation did not induce oxidative stress by itself, nor did reduced rotenone-induced oxidative stress, maintaining in both cases the mean DCF fluorescence value (16.6 *vs* control and 125.0 *vs* control, respectively; Figure 4.6 B) and percentage of DCF-positive cells value (3.8% *vs* control and 52.3% *vs* control, respectively; Figure 4.6 D) similar to the respective control. The free and liposomal forms of quercetin achieved a similar reduction of rotenone-induced oxidative stress, either in the mean DCF fluorescence (32.6 *vs* control and 66.6 *vs* control, respectively; Figure 4.6 B) or in the percentage of DCF-positive cells (9.0% *vs* control and 14.3% *vs* control, respectively; Figure 4.6 D). This was also validated by quantification of the ratio between the quercetin form and the corresponding control (DMSO for the free quercetin form and the empty liposomal formulation for the liposomal form), which was 4.83 for free quercetin and 3.66 for quercetin liposomal formulation. Alone, both quercetin forms did not induce any effect on the basal ROS levels, either in the mean DCF fluorescence (14.5 *vs* control for the free form and 11.3 *vs* control for the liposomal form; Figure 4.6 B) or in the percentage of DCF-positive cells (2.6% *vs* control for the free form and 2.7% *vs* control for the liposomal form; Figure 4.6 D).

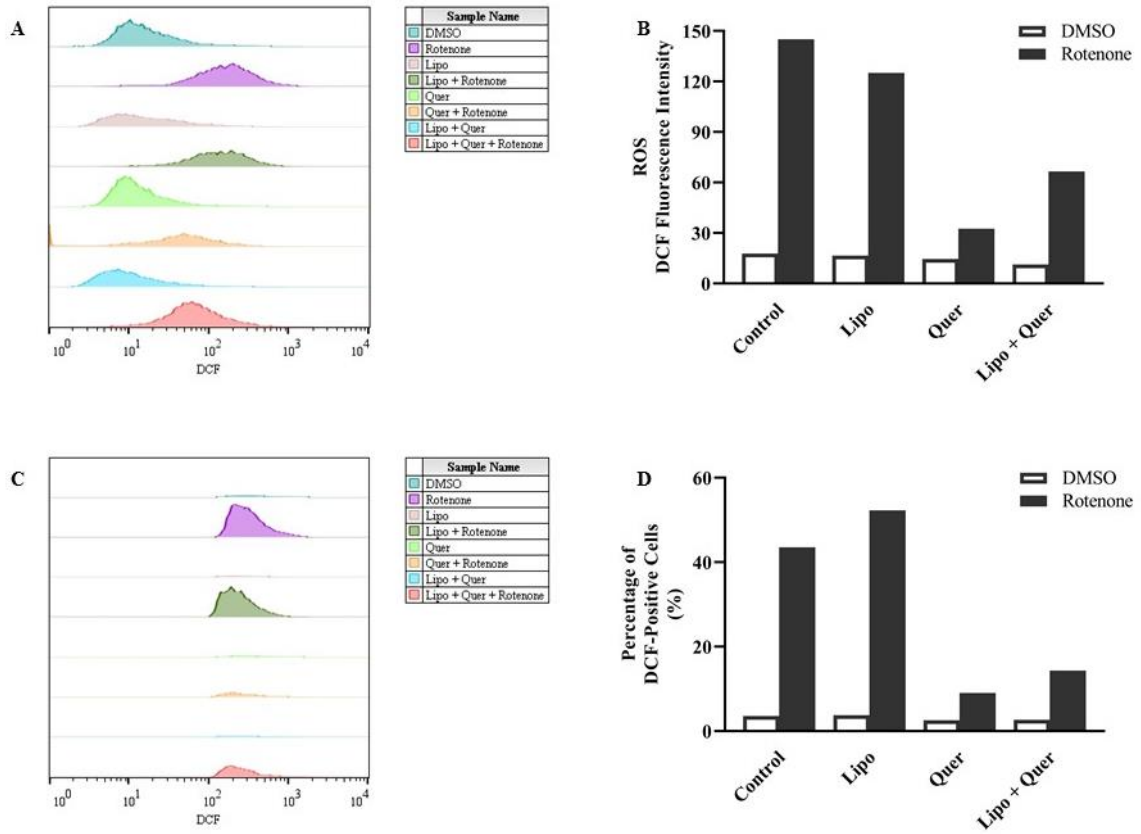

<u>Figure 4.6</u> – Free and Liposomal Forms of Quercetin reduced equally Rotenone-Induced Oxidative Stress. (A/C) – DCF fluorescence intensity distribution of the live cell group **(A)** or the DCF-positive cell group **(C)** of each condition via Flow Cytometry of the C6 cell culture preincubated with the empty liposomal formulation [Lipo; SPC:Chol:DSPE-PEG2000 (8.00:1.50:0.50:1.00); lipid concentration: 140 μM], quercetin (Quer; quercetin concentration: 10 μM) and the quercetin liposomal formulation [Lipo + Quer; SPC:Chol:DSPE-PEG2000:Quercetin (8.00:1.50:0.50:1.00); lipid concentration: 140 μM; quercetin concentration: 10 μM] for 24 hours and incubated with rotenone (Rotenone/X + Rotenone; 5 μM) for 4 hours, compared to the respective control (DMSO; DMSO 0.15%). The histogram range is equal and data derived from one independent experiment (N = 1). **(B)** – Quantification of the mean DCF fluorescence intensity value derived from the DCF fluorescence intensity distribution of the live cell group (DMSO – White bars; Rotenone – Black bars). Data derived from one independent experiment (N = 1). **(D)** – Quantification of the percentage of DCF-positive Cells from the DCF fluorescence intensity distribution of the DCF-positive cell group of each condition (DMSO – White bars; Rotenone – Black bars). Data derived from one independent experiment (N = 1).

While both quercetin forms had little effect on basal ROS production after 4 hours of incubation, both forms had a clear effect on basal ROS production after 16 hours (Figure 4.7).

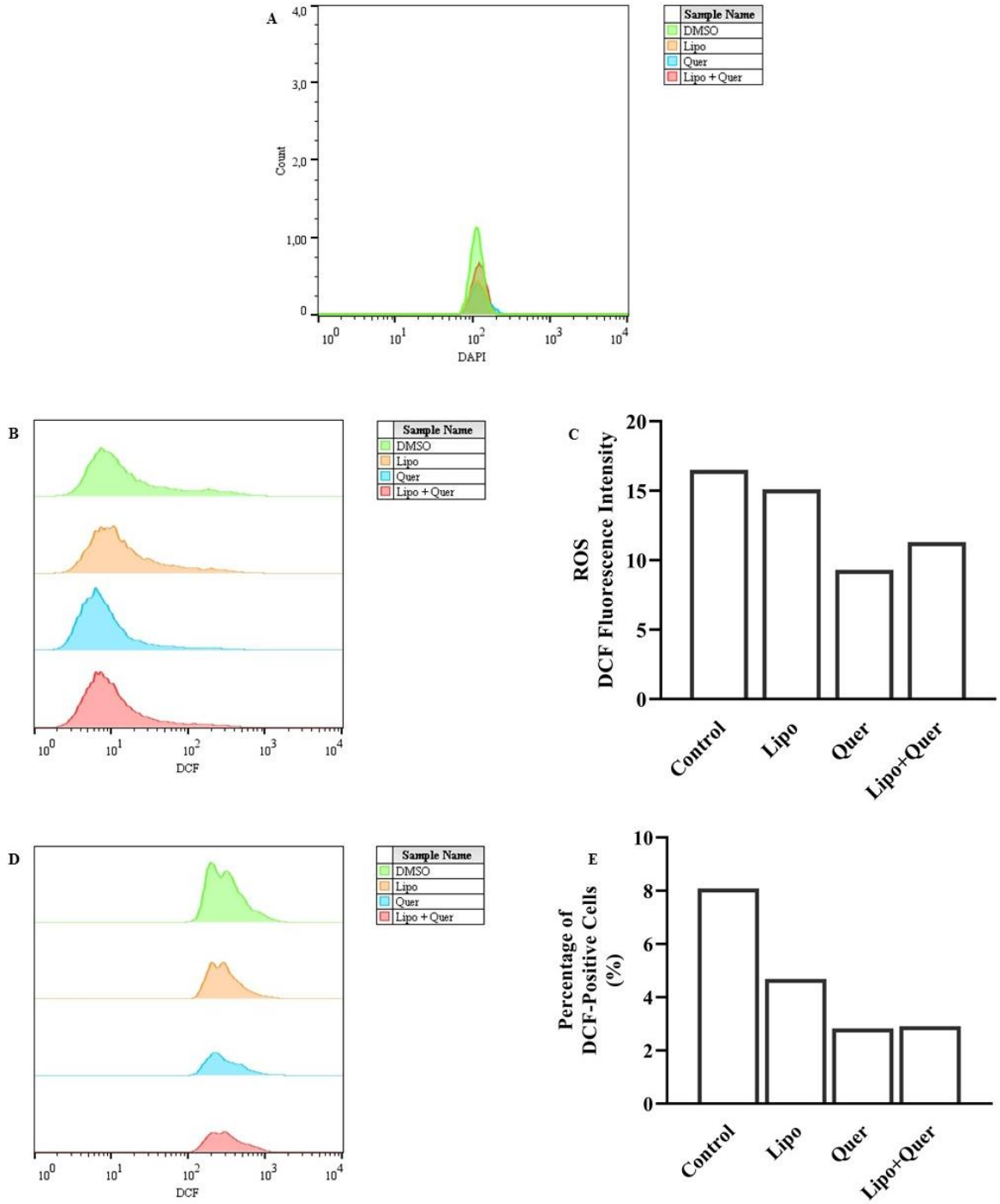

Figure 4.7 – **Free and Liposomal Forms of Quercetin reduced equally Basal ROS Production. (A)** – DAPI fluorescence intensity distribution of the dead cell group of each condition via Flow Cytometry of the C6 cell culture preincubated with the empty liposomal formulation [Lipo; SPC:Chol:DSPE-PEG2000 (8.00:1.50:0.50:1.00); lipid concentration: 140 µM], quercetin (Quer; quercetin concentration: 10 µM) and the quercetin liposomal formulation [Lipo + Quer; SPC:Chol:DSPE-PEG2000:Quercetin (8.00:1.50:0.50:1.00); lipid concentration: 140 µM; quercetin concentration: 10 µM] for 24 hours and incubated with rotenone vehicle (DMSO; DMSO 0.15%) for 16 hours. Data derived from one independent experiment (N = 1). **(B/D)** – DCF fluorescence intensity distribution of the live cell group **(B)** or the DCF-positive cell group **(D)** of each condition. The histogram range is equal and data derived from one independent experiment (N = 1). **(C)** – Quantification of the mean DCF fluorescence intensity value derived from the DCF fluorescence intensity distribution of the live cell group. Data derived from one independent experiment (N = 1). **(E)** – Quantification of the percentage of DCF-positive Cells from the DCF fluorescence intensity distribution of the DCF-positive cell group of each condition. Data derived from one independent experiment (N = 1).

Even though the results are preliminary, since these experiments were only performed once and with only one liposomal formulation, requiring further studies to prove the results, they suggested that there is a possibility that either quercetin form reduced similarly rotenone-induced oxidative stress.

5. DISCUSSION

Hepatic IRI is described as a very complex mechanistic process that involves various parts of the biological function of an organism, most of them involved in oxidative stress or the inflammation cascade [1, 3, 5, 7, 10, 11, 18, 22, 51]. Since some of these variables involved are still unknown [11-13, 25, 50, 51], Hepatic IRI does not have a clear and highly reliable treatment strategy [11, 50]. However, new possibilities are being studied, such as quercetin, an antioxidant and an anti-inflammatory compound with indications of treating Hepatic IRI *in vivo* in animals [4, 64-70, 72-74]. While quercetin has some issues that hinder its administration in humans [64, 66-68, 72,73, 81-84], these issues can possibly be overcome by its incorporation into liposomal formulations [81, 83, 87], which was the purpose of this research project.

In this project, quercetin was unable to protect cells against a rotenone insult (Figures 4.2 and 4.4), regardless of the formulation. Although these results are preliminary, the behavior behind both forms of quercetin against rotenone-induced toxicity could be explained by the cell uptake mechanisms, the different action mechanisms and the different abilities of each compound to perform a cellular effect. Unlike rotenone, which does not require a specific transporter for cell import [173], quercetin's cell import is possibly done via active transport mediated by a cell transporter [174]. Furthermore, the liposomal quercetin form has two additional hinders: the use of PEG in the liposomal lipid composition and the liposome-cell interaction mechanism. Although PEG masks the liposomal formulation from the organism's immune system, increasing the liposomal formulation's circulation time [87, 94, 102, 120], PEG also hinders liposomal cell uptake [123, 153, 158]. As it hinders liposomal cell uptake, PEG needs to be removed from the liposomal formulation. *In vivo*, PEG removal can be achieved by the cell's microenvironment (e.g., the tumor's acidic microenvironment) [94, 120, 147] but *in vitro*, it can be difficult [175], which results in the quercetin's import being delayed. Furthermore, the liposomal formulation has to interact with the target cells, a multistep process for each mechanism [117, 121, 122, 136, 154, 155] which takes extra time to occur, delaying even more quercetin's cell uptake. In both cases, this time difference between quercetin's (free and liposomal) and rotenone's cell uptake can provoke the delay of quercetin's therapeutic effect against rotenone. To circumvent this, quercetin can be preincubated in order to give more time to enter the cells (Figure 4.2 C-E and Figure 4.4) but, as it was possible to observe, both forms of quercetin maintained the same behavior against rotenone-induced toxicity. Although these results are preliminary, they do not support this cell uptake hypothesis. After entering the cells, rotenone goes straight to the mitochondria and inhibits the Complex I of the respiratory chain [35-40]. Even though quercetin is also directed to the mitochondria [174], it has other cell targets [64-66, 69, 70, 72-74]. From the moment that quercetin enters the cells, it is used throughout various cellular pathways [64-66, 69, 70, 72-74] and when it reaches the mitochondria, quercetin accumulates in the mitochondria at lower levels than initially, which can impede its protective effects against rotenone-induced toxicity. These results are also connected with the hypothesis that, as quercetin does not affect rotenone-induced toxicity levels, either quercetin is not strong enough to overcome the nefarious rotenone effects or rotenone is too toxic under the studied conditions. This could be why quercetin works in other models that have a higher basal cell viability level or at other rotenone concentrations [72, 176]. Furthermore, although the protection provided by quercetin is weak, there is some similarity between the free and liposomal quercetin formulations, which strengthens the observations.

On the other hand, both forms of quercetin reduced similarly rotenone-induced oxidative stress after 4 hours of incubation (Figure 4.6). Even though these results are still preliminary, some of the previous hypotheses are consistent with them. As for the cell uptake hypothesis, these results showed that either quercetin form reduced equally rotenone-induced oxidative stress, which indicated that

quercetin entered the cells at the same levels as rotenone. Even more, as both forms of quercetin reduced also similarly the basal ROS levels (Figure 4.7), the liposomal quercetin form was imported at the same rate as the free quercetin, which devaluates the cell import hypothesis. The other two hypotheses are supported by the results in Figure 4.6. In this case, cells were exposed for the longest incubation time considered here to quercetin but only for the shortest incubation time to rotenone. This resulted in quercetin cellular levels being possibly higher than rotenone cellular levels, causing the reduction of rotenone's effects in the mean DCF fluorescence intensity or the percentage of DCF-positive cells. This could be because as rotenone's incubation time was lower, it had a lower possibility to cause cell harm, which resulted in quercetin having an additional strength to overcome rotenone's effects. Furthermore, to strengthen these observations, both forms of quercetin had a similar effect against rotenone's effects.

In summary, based on these results, it is possible to infer that, although the protection against a rotenone insult was very reduced, both forms of quercetin act similarly in both standpoints, which indicates that liposomal quercetin was successfully delivered to the cells. Also, both forms of quercetin reduced equally rotenone-induced oxidative stress, which indicates that quercetin can be a good treatment option against oxidative stress *in vitro*.

6. CONCLUSIONS AND FUTURE PERSPECTIVES

In this project, it was shown that none of the quercetin forms had a protective effect against rotenone-induced toxicity. Instead, either quercetin form had a similar protective effect against rotenone-induced oxidative stress. As both quercetin forms reduced equally oxidative stress, it can be concluded that, *in vitro*, quercetin can be a good treatment option for oxidative stress issues, such as Hepatic IRI. Furthermore, since there is some similarity between free quercetin and the quercetin liposomal formulation *in vitro*, the used liposomal formulation can delivery successfully quercetin at the same level as free quercetin. This indicates that the used liposomal formulation could be a useful tool to deliver quercetin *in vivo*. As quercetin is a possible option against Hepatic IRI and with the success of the used liposomal formulation in quercetin delivery, this quercetin liposomal formulation can possibly be used as a new pharmacological treatment for Hepatic IRI.

As these conclusions are based on preliminary results, further studies are required to confirm this possible new Hepatic IRI pharmacological treatment. First, to confirm if the used Q:L molar ratio is the appropriate one for these studies; and second, to infer if the described effects are significant, using also liposomal formulation replicates. If the conclusions are the same, the next step is to replicate these studies in a more physiological model of Hepatic IRI to conclude definitely that this quercetin liposomal formulation is a possible new pharmacological treatment for Hepatic IRI. Besides this, there are a variety of new perspectives that this study can take for the future, depending on the validity of the previously described conclusions. A possibility is to test how quercetin, either in the free or in the incorporated form, can affect different key parameters of the Hepatic IRI cascade. For example, quantify the GSH/GSSG levels to understand the antioxidant cellular balance, quantify the Ca^{2+} levels to comprehend if quercetin can affect the Ca^{2+} overload characteristic in Hepatic IRI [3, 18] and know what is the effect on the $NO^{\bullet}$ system [4, 5, 15, 18, 23, 27] to understand if quercetin can reduce the damage caused by this system. Furthermore, instead of focusing solely on oxidative stress, one possible target for quercetin is the inflammation cascade, one of the Hepatic IRI hallmarks [3, 10, 15]. In this case, it can be evaluated the expression and the intracellular levels of different molecules such as NF-κB, IL-1β, IL-6 and TNF-α [3, 7, 8, 15, 17, 18, 21, 25] to understand the effects of both quercetin forms against the inflammation cascade. Furthermore, if the liposomal formulation does not present the same effect *in vivo*, other liposomal formulations could be tested to improve delivery or intensify quercetin's effect. In the same line, since there was no comparison between other molecules, these studies can be performed with other antioxidant or anti-inflammatory compounds such as resveratrol [5, 21, 26] to observe if there is a better pharmacological approach. Also, one hypothesis was that rotenone was too toxic for the cells and did not allow a correct analysis of the effects. Instead of using rotenone as an oxidative stress inducer, other compounds can replace it such as H_2O_2 [177], MG-132 [178], or tertiary-butylhydroperoxide [179].

7. REFERENCES

[1] – Harada, N., Hatano, E., Koizumi, N., Nitta, T., Yoshida, M., Yamamoto, N., Brenner, D. A., & Yamaoka, Y. (2004). Akt Activation Protects Rat Liver from Ischemia/Reperfusion Injury. *Journal of Surgical Research*, *121*(2), 159 – 170.

[2] – Kalogeris, T., Baines, C. P., Krenz, M., & Korthuis, R. J. (2016). Ischemia/Reperfusion. *Comprehensive Physiology*, *7*(1), 113 – 170.

[3] – Arii, S., Teramoto, K., & Kawamura, T. (2003). Current progress in the understanding of and therapeutic strategies for ischemia and reperfusion injury of the liver. *Journal of Hepato-Biliary-Pancreatic Surgery*, *10*(3), 189 – 194.

[4] – Atef, Y., El-Fayoumi, H. M., Abdel-Mottaleb, Y., & Mahmoud, M. F. (2017). Quercetin and tin protoporphyrin attenuate hepatic ischemia reperfusion injury: role of HO-1. *Naunyn-Schmiedeberg's Archives of Pharmacology*, *390*(9), 871 – 881.

[5] – Cannistrà, M., Ruggiero, M., Zullo, A., Gallelli, G., Serafini, S., Maria, M., Naso, A., Grande, R., Serra, R., & Nardo, B. (2016). Hepatic ischemia reperfusion injury: A systematic review of literature and the role of current drugs and biomarkers. *International Journal of Surgery*, *33*, S57 – S70.

[6] – Kawachi, S., Hines, I. N., Laroux, F. S., Hoffman, J., Bharwani, S., Gray, L., Leffer, D., & Grisham, M. B. (2000). Nitric Oxide Synthase and Postischemic Liver Injury. *Biochemical and Biophysical Research Communications*, *276*(3), 851 – 854.

[7] – Konishi, T., & Lentsch, A. B. (2017). Hepatic Ischemia/Reperfusion: Mechanisms of Tissue Injury, Repair, and Regeneration. *Gene Expression*, *17*(4), 277 – 287.

[8] – Marcelino, P., Marinho, H. S., Campos, M. C., Neves, A. R., Fontes, F. S., Carvalho, A., Feio, G., Martins, M. B. F., & Corvo, M. L. (2017). Therapeutic activity of superoxide dismutase-containing enzymosomes on rat liver ischaemia-reperfusion injury followed by magnetic resonance microscopy. *European Journal of Pharmaceutical Sciences*, *109*(September), 464 – 474.

[9] – Martins, M. B. A. F., Corvo, M. L., Marcelino, P., Marinho, H. S., Feio, G., & Carvalho, A. (2014). New long circulating magnetoliposomes as contrast agents for detection of ischemia-reperfusion injuries by MRI. *Nanomedicine: Nanotechnology, Biology, and Medicine*, *10*(1), 207 – 214.

[10] – Marinho, H. S., Marcelino, P., Soares, H., & Corvo, M. L. (2018). Gene Silencing using siRNA for Preventing Liver Ischaemia-Reperfusion Injury. *Current Pharmaceutical Design*, *24*(23), 2692 – 2700.

[11] – Ferreira-Silva, M., Faria-Silva, C., Baptista, P. V., Fernandes, E., Fernandes, A. R., & Corvo, M. L. (2021). Drug delivery nanosystems targeted to hepatic ischemia and reperfusion injury. *Drug Delivery and Translational Research*, *11*(2), 397 – 410.

[12] – Koti, R. S., Seifalian, A. M., & Davidson, B. R. (2003). Protection of the Liver by Ischemic Preconditioning: A Review of Mechanisms and Clinical Applications. *Digestive Surgery*, *20*(5), 383 – 396.

[13] – Mendes-Braz, M., Elias-Miró, M., Jiménez-Castro, M. B., Casillas-Ramírez, A., Ramalho, F. S., & Peralta, C. (2012). The Current State of Knowledge of Hepatic Ischemia-Reperfusion Injury Based on Its Study in Experimental Models. *Journal of Biomedicine & Biotechnology*, *2012*, 298657.

[14] – Saidi, R. F., & Kenari, S. K. (2014). Liver Ischemia/Reperfusion Injury: an Overview. *Journal of Investigative Surgery*, *27*(6), 366 – 379.

[15] – Song, X., Zhang, N., Xu, H., Cao, L., & Zhang, H. (2012). Combined Preconditioning and Postconditioning Provides Synergistic Protection against Liver Ischemic Reperfusion Injury. *International Journal of Biological Sciences*, *8*(5), 707 – 718.

[16] – Cowled, P., & Fitridge, R. (2011). Pathophysiology of Reperfusion Injury. In R. Fitridge & M. M. Thompson (Eds.), *Mechanisms of Vascular Disease: A Reference Book for Vascular Specialists* (pp. 331 – 350). Barr Smith Press.

[17] – Peralta, C., Jiménez-Castro, M. B., & Gracia-Sancho, J. (2013). Hepatic ischemia and reperfusion injury: Effects on the liver sinusoidal milieu. *Journal of Hepatology*, *59*(5), 1094 – 1106.

[18] – Rampes, S., & Ma, D. (2019). Hepatic ischemia-reperfusion injury in liver transplant setting: mechanisms and protective strategies. *The Journal of Biomedical Research*, *33*(4), 221 – 234.

[19] – Pacher, P., Nivorozhkin, A., & Szabó, C. (2006). Therapeutic Effects of Xanthine Oxidase Inhibitors: Renaissance Half a Century after the Discovery of Allopurinol. *Pharmacological Reviews*, *58*(1), 87 – 114.

[20] – Wang, M., Shen, F., Shi, L. H., Xi, T., Li, X. F., Chen, X., & Wu, M. C. (2008). Protective effect of prednisolone on ischemia-induced liver injury in rats. *World Journal of Gastroenterology*, *14*(27), 4332 – 4337.

[21] – Dossi, C. G., Vargas, R. G., Valenzuela, R., & Videla, L. A. (2021). Beneficial effects of natural compounds on experimental liver ischemia-reperfusion injury. *Food & Function*, *12*(9), 3787 – 3798.

[22] – Nastos, C., Kalimeris, K., Papoutsidakis, N., Tasoulis, M. K., Lykoudis, P. M., Theodoraki, K., Nastou, D., Smyrniotis, V., & Arkadopoulos, N. (2014). Global Consequences of Liver Ischemia/Reperfusion Injury. *Oxidative Medicine and Cellular Longevity*, *2014*, 906965

[23] – Gomes, A., Fernandes, E., Lima, J. L. F. C., Mira, L., & Corvo, M. L. (2008). Molecular Mechanisms of Anti-Inflammatory Activity Mediated by Flavonoids. *Current Medicinal Chemistry*, *15*(16), 1586 – 1605.

[24] – Lyngsie, G., Krumina, L., Tunlid, A., & Persson, P. (2018). Generation of hydroxyl radicals from reactions between a dimethoxyhydroquinone and iron oxide nanoparticles. *Scientific Reports*, *8*(1), 10834.

[25] – Jaeschke, H. (2003). Molecular mechanisms of hepatic ischemia-reperfusion injury and preconditioning. *American Journal of Physiology – Gastrointestinal and Liver Physiology*, *284*(1), G15 – G26.

[26] – Jaeschke, H., & Woolbright, B. L. (2012). Current strategies to minimize hepatic ischemia-reperfusion injury by targeting reactive oxygen species. *Transplantation Reviews*, *26*(2), 103 – 114.

[27] – Li, Y., Yang, Y., Feng, Y., Yan, J., Fan, C., Jiang, S., & Qu, Y. (2014). A review of melatonin in hepatic ischemia/reperfusion injury and clinical liver disease. *Annals of Medicine*, *46*(7), 503 – 511.

[28] – Sousa, J. S., D'Imprima, E., & Vonck, J. (2018). Mitochondrial Respiratory Chain Complexes. In J. R. Harris & E. J. Boekema (Eds.), *Membrane Protein Complexes: Structure and Function* (pp. 167 – 227). Springer Nature Singapore Pte Ltd.

[29] – Voet, D., & Voet, J. G. (Eds.). (2010). Electron Transport and Oxidative Phosphorylation. In *Biochemistry* (pp. 823 – 870). John Wiley & Sons.

[30] – Dudkina, N. V., Kouřil, R., Peters, K., Braun, H. P., & Boekema, E. J. (2010). Structure and function of mitochondrial supercomplexes. *Biochimica et Biophysica Acta - Bioenergetics*, *1797*(6-7), 664–670.

[31] – Zhao, R. Z., Jiang, S., Zhang, L., & Yu, Z. B. (2019). Mitochondrial electron transport chain, ROS generation and uncoupling (Review). *International Journal of Molecular Medicine*, *44*(1), 3 – 15.

[32] – Nelson, L. D., & Cox, M. M. (Eds.). (2012). The Citric Acid Cycle. In *Principles of Biochemistry* (Sixth Edition, pp. 633 – 665). W. H. Freeman and Company.

[33] – Jonckheere, A. I., Smeitink, J. A. M., & Rodenburg, R. J. T. (2012). Mitochondrial ATP synthase: architecture, function and pathology. *Journal of Inherited Metabolic Disease*, *35*(2), 211 – 225.

[34] – Nelson, L. D., & Cox, M. M. (Eds.). (2012). Oxidative Phosphorylation and Photophosphorylation. In *Principles of Biochemistry* (Sixth Edition, pp. 731 – 797). W. H. Freeman and Company.

[35] – Gupta, R. C. (2014). Rotenone. In P. Wexler (Ed.), *Encyclopedia of Toxicology* (Third Edition, Vol. 4, pp. 185 – 187). Academic Press.

[36] – Heinz, S., Freyberger, A., Lawrenz, B., Schladt, L., Schmuck, G., & Ellinger-Ziegelbauer, H. (2017). Mechanistic Investigations of the Mitochondrial Complex I Inhibitor Rotenone in the Context of Pharmacological and Safety Evaluation. *Scientific Reports*, *7*(February), 45465.

[37] – Ichikawa, H., Takagi, T., Uchiyama, K., Higashihara, H., Katada, K., Isozaki, Y., Naito, Y., Yoshida, N., & Yoshikawa, T. (2004). Rotenone, a mitochondrial electron transport inhibitor, ameliorates ischemia-reperfusion-induced intestinal mucosal damage in rats. *Redox Report*, *9*(6), 313 – 316.

[38] – Li, N., Ragheb, K., Lawler, G., Sturgis, J., Rajwa, B., Melendez, J. A., & Robinson, J. P. (2003). Mitochondrial Complex I Inhibitor Rotenone Induces Apoptosis through Enhancing Mitochondrial Reactive Oxygen Species Production. *The Journal of Biological Chemistry*, *278*(10), 8516 – 8525.

[39] – Pan, P. K., Qiao, L. Y., & Wen, X. N. (2016). Safranal prevents rotenone-induced oxidative stress and apoptosis in an *in vitro* model of Parkinson's disease through regulating Keap1/Nrf2 signaling pathway. *Cellular and Molecular Biology*, *62*(14), 11 – 17.

[40] – Yu, Y. X., Li, Y. P., Gao, F., Hu, Q. S., Zhang, Y., Chen, D., & Wang, G. H. (2016). Vitamin K_2 suppresses rotenone-induced microglial activation *in vitro*. *Acta Pharmacologica Sinica*, *37*(9), 1178 – 1189.

[41] – Huang, C. W., Lin, K. M., Hung, T. Y., Chuang, Y. C., & Wu, S. N. (2018). Multiple Actions of Rotenone, an Inhibitor of Mitochondrial Respiratory Chain, on Ionic Currents and Miniature End-Plate Potential in Mouse Hippocampal (mHippoE-14) Neurons. *Cellular Physiology and Biochemistry*, *47*(1), 330 – 343.

[42] – Martin, J. L., Gruszczyk, A. V., Beach, T. E., Murphy, M. P., & Saeb-Parsy, K. (2019). Mitochondrial mechanisms and therapeutics in ischaemia reperfusion injury. *Pediatric Nephrology*, *34*(7), 1167 – 1174.

[43] – Han, G., Casson, R. J., Chidlow, G., & Wood, J. P. M. (2014). The Mitochondrial Complex I Inhibitor Rotenone Induces Endoplasmic Reticulum Stress and Activation of GSK-3β in Cultured Rat Retinal Cells. *Investigative Ophthalmology & Visual Science*, *55*(9), 5616 – 5628.

[44] – Thakur, P., & Nehru, B. (2015). Inhibition of Neuroinflammation and Mitochondrial Dysfunctions by Carbenoxolone in the Rotenone Model of Parkinson's Disease. *Molecular Neurobiology*, *51*(1), 209 – 219.

[45] – Fato, R., Bergamini, C., Bortolus, M., Maniero, A. L., Leoni, S., Ohnishi, T., & Lenaz, G. (2009). Differential effects of mitochondrial Complex I inhibitors on production of reactive oxygen species. *Biochimica et Biophysica Acta*, *1787*(5), 384 – 392.

[46] – Mohammed, F., Gorla, M., Bisoyi, V., Tammineni, P., & Sepuri, N. (2020). Rotenone-induced reactive oxygen species signal the recruitment of STAT3 to mitochondria. *FEBS Letters*, *594*(9), 1403 – 1412.

[47] – Knaryan, V. H., Samantaray, S., Park, S., Azuma, M., Inoue, J., & Banik, N. L. (2014). SNJ-1945, a calpain inhibitor, protects SH-SY5Y cells against MPP^+ and rotenone. *Journal of Neurochemistry*, *130*(2), 280 – 290.

[48] – Orellana, C., Villagrán, R., Zang, J., & Rodrigo, R. (2019). The role of oxidative stress in hepatic ischemia-reperfusion injury: potential target for interventions in liver transplantation. *Clinical Research and Trials*, *5*(2), 1 – 4.

[49] – Zhang, H., Yan, Q., Wang, X., Chen, X., Chen, Y., Du, J., & Chen, L. (2021). The Role of Mitochondria in Liver Ischemia-Reperfusion Injury: From Aspects of Mitochondrial Oxidative Stress, Mitochondrial Fission, Mitochondrial Membrane Permeable Transport Pore Formation, Mitophagy, and Mitochondria-Related Protective Measures. *Oxidative Medicine and Cellular Longevity*, *2021*, 6670579.

[50] – Cornide-Petronio, M. E., Jiménez-Castro, M. B., Gracia-Sancho, J., & Peralta, C. (2019). Ischemic Preconditioning Directly or Remotely Applied on the Liver to Reduce Ischemia-Reperfusion Injury in Resections and Transplantation. In G. Tsouflas (Ed.), *Liver Disease and Surgery* (pp. 1 – 15). IntechOpen.

[51] – Yamanaka, K., Houben, P., Bruns, H., Schultze, D., Hatano, E., & Schemmer, P. (2015). A Systematic Review of Pharmacological Treatment Options Used to Reduce Ischemia Reperfusion Injury in Rat Liver Transplantation. *PloS ONE*, *10*(4), e0122214.

[52] – Desai, K. K., Dikdan, G. S., Shareef, A., & Koneru, B. (2008). Ischemic Preconditioning of the Liver: A Few Perspectives from the Bench to Bedside Translation. *Liver Transplantation*, *14*(11), 1569 – 1577.

[53] – Guo, J. Y., Yang, T., Sun, X. G., Zhou, N. Y., Li, F. S., Long, D., Lin, T., Li, P. Y., & Feng, L. (2011). Ischemic postconditioning attenuates liver warm ischemia-reperfusion injury through Akt-eNOS-NO-HIF pathway. *Journal of Biomedical Science*, *18*(1), 79.

[54] – Schewe, J., Makeschin, M. C., Liss, I., Mayr, D., Zhang, J., Khandoga, A., Rothenfußer, S., Schnurr, M., Gerbes, A. L., & Steib, C. J. (2019). Ischemic Postconditioning (IPostC) Protects Fibrotic and Cirrhotic Rat Livers after Warm Ischemia. *Canadian Journal of Gastroenterology and Hepatology*, *2019*, 5683479.

[55] – Ceresa, C. D. L., Nasralla, D., & Jassem, W. (2018). Normothermic Machine Preservation of the Liver: State of the Art. *Current Transplantation Reports*, *5*(1), 104 – 110.

[56] – Reiter, R., Tang, L., Garcia, J. J., & Muñoz-Hoyos, A. (1997). Pharmacological Actions of Melatonin in Oxygen Radical Pathophysiology. *Life Sciences*, *60*(25), 2255 – 2271.

[57] – Rodriguez, C., Mayo, J. C., Sainz, R. M., Antolín, I., Herrera, F., Martín, V., & Reiter, R. J. (2004). Regulation of antioxidant enzymes: a significant role for melatonin. *Journal of Pineal Research*, *36*(1), 1 – 9.

[58] – Park, S. W., & Lee, S. M. (2008). Antioxidant and prooxidant properties of ascorbic acid on hepatic dysfunction induced by cold ischemia/reperfusion. *European Journal of Pharmacology*, *580*(3), 401 – 406.

[59] – Timoshnikov, V. A., Kobzeva, T. V., Polyakov, N. E., & Kontoghiorghes, G. J. (2020). Redox Interactions of Vitamin C and Iron: Inhibition of the Pro-Oxidant Activity by Deferiprone. *International Journal of Molecular Sciences*, *21*(11), 3967.

[60] – Flower, R. J. (2009). Prednisone. In S. J. Enna & D. B. Bylund (Eds.), *xPharm: The Comprehensive Pharmacology Reference* (pp. 1 – 6). Elsevier.

[61] – Wang, M., Sakon, M., Umeshita, K., Okuyama, M., Shiozaki, K., Nagano, H., Dohno, K., Nakamori, S., & Monden, M. (2001). Prednisolone suppresses ischemia-reperfusion injury of the rat liver by reducing cytokine production and calpain μ activation. *Journal of Hepatology*, *34*(2), 278 – 283.

[62] – Moini, M., Schilsky, M. L., & Tichy, E. M. (2015). Review on immunosuppression in liver transplantation. *World Journal of Hepatology*, *7*(10), 1355 – 1368.

[63] – Pillai, A. A., & Levitsky, J. (2009). Overview of immunosuppression in liver transplantation. *World Journal of Gastroenterology*, *15*(34), 4225 – 4233.

[64] – Andres, S., Pevny, S., Ziegenhagen, R., Bakhiya, N., Schäfer, B., Hirsch-Ernst, K. I., & Lampen, A. (2018). Safety Aspects of the Use of Quercetin as a Dietary Supplement. *Molecular Nutrition & Food Research*, *62*(1), 1700447.

[65] – Bahadir, H. M., Sarigoz, T., Topuz, O., Sevim, Y., Ertan, T., & Sarici, I. S. (2018). Protective Effects of Quercetin on Hepatic Ischemia-Reperfusion Injury. *Istanbul Medical Journal*, *19*, 47 – 51.

[66] – Harwood, M., Danielewska-Nikiel, B., Borzelleca, J. F., Flamm, G. W., Williams, G. M., & Lines, T. C. (2007). A critical review of the data related to the safety of quercetin and lack of evidence of *in vivo* toxicity, including lack of genotoxic/carcinogenic properties. *Food and Chemical Toxicology*, *45*(11), 2179 – 2205.

[67] – Kelly, G. S. (2011). Quercetin. Monograph. *Alternative Medicine Review*, *16*(2), 172 – 194.

[68] – Li, Y., Yao, J., Han, C., Yang, J., Chaudhry, M. T., Wang, S., Liu, H., & Yin, Y. (2016). Quercetin, Inflammation and Immunity. *Nutrients*, *8*(3), 167.

[69] – Mlcek, J., Jurikova, T., Skrovankova, S., & Sochor, J. (2016). Quercetin and Its Anti-Allergic Immune Response. *Molecules*, *21*(5), 623.

[70] – Xu, D., Hu, M. J., Wang, Y. Q., & Cui, Y. L. (2019). Antioxidant Activities of Quercetin and Its Complexes for Medicinal Application. *Molecules*, *24*(6), 1123.

[71] – Zheng, Y., & Chow, A. H. (2009). Production and characterization of a spray-dried hydroxypropyl-β-cyclodextrin/quercetin complex. *Drug Development and Industrial Pharmacy*, *35*(6), 727 – 734.

[72] – Ferreira-Silva, M., Faria-Silva, C., Carvalheiro, M. C., Simões, S., Marinho, H. S., Marcelino, P., Campos, M. C., Metselaar, J. M., Fernandes, E., Baptista, P. V., Fernandes, A. R., & Corvo, M. L. (2022). Quercetin Liposomal Nanoformulation for Ischemia and Reperfusion Injury Treatment. *Pharmaceutics*, *14*(1), 104.

[73] – Rich, G. T., Buchweitz, M., Winterbone, M. S., Kroon, P. A., & Wilde, P. J. (2017). Towards an Understanding of the Low Bioavailability of Quercetin: A Study of Its Interaction with Intestinal Lipids. *Nutrients*, *9*(2), 111.

[74] – Yuan, Z., Yao, F., Hu, Z., Sun, S., & Wu, B. (2015). Quercetin inhibits the migration and proliferation of astrocytes in wound healing. *NeuroReport*, *26*(7), 387–393.

[75] – Proença, C., Ribeiro, D., Soares, T., Tomé, S. M., Silva, A., Lima, J., Fernandes, E., & Freitas, M. (2017). Chlorinated Flavonoids Modulate the Inflammatory Process in Human Blood. *Inflammation*, *40*(4), 1155 – 1165.

[76] – Atkinson, J., Manor, D., & Parker, R. (2013). Vitamin E. In W. J. Lennarz & M. D. Lane (Eds.), *Encyclopedia of Biological Chemistry* (Second Edition, pp. 545 – 550). Waltham: Academic Press.

[77] – Ribeiro, D., Freitas, M., Lima, J. L. F. C., & Fernandes, E. (2015). Proinflammatory Pathways: The Modulation by Flavonoids. *Medicinal Research Reviews*, *35*(5), 877 – 936.

[78] – Chen, C., Zhou, J., & Ji, C. (2010). Quercetin: A potential drug to reverse multidrug resistance. *Life Sciences*, *87*(11 – 12), 333 – 338.

[79] – Marín-García, J. (2014). Chapter 14 – Oxidative Stress and Cell Death in Cardiovascular Disease: A Post-Genomic Appraisal. In J. Marín-García (Ed.), *Post-Genomic Cardiology* (Second Edition, pp. 471 – 498). Boston: Academic Press.

[80] – Nabar, N. R., Shi, C. S., & Kehrl, J. H. (2018). Chapter 6 – Signaling by the Toll-Like Receptors Induces Autophagy Through Modification of Beclin 1: Molecular Mechanism. In M. A. Hayat (Ed.), *Immunology* (pp. 75 – 84). Academic Press.

[81] – Goniotaki, M., Hatziantoniou, S., Dimas, K., Wagner, M., & Demetzos, C. (2004). Encapsulation of naturally occurring flavonoids into liposomes: physicochemical properties and biological activity against human cancer cell lines. *Journal of Pharmacy and Pharmacology*, *56*(10), 1217 – 1224.

[82] – Grgić, J., Šelo, G., Planinić, M., Tišma, M., & Bucić-Kojić, A. (2020). Role of the Encapsulation in Bioavailability of Phenolic Compounds. *Antioxidants*, *9*(10), 923.

[83] – Huang, M., Su, E., Zheng, F., & Tan, C. (2017). Encapsulation of Flavonoids in Liposomal Delivery Systems: Case of Quercetin, Kaempferol and Luteolin. *Food & Function*, *8*(9), 3198 – 3208.

[84] – Toniazzo, T., Peres, M. S., Ramos, A. S., & Pinho, S. C. (2017). Encapsulation of quercetin in liposomes by ethanol injection and physicochemical characterization of dispersions and lyophilized vesicles. *Food Bioscience*, *19*, 17 – 25.

[85] – David, M. N. V., & Shetty, M. (2021). Digoxin. In *StatPearls*. StatPearls Publishing.

[86] – Wang, Y. H., Chao, P. D., Hsiu, S. L., Wen, K. C., & Hou, Y. C. (2004). Lethal quercetin-digoxin interaction in pigs. *Life Sciences*, *74*(10), 1191 – 1197.

[87] – Beltrán-Gracia, E., López-Camacho, A., Higuera-Ciapara, I., Velázquez-Fernández, J. B., & Vallejo-Cardona, A. A. (2019). Nanomedicine review: clinical developments in liposomal applications. *Cancer Nanotechnology*, *10*, 11.

[88] – Almeida, B., Nag, O. K., Rogers, K. E., & Delehanty, J. B. (2020). Recent Progress in Bioconjugation Strategies for Liposome-Mediated Drug Delivery. *Molecules*, *25*(23), 5672.

[89] – Gadekar, V., Borade, Y., Kannaujia, S., Rajpoot, K., Anup, N., Tambe, V., Kalia, K., & Tekade, R. K. (2021). Nanomedicines accessible in the market for clinical interventions. *Journal of Controlled Release*, *330*, 372–397.

[90] – Inglut, C. T., Sorrin, A. J., Kuruppu, T., Vig, S., Cicalo, J., Ahmad, H., & Huang, H. (2020). Immunological and Toxicological Considerations for the Design of Liposomes. *Nanomaterials*, *10*(2), 190.

[91] – Laouini, A., Jaafar-Maalej, C., Limayem-Blouza, I., Sfar, S., Charcosset, C., & Fessi, H. (2012). Preparation, Characterization and Applications of Liposomes: State of the Art. *Journal of Colloid Science and Biotechnology*, *1*(2), 147 – 168.

[92] – Sercombe, L., Veerati, T., Moheimani, F., Wu, S. Y., Sood, A. K., & Hua, S. (2015). Advances and Challenges of Liposome Assisted Drug Delivery. *Frontiers in Pharmacology*, *6*, 286.

[93] – Trucillo, P., Campardelli, R., & Reverchon, E. (2020). Liposomes: From Banghan to Supercritical Fluids. *Processes*, *8*, 1022.

[94] – Zylberberg, C., & Matosevic, S. (2016). Pharmaceutical liposomal drug delivery: a review of new delivery systems and a look at the regulatory landscape. *Drug Delivery*, *23*(9), 3319 – 3329.

[95] – Najlah, M., Said Suliman, A., Tolaymat, I., Kurusamy, S., Kannappan, V., Elhissi, A. M. A., & Wang, W. (2019). Development of Injectable PEGylated Liposome Encapsulating Disulfiram for Colorectal Cancer Treatment. *Pharmaceutics*, *11*(11), 610.

[96] – Allen, T. M., Hansen, C. B., & de Menezes, D. E. L. (1995). Pharmacokinetics of long-circulating liposomes. *Advanced Drug Delivery Reviews*, *16*(2), 267 – 284.

[97] – Bangham, A. D., & Horne, R. W. (1964). Negative Staining of Phospholipids and their Structural Modification by Surface-active Agents as observed in the Electron Microscope. *Journal of Molecular Biology*, *8*(5), 660 – 668.

[98] – Bangham, A. D., Standish, M. M., & Watkins, J. C. (1965). Diffusion of Univalent Ions across the Lamellae of Swollen Phospholipids. *Journal of Molecular Biology*, *13*(1), 238 – 252.

[99] – Deamer, D. W. (2010). From "Banghasomes" to liposomes: A memoir of Alec Bangham, 1921-2010. *The FASEB Journal*, *24*(5), 1308 – 1310.

[100] – Heap, B., & Gregoriadis, G. (2011). Alec Douglas Bangham. 10 November 1921 -- 9 March 2010. *Biographical Memoirs of Fellows of the Royal Society*, *57*, 25 – 43.

[101] – Bangham, A. D. (1989). The First Description of Liposomes – A Citation Classic Commentary on Diffusion of Univalent Ions across the Lamellae of Swollen Phospholipids by Bangham, A. D., Standish, M. M., & Watkins, J. C.. *Current Contentes/Life Sciences*, *I*(13), 14.

[102] – Weissig, V. (2017). Liposomes Came First: The Early History of Liposomology. In: G. G. M. D'Souza (ed.), *Liposomes - Methods and Protocols* (Second Edition, pp. 1 – 16). Humana Press.

[103] – Leserman, L. (2008). The Gregoriadyssey: From smetic mesophases to liposomal drug carriers, a personal reflection of Gregory Gregoriadis. *Journal of Drug Targeting*, *16*(7 – 8), 525 – 528.

[104] – Sessa, G., & Weissmann, G. (1968). Phospholipid spherules (liposomes) as a model for biological membranes. *Journal of Lipid Research*, *9*(3), 310 – 318.

[105] – Gregoriadis, G., & Ryman, B. E. (1971). Liposomes as Carriers of Enzymes or Drugs: a New Approach to the Treatment of Storage Diseases. *The Biochemical Journal*, *124*(5), 58P.

[106] – Gregoriadis, G., & Neerunjun, E. D. (1975). Treatment of tumour bearing mice with liposome-entrapped actinomycin D prolongs their survival. *Research Communications in Chemical Pathology and Pharmacology*, *10*(2), 351 – 362.

[107] – Matos, C., Moutinho, C., & Lobão, P. (2012). Liposomes as a Model for the Biological Membrane: Studies on Daunorubicin Bilayer Interaction. *Journal of Membrane Biology*, *245*(2), 69 – 75.

[108] – Anselmo, A. C., & Mitragotri, S. (2019). Nanoparticles in the clinic: An update. *Bioengineering & Translational Medicine*, *4*(3), e10143.

[109] – Barenholz, Y. (2012). Doxil® – The first FDA-approved nano-drug: Lessons learned. *Journal of Controlled Release*, *160*(2), 117 – 134.

[110] – Bovier, P. A. (2008). Epaxal®: a virosomal vaccine to prevent hepatitis A infection. *Expert Review of Vaccines*, *7*(8), 1141 – 1150.

[111] – Hobbs, S. D., & Pierce, K. (2022). Wet Age-related Macular Degeneration (Wet AMD). In *StatPearls*. StatPearls Publishing.

[112] – Scott, L. J., & Goa, K. L. (2000). Verteporfin. *Drugs & Aging*, *16*(2), 139 – 148.

[113] – van der Veen, J. N., Kennelly, J. P., Wan, S., Vance, J. E., Vance, D. E., & Jacobs, R. L. (2017). The critical role of phosphatidylcholine and phosphatidylethanolamine metabolism in health and disease. *Biochimica et Biophysica Acta*, *1859*(9), 1558 – 1572.

[114] – Di Sotto, A., Paolicelli, P., Nardoni, M., Abete, L., Garzoli, S., Di Giacomo, S., Mazzanti, G., Casadei, M. A., & Petralito, S. (2018). SPC Liposomes as Possible Delivery Systems for Improving Bioavailability of the Natural Sesquiterpene β-Caryophyllene: Lamellarity and Drug-Loading as Key Features for a Rational Drug Delivery Design. *Pharmaceutics*, *10*(4), 274.

[115] – Eeman, M., & Deleu, M. (2010) From biological membranes to biomimetic model membranes. *Biotechnology, Agronomy, Society and Environment (BASE)*, *14*(4), 719 – 736.

[116] – Briuglia, M. L., Rotella, C., McFarlane, A., & Lamprou, D. A. (2015). Influence of cholesterol on liposome stability and on *in vitro* drug release. *Drug Delivery and Translational Research*, *5*(3), 231 – 242.

[117] – Nakhaei, P., Margiana, R., Bokov, D. O., Abdelbasset, W. K., Jadidi Kouhbanani, M. A. J., Varma, R. S., Marofi, F., Jarahian, M., & Beheshtkhoo, N. (2021). Liposomes: Structure, Biomedical Applications, and Stability Parameters With Emphasis on Cholesterol. *Frontiers in Bioengineering and Biotechnology*, *9*(September), 705886.

[118] – Allen, T. M., & Cullis, P. R. (2013). Liposomal drug delivery systems: From concept to clinical applications. *Advanced Drug Delivery Reviews*, *65*(1), 36 – 48.

[119] – Klibanov, A. L., Maruyama, K., Torchilin, V. P., & Huang, L. (1990). Amphipathic polyethyleneglycols effectively prolong the circulation time of liposomes. *FEBS Letters*, *268*(1), 235 – 237.

[120] – Attia, M. F., Anton, N., Wallyn, J., Omran, Z., & Vandamme, T. F. (2019). An overview of active and passive targeting strategies to improve the nanocarriers efficiency to tumour sites. *Journal of Pharmacy and Pharmacology*, *71*(8), 1185 – 1198.

[121] – Bozzuto, G., & Molinari, A. (2015). Liposomes as nanomedical devices. *International Journal of Nanomedicine*, *10*, 975 – 999.

[122] – Bitounis, D., Fanciullino, R., Iliadis, A., & Ciccolini, J. (2012). Optimizing Druggability through Liposomal Formulations: New Approaches to an Old Concept. *ISRN Pharmaceutics*, *2012*, 738432.

[123] – Fang, Y., Xue, J., Gao, S., Lu, A., Yang, D., Jiang, H., He, Y., & Shi, K. (2017). Cleavable PEGylation: a strategy for overcoming the "PEG dilemma" in efficient drug delivery. *Drug Delivery*, *24*(2), 22 – 32.

[124] – Malvern. *Zetasizer Nano Series User Manual*. (Malvern Instruments Ltd., 2013).

[125] – Shaw, R. *Dynamic Light Scattering Training*. (Malvern Instruments Ltd., 2014).

[126] – Danaei, M., Dehghankhold, M., Ataei, S., Hasanzadeh Davarani, F., Javanmard, R., Dokhani, A., Khorasani, S., & Mozafari, M. R. (2018). Impact of Particle Size and Polydispersity Index on the Clinical Applications of Lipidic Nanocarrier Systems. *Pharmaceutics*, *10*(2), 57.

[127] – Clogston, J. D., & Patri, A. K. (2011). Zeta Potential Measurement. In S. E. McNeil (Ed.), *Characterization of Nanoparticles Intended for Drug Delivery* (First Edition, Vol. 697, pp. 63 – 70). Humana Press.

[128] – Manaia, E. B., Abuçafy, M. P., Chiari-Andréo, B. G., Silva, B. L., Junior, J. A. O., & Chiavacci, L. A. (2017). Physicochemical characterization of drug nanocarriers. *International Journal of Nanomedicine*, *12*, 4991 – 5011.

[129] – Smith, M. C., Crist, R. M., Clogston, J. D., & McNeil, S. E. (2017). Zeta potential: a case study of cationic, anionic, and neutral liposomes. *Analytical and Bioanalytical Chemistry*, *409*(24), 5779 – 5787.

[130] – Gaikwad, V. L., Choudhari, P. B., Bhatia, N. M., & Bhatia, M. S. (2019). Characterization of pharmaceutical nanocarriers: in vitro and in vivo studies. In A. M. Grumezescu (Ed.), *Nanomaterials for Drug Delivery and Therapy* (pp. 33 – 58). Elsevier.

[131] – Honary, S., & Zahir, F. (2013). Effect of Zeta Potential on the Properties of Nano-Drug Delivery Systems - A Review (Part 1). *Tropical Journal of Pharmaceutical Research*, *12*(2), 255 – 264.

[132] – Meure, L. A., Foster, N. R., & Dehghani, F. (2008). Conventional and Dense Gas Techniques for the Production of Liposomes: A Review. *AAPS PharmSciTech*, *9*(3), 798 – 809.

[133] – Shah, S., Dhawan, V., Holm, R., Nagarsenker, M. S., & Perrie, Y. (2020). Liposomes: Advancements and innovation in the manufacturing process. *Advanced Drug Delivery Reviews*, *154 – 155*, 102 – 122.

[134] – Olson, F., Hunt, C. A., Szoka, F. C., Vail, W. J., & Papahadjopoulos, D. (1979). Preparation of liposomes of defined size distribution by extrusion through polycarbonate membranes. *Biochimica et Biophysica Acta*, *557*(1), 9 – 23.

[135] – Hope, M. J., Nayar, R., Mayer, L. D., & Cullis, P. R. (1993). Reduction of Liposome Size and Preparation of Unilamellar Vesicles by Extrusion Techniques. In G. Gregoriadis (Ed.), *Liposome Technology* (pp. 123 – 139). CRC Press.

[136] – Gonzalez Gomez, A., & Hosseinidoust, Z. (2020). Liposomes For Antibiotic Encapsulation and Delivery. *ACS Infectious Diseases*, *6*(5), 896 – 908.

[137] – Grabielle-Madelmont, C., Lesieur, S., & Ollivon, M. (2003). Characterization of loaded liposomes by size exclusion chromatography. *Journal of Biochemical and Biophysical Methods*, *56*(1 – 3), 189 – 217.

[138] – Ruysschaert, T., Marque, A., Duteyrat, J. L., Lesieur, S., Winterhalter, M., & Fournier, D. (2005). Liposome retention in size exclusion chromatography. *BMC Biotechnology*, *5*, 11.

[139] – Chiba, M., Miyazaki, M., & Ishiwata, S. (2014). Quantitative Analysis of the Lamellarity of Giant Liposomes Prepared by the Inverted Emulsion Method. *Biophysical Journal*, *107*(2), 346 – 354.

[140] – Di Muzio, M., Millan-Solsona, R., Dols-Perez, A., Borrell, J. H., Fumagalli, L., & Gomila, G. (2021). Dielectric properties and lamellarity of single liposomes measured by in-liquid scanning dielectric microscopy. *Journal of Nanobiotechnology*, *19*(1), 167.

[141] – Nele, V., Holme, M. N., Kauscher, U., Thomas, M. R., Doutch, J. J., & Stevens, M. M. (2019). Effect of Formulation Method, Lipid Composition, and PEGylation on Vesicle Lamellarity: A Small-Angle Neutron Scattering Study. *Langmuir*, *35*(18), 6064 – 6074.

[142] – Almgren, M., Edwards, K., & Karlsson, G. (2000). Cryo transmission electron microscopy of liposomes and related structures. *Colloids and Surfaces A: Physicochemical and Engineering Aspects*, *174*, 3 – 21.

[143] – Nii, T., & Ishii, F. (2005). Encapsulation efficiency of water-soluble and insoluble drugs in liposomes prepared by the microencapsulation vesicle method. *International Journal of Pharmaceutics*, *298*(1), 198 – 205.

[144] – Piacentini, E. (2016). Encapsulation Efficiency. In E. Drioli & L. Giorno (Eds.), *Encyclopedia of Membranes* (pp. 706 – 707). Springer-Verlag Berlin Heidelberg.

[145] – Rouser, G., Fkeischer, S., & Yamamoto, A. (1970). Two Dimensional Thin Layer Chromatographic Separation of Polar Lipids and Determination of Phospholipids by Phosphorus Analysis of Spots. *Lipids*, *5*(5), 494 – 496.

[146] – Nehoff, H., Parayath, N. N., Domanovitch, L., Taurin, S., & Greish, K. (2014). Nanomedicine for drug targeting: strategies beyond the enhanced permeability and retention effect. *International Journal of Nanomedicine*, *9*, 2539–2555.

[147] – Torchilin, V. (2011). Tumor delivery of macromolecular drugs based on the EPR effect. *Advanced Drug Delivery Reviews*, *63*(3), 131 – 135.

[148] – Brown, S., & Khan, D. R. (2012). The Treatment of Breast Cancer Using Liposome Technology. *Journal of Drug Delivery*, *2012*, 212965.

[149] – Pate, M., Damarla, V., Chi, D. S., Negi, S., & Krishnaswamy, G. (2010). Endothelial cell biology: role in the inflammatory response. *Advances in Clinical Chemistry*, *52*, 109–130.

[150] – Pober, J. S., & Sessa, W. C. (2007). Evolving functions of endothelial cells in inflammation. *Nature Reviews Immunology*, *7*(10), 803–815.

[151] – Sutton, N. R., Baek, A., & Pinsky, D. J. (2014). Endothelial Cells and Inflammation. In I. R. Mackay & N. R. Rose (Eds.), *Encyclopedia of Medical Immunology – Autoimmune Diseases* (pp. 367 – 412). Springer Science+Business Media New York.

[152] – Akbarzadeh, A., Rezaei-Sadabady, R., Davaran, S., Joo, S. W., Zarghami, N., Hanifehpour, Y., Samiei, M., Kouhi, M., & Nejati-Koshki, K. (2013). Liposome: classification, preparation, and applications. *Nanoscale Research Letters*, *8*(1), 102.

[153] – Kuai, R., Yuan, W., Qin, Y., Chen, H., Tang, J., Yuan, M., Zhang, Z., & He, Q. (2010). Efficient Delivery of Payload into Tumor Cells in a Controlled Manner by TAT and Thiolytic Cleavable PEG Co-Modified Liposomes. *Molecular Pharmaceutics*, *7*(5), 1816 – 1826.

[154] – Liu, W., Hou, Y., Jin, Y., Wang, Y., Xu, X., & Han, J. (2020). Research progress on liposomes: Application in food, digestion behavior and absorption mechanism. *Trends in Food Science & Technology*, *104*(August), 177 – 189.

[155] – Torchilin, V. P. (2005). Recent advances with liposomes as pharmaceutical carriers. *Nature Reviews Drug Discovery*, *4*(2), 145 – 160.

[156] – Pagano, R. E., & Weinstein, J. N. (1978). Interactions of liposomes with mammalian cells. *Annual Review of Biophysics and Bioengineering*, *7*, 435 – 468.

[157] – Rommasi, F., & Esfandiari, N. (2021). Liposomal Nanomedicine: Applications for Drug Delivery in Cancer Therapy. *Nanoscale Research Letters*, *16*(1), 95.

[158] – Magar, K. T., Boafo, G. F., Li, X., Chen, Z., & He, W. (2022). Liposome-based delivery of biological drugs. *Chinese Chemical Letters*, *33*(2), 587 – 596.

[159] – Chacon, E., Acosta, D., & Lemasters, J. (1997). Primary Cultures of Cardiac Myocytes as *In Vitro* Models for Pharmacological and Toxicological Assessments. In J. V. Castell & M. J. Gómez-Lechón (Eds.), *In Vitro Methods in Pharmaceutical Research* (pp. 209 – 223). Academic Press.

[160] – Gutiérrez, L., Stepien, G., Pérez-Hernández, M., Pardo, J., Grazú, V., & de la Fuente, J. M. (2017). Nanotechnology in Drug Discovery and Development. In S. Chackalamannil, D. Rotella, & S. E. Ward (Eds.), *Comprehensive Medicinal Chemistry III* (pp. 264 – 295). Elsevier.

[161] – Kuete, V., Karaosmanoğlu, O., & Sivas, H. (2017). Anticancer Activities of African Medicinal Spices and Vegetables. In V. Kuete (Ed.), *Medicinal Spices and Vegetables from Africa: Therapeutic Potential Against Metabolic, Inflammatory, Infectious and Systemic Diseases* (pp. 271 – 297). Academic Press.

[162] – Eruslanov, E., & Kusmartsev, S. (2010). Identification of ROS Using Oxidized DCFDA and Flow-Cytometry. In D. Armstrong (Ed.), *Advanced Protocols in Oxidative Stress II* (Vol. 594, pp. 57 – 72). Humana Press.

[163] – Yang, C., Jiang, L., Zhang, H., Shimoda, L. A., DeBerardinis, R. J., & Semenza, G. L. (2014). Analysis of Hypoxia-Induced Metabolic Reprogramming. In L. Galluzzi & G. Kroemer (Eds.), *Conceptual Background and Bioenergetic/Mitochondrial Aspects of Oncometabolism* (Vol. 542, pp. 425 – 455). Academic Press.

[164] – Kepp, O., Galluzzi, L., Lipinski, M., Yuan, J., & Kroemer, G. (2011). Cell death assays for drug discovery. *Nature Reviews Drug Discovery*, *10*(3), 221 – 237.

[165] – Wallberg, F., Tenev, T., & Meier, P. (2016). Analysis of Apoptosis and Necroptosis by Fluorescence-Activated Cell Sorting. *Cold Spring Harbor Protocols*, *2016*(4), 347 – 352.

[166] – Ma, J., Gao, S. S., Yang, H. J., Wang, M., Cheng, B. F., Feng, Z. W., & Wang, L. (2018). Neuroprotective Effects of Proanthocyanidins, Natural Flavonoids Derived From Plants, on Rotenone-Induced Oxidative Stress and Apoptotic Cell Death in Human Neuroblastoma SH-SY5Y Cells. *Frontiers in Neuroscience*, *12*(May), 369.

[167] – Testa, C. M., Sherer, T. B., & Greenamyre, J. T. (2005). Rotenone induces oxidative stress and dopaminergic neuron damage in organotypic substantia nigra cultures. *Molecular Brain Research*, *134*(1), 109 – 118.

[168] – Chen, Y., McMillan-Ward, E., Kong, J., Israels, S. J., & Gibson, S. B. (2008). Oxidative stress induces autophagic cell death independent of apoptosis in transformed and cancer cells. *Cell Death and Differentiation*, *15*(1), 171 – 182.

[169] – Ott, M., Gogvadze, V., Orrenius, S., & Zhivotovsky, B. (2007). Mitochondria, oxidative stress and cell death. *Apoptosis*, *12*(5), 913 – 922.

[170] – Nishimura, Y., Oyama, T. B., Sakanashi, Y., Oyama, T. M., Matsui, H., Okano, Y., & Oyama, Y. (2008). Some characteristics of quercetin-induced cytotoxicity on rat thymocytes under *in vitro* condition. *Toxicology in Vitro*, *22*(4), 1002 – 1007.

[171] – Sundaram, M. K., Raina, R., Afroze, N., Bajbouj, K., Hamad, M., Haque, S., & Hussain, A. (2019). Quercetin modulates signaling pathways and induces apoptosis in cervical cancer cells. *Bioscience Reports*, *39*(8), 1 – 17.

[172] – Zielińska, M., Gülden, M., & Seibert, H. (2003). Effects of quercetin and quercetin-3-*O*-glycosides on oxidative damage in rat C6 glioma cells. *Environmental Toxicology and Pharmacology*, *13*(1), 47 – 53.

[173] – Xue, X., & Bian, J. S. (2015). Neuroprotective Effects of Hydrogen Sulfide in Parkinson's Disease Animal Models: Methods and Protocols. *Methods in Enzymology*, *554*, 169 – 186.

[174] – Notas, G., Nifli, A. P., Kampa, M., Pelekanou, V., Alexaki, V. I., Theodoropoulos, P., Vercauteren, J, & Castanas, E. (2012). Quercetin accumulates in nuclear structures and triggers specific gene expression in epithelial cells. *Journal of Nutritional Biochemistry*, *23*(6), 656 – 666.

[175] – Verhoef, J. J. F., & Anchordoquy, T. J. (2013). Questioning the Use of PEGylation for Drug Delivery. *Drug Delivery and Translational Research*, *3*(6), 499 – 503.

[176] – Pakrashi, S., Chakraborty, J., & Bandyopadhyay, J. (2020). Neuroprotective Role of Quercetin on Rotenone-Induced Toxicity in SH-SY5Y Cell Line Through Modulation of Apoptotic and Autophagic Pathways. *Neurochemical Research*, *45*(8), 1962 – 1973.

[177] – Choi, E. O., Jeong, J. W., Park, C., Hong, S. H., Kim, G. Y., Hwang, H. J., Cho, E. J., & Choi, Y. H. (2016). Baicalein protects C6 glial cells against hydrogen peroxide-induced oxidative stress and apoptosis through regulation of the Nrf2 signaling pathway. *International Journal of Molecular Medicine*, *37*(3), 798 – 806.

[178] – Fan, W. H., Hou, Y., Meng, F. K., Wang, X. F., Luo, Y. N., & Ge, P. F. (2011). Proteasome inhibitor MG-132 induces C6 glioma cell apoptosis via oxidative stress. *Acta Pharmacologica Sinica*, *32*(5), 619 – 625.

[179] – Krylova, N. G., Drobysh, M. S., Semenkova, G. N., Kulahava, T. A., Pinchuk, S. V., & Shadyro, O. I. (2019). Cytotoxic and antiproliferative effects of thymoquinone on rat C6 glioma cells depend on oxidative stress. *Molecular and Cellular Biochemistry*, *462*(1 – 2), 195 – 206.